Kasdi Merbah University Ouargla

FACULTY OF HYDROCARBONS, RENEWABLE ENERGIES AND EARTH AND UNIVERSE SCIENCES

Department of Earth and Universe Sciences

Academic Master's Thesis

Domain: Earth and Universe Sciences

Sector: Geology

Specialty: Petroleum Geology

THEME

Geological and Petrophysical Modeling of the Reservoir in the Ben Kahla Region South Algeria.

Presented by:

Djoudi Nour El Houda

Mihoubi Floura

Publicly defended on:--/--/2025

In front of the jury:

President	**Kachiched Rabah**	**Pr. UKM. Ouargla**
Promoter	**Sahri Leila**	**MCB. UKM. Ouargla**
Examiner	**Medjani Fethi**	**Pr. UKM . Ouargla**

Academic year : 2024/2025

Acknowledgment

First and foremost, we thank our Creator ALLAH, who gave us the will, strength, and patience to complete this work. Without His will, none of this would have been possible.

We sincerely express our gratitude to our supervisor, Mrs. Sahri Leila, for her guidance, availability, and efforts throughout this thesis. Thank you for your valuable advice and clear direction.

We also thank the jury members who accepted to examine and evaluate this work.

A special thank you to Mr. Malek, who supported us step by step in this project — both in the technical and theoretical parts. His constant help, advice, and encouragement made a real difference.

We are also deeply grateful to our families and friends, especially Amel, Houria, and everyone who supported us, directly or indirectly. Your presence and encouragement were essential.

Finally, we thank our faculty and all the teachers of the department for the knowledge and support they provided during our academic journey

Dedication

The name of Allah, the Most Merciful, the Most Compassionate First and foremost, all praise goes to Allah, whose guidance and support have been my strength throughout this journey. Without His blessings, I would not have made it this far, and for that, I am truly grateful. A special thank you goes to my dear friend **Flora**, who has been my constant companion. Together, we tackled every challenge, shared countless ideas, and pushed each other to do better. The support she's given me throughout this process means the world, and I can't imagine having done this without her. To my amazing parents, whose love, sacrifices, and encouragement have been my foundation, I owe everything. Your belief in me has carried me through the toughest moments. And to my wonderful brothers and sisters, your unwavering support has always been my source of strength. I am deeply grateful for each of you. Although this is the first time I've been away from my family, I've been fortunate to meet incredible people who have become like family to me. You've made this experience so much richer, and I thank you from the bottom of my heart. Lastly, I want to express my gratitude to the professors who have guided me with their wisdom and helped me grow in ways I never expected. Your support has been invaluable.

Nour EL Houda

Dedication

I dedicate this work to myself and to **Houda** because only we truly know the journey we've taken and the challenges we've overcome to make this thesis a reality.

To my father, my mother, and my brothers I am here today thanks to your endless love, support, and sacrifices.

To all my family members your presence in my life has always been a source of strength.

To the one who has stood by my side for a long time and walked with me, step by step, until today your unwavering support means the world to me.

To all my friends who believed in me and supported me thank you for always being there.

To everyone I met in Ouargla who became my second family your kindness and warmth will never be forgotten.

This thesis is the fruit of love, effort, patience, and persistence. Thank you all for being part of this beautiful chapter in my life.

Flora

Abstract

The Ben Kahla reservoir, located in Algeria's Ouargla province within the Ouad Mya basin of the Triassic Houad Berkaoui formation, stands out as one of the region's most productive oil fields and has been under active exploitation for many years. Its geological structure is highly integrated, consisting of Silurian shale as the source rock, Triassic sandstone with varying clay content as the reservoir rock, and a Liassic evaporitic salt layer serving as a cap rock—all sealed by effective structural traps. Recent geological studies pointing to additional untapped potential in the southern area have spurred several companies to undertake exploration efforts and develop a comprehensive 3D geological model using Petrel software. This model integrates crucial data such as porosity (Φ), fluid saturation (Sw), and reservoir thickness, derived from well logs and petrophysical evaluations. These results enable us to conduct dynamic simulations that enhance understanding of fluid behavior within the reservoir, and support more informed and efficient extraction strategies.

Résumé

Le réservoir de Ben Kahla, situé dans la province algérienne d'Ouargla dans le bassin d'Ouad Mya de la formation triasique Houad Berkaoui, se distingue comme l'un des champs pétrolifères les plus productifs de la région et est en exploitation active depuis de nombreuses années. Sa structure géologique est hautement intégrée, constituée de schiste silurien comme roche mère, de grès triasique avec une teneur en argile variable comme roche réservoir et d'une couche de sel évaporitique liassique servant de roche de coiffe—le tout scellé par des pièges structurels efficaces. Des études géologiques récentes indiquant un potentiel inexploité supplémentaire dans la région sud ont incité plusieurs entreprises à entreprendre des efforts d'exploration et à développer un modèle géologique 3D complet à l'aide du logiciel Petrel. Ce modèle intègre des données cruciales telles que la porosité (Φ), la saturation du fluide (Sw) et l'épaisseur du réservoir, dérivées des diagraphies des puits et des évaluations pétrophysiques. Ces résultats nous permettent de mener des simulations dynamiques qui améliorent la compréhension du comportement des fluides dans le réservoir et soutiennent des stratégies d'extraction plus éclairées et plus efficaces.

مـلـخص

يقع خزان بن كحلة في ولاية ورقلة الجزائرية داخل حوض ود ميا في تكوين هواد بركاوي التريـاسي ، ويبرز كواحد من أكثر حقول النفط إنتاجية في المنطقة ويخضع للاستغلال النشط لسنوات عديدة. هيكلها الجيولوجي متكامل للغاية, تتكون من الصخر الزيتي السيلوري كصخرة المصدر, الحجر الرملي التريـاسي مع محتوى طيني متفاوت مثل صخور الخزان, وطبقة ملح تبخيري لياسي تعمل كصخرة سقف—كلها مختومة بمصائد هيكلية فعالة. دفعت الدراسات الجيولوجية الحديثة التي تشير إلى إمكانات إضافية غير مستغلة في المنطقة الجنوبية العديد من الشركات إلى بذل جهود الاستكشاف وتطوير نموذج جيولوجي شامل 3 د باستخدام برمجيات بترل. يدمج هذا النموذج بيانات مهمة مثل المسامية (saturation) ، وتشبع السوائل (جنوب غرب) ، وسمك الخزان ، المستمدة من سجلات الآبار والتقييمات البتروفيزيائية. وقد تمكننا هذه النتائج من اجراء محاكاة ديناميكية تعزز فهم سلوك السوائل داخل الخزان ، وتدعم استراتيجيات استخراج أكثر استنارة وكفاءة.

Chapter 3 : Reservoirs modeling

List of figures

List of table

list of abreviation

Qc : Quality control .
Sw : Water saturation.
Vsh : Shale volume.
SH : Sonatrach .
SIS: Sequential Indicator Simulation.
SIG: Sequential Gaussian Simulation.
PS: Spontaneous Potential

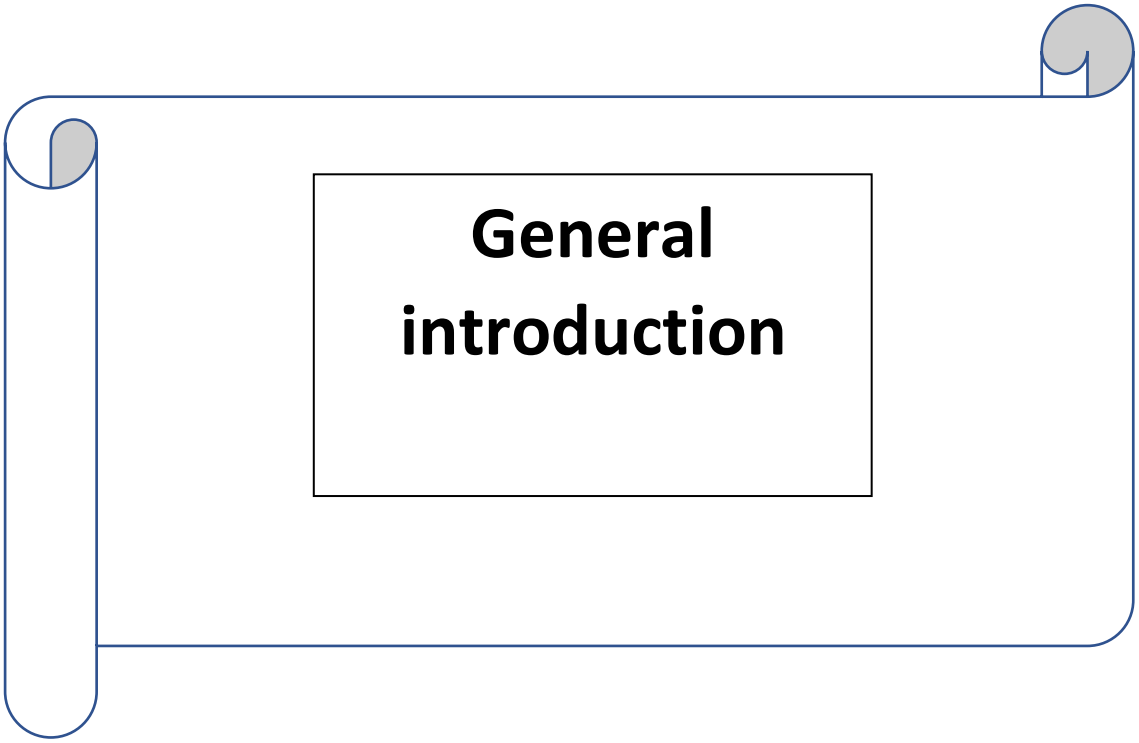
General
introduction

General Introduction

Algeria's geological landscape is characterized by a diverse array of provinces that host significant natural resources. The Saharan Platform, which contains the country's major hydrocarbon basins—including Oued Mya, Berkine, and Illizi—rests on a stable Precambrian basement. Within this platform, the Oued Mya Basin stands out as one of the most intensively explored and developed basins in the Algerian Sahara. It is in this context that the Ben Kahla field, located southeast of the Berkaoui field, emerges as a key hydrocarbon target.

Exploration in the Ben Kahla area began in 1956, and to date, the field contains over 40 producing wells, 6 injectors, and 7 dry wells, primarily targeting the TAG reservoir. This reservoir is dated to the Upper Triassic and was deposited in a post-Hercynian extensional tectonic setting, associated with continental rifting following the Variscan orogeny at the end of the Paleozoic era (Ziegler, 1990). These tectonic conditions promoted the development of subsiding basins that favored the accumulation of thick sedimentary sequences with favorable reservoir properties.

The reservoir's structure has been significantly modified by Cenozoic Alpine compressional events, which reactivated deep-seated faults and induced reservoir compartmentalization (Guiraud & Bosworth, 1997). This complex tectonostratigraphic history necessitates the construction of a detailed three-dimensional geological model to understand the internal architecture of the reservoir and improve development strategies.

At the heart of modern field management lies reservoir modeling, a critical tool for understanding subsurface heterogeneities and predicting production behavior. The geological model enables the spatial reconstruction of lithostratigraphic units, the geometry and continuity of reservoir bodies, and the major structural elements controlling hydrocarbon distribution (Ringrose & Bentley, 2011). In parallel, the petrophysical model quantifies key reservoir properties—such as porosity, permeability, and fluid saturations—which directly influence dynamic performance (Tiab & Donaldson, 2015).

Accurate integration of geological, petrophysical, and production data is essential for reducing geological uncertainties, improving hydrocarbon volume estimations, and optimizing field development (Haldorsen & Damsleth, 1990). In the case of the Ben Kahla field, the persistent production challenges and observed heterogeneities highlight the urgent need for a robust and integrated modeling approach.

This thesis is devoted to the characterization and modeling of the TAG reservoir in the Ben Kahla field. It is structured into three main chapters:

- **Chapter 1**: A general overview of the Oued Mya Basin and the Ben Kahla field, including its geological and tectonic framework, as well as its exploration and production history.
- **Chapter 2**: A detailed presentation of the methodology used for data acquisition, processing, and integration into the modeling workflow.
- **Chapter 3**: The construction and interpretation of the geological and petrophysical model of the TAG reservoir, followed by a discussion of its operational implications and recommendations for improving production strategies.

Chapter1 : Regional and local Geology of the study area.

CHAPITRE 1

Regional and local Geology of the study area.

1. Introduction

The Algerian Saharan Platform, a vast geological region in North Africa, is subdivided into three major provinces. Among them, the northern Triassic province stands out for its complex tectonic architecture, characterized by an east-west-oriented anticlinorium. Key structural elements include the Tilrhemt Arch, the Djemâa-Touggourt structural system, and the El Agreb–Messaoud fault system, which are delineated by the Oued Mya depression. Shaped by ancient tectonic movements and erosion processes, this province is largely covered by sedimentary sequences ranging from the Mesozoic to the Mio-Pliocene, which are considered potentially hydrocarbon-bearing, though many accumulations remain unconfirmed.

This region hosts several significant hydrocarbon fields such as Hassi Messaoud and Hassi R'mel, as well as fields located along the Oued Mya axis, including Haoud Berkaoui and Ben Kahla. The Ben Kahla field, which serves as the central case study of this project, is one of the most thoroughly explored zones within the Triassic province and offers valuable insights into the petroleum potential of the region.

2.9. Regional framework of the Oued M'ya basin:

1.1.A. Geographical location of Oued M'ya basin:

The Oued M'ya is a basin within the Saharan Platform, corresponding to the western compartment of the Triassic Province and covering an area of 400,000 km². Its geographical boundaries provide the best references.

It is bounded to the south and north by the parallels 31˚15' and 33˚00', respectively, and to the east and west by the meridians 6˚15' and 3˚30', respectively. The basin includes blocks 438, 425, 422, 437, 436, 3178, 420, 419, 418, 417, and 416, all belonging to District IV of Sonatrach.

Structurally, the basin is bounded by the Djemaa-Touggourt High to the north, the Mouydir Basin to the south, the Amguid-Messaoud High to the east, and the Allal Arch to the west.

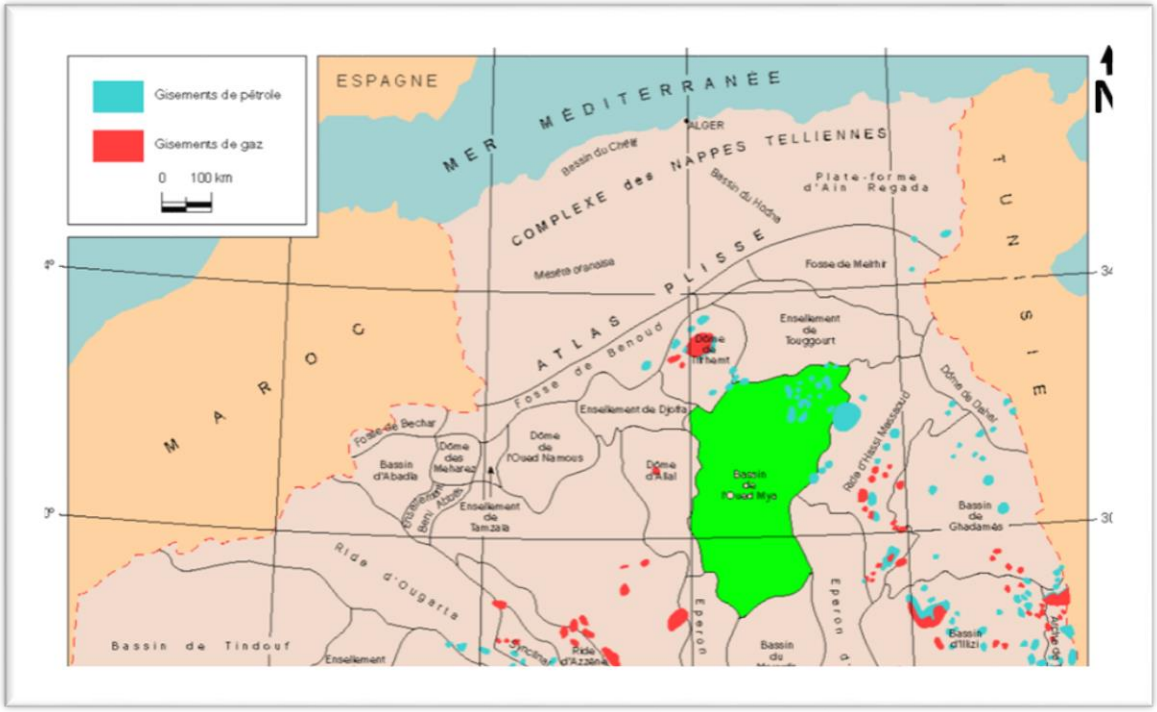

Figure 1:: geographical location of Oued M'ya basin.(SONATRACH1995).

1.1.B. Geological location of Oued M'ya basin:

Only a minor sub-basin with respect to the intracratonic setting is the M'ya Valley region. Its northern border tends to slope into the Saharan Flexure, where during the Mesozoic, there existed an area of highly subsiding trough that organized the pericratonic chain of the Saharan Atlas (Figure 02).

The bi segment parasmiting the geological evolution of the area known as Oued M'ya since the Cambrian is:

a. Paleozoic sedimentation mostly confined to Lower Paleozoic and its pre-Hercynian structuring.

b. The formation of a basin during the Triassic and evolution throughout the Mesozoic and Tertiary.

Thus, these two major stages in the history of this region are used to identify the two major sedimentary "megacycles" of the Paleozoic and the Mesozoic that are classically separated by an unconformity known as Hercynian. Structural highs persisted features that clearly shaped the area throughout the whole Paleozoic.

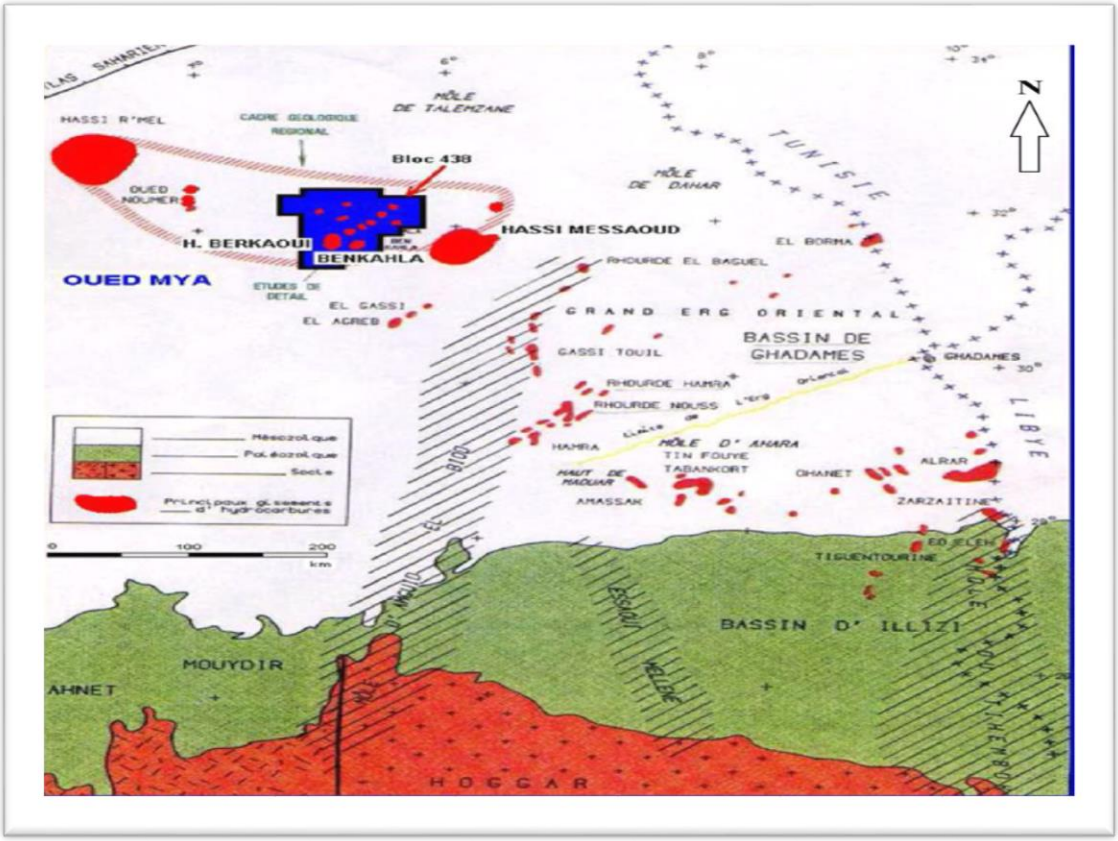

Figure 2 : geological location of the Oued M'ya basin. (SONATRAH/PRODUCTION1995).

1.1.C. **Stratigraphical**

The typical lithostratigraphic section of the Oued Mya basin is essentially by deposits that extend in age from Paleozoic to Cenozoic, with thicknesses reaching up to 5000m (fig.03).

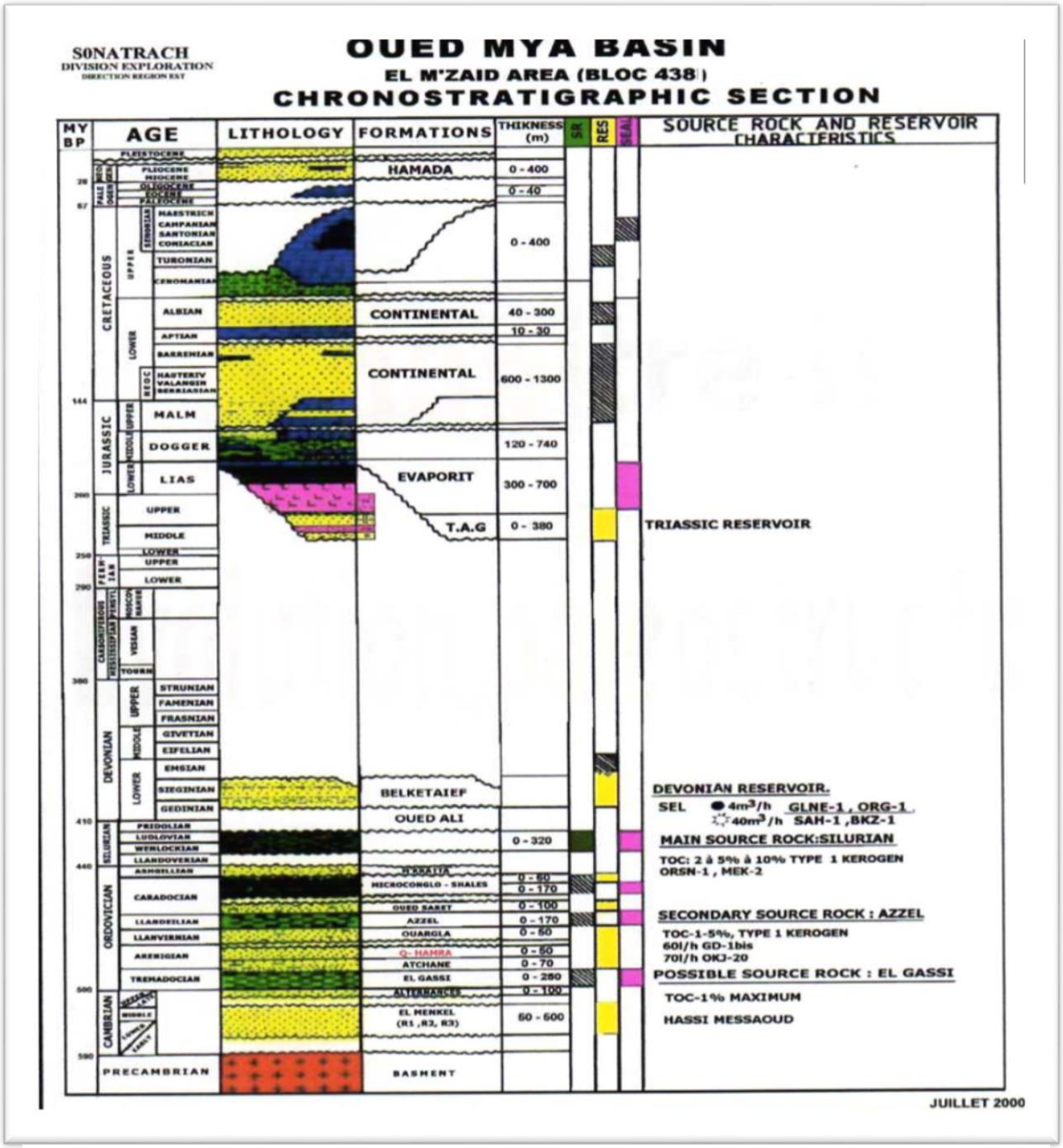

Figure 3: Typical lithostratigraphic section of the Wadi Mya basins.(SONATRACH 2000).

1.1.D. **Tectonic**

1. The Major Stages in the Structural Evolution of the Saharan Platform during the Paleozoic

The major states of structural evolution of the Saharan Platform would need to be reexamined throughout the Paleozoic due to difficulties occasioned by the sparse thickness, or the absence altogether, of certain sedimentary units on account of local unconformities or lack of deposition (Table 01).

1.A. The Pan-African Orogeny and the Origin of the Fracture Network in the North African Craton Dramatic vertical movements and volcanic eruptions, followed by uplift, characterized the final phase of the Pan-African orogeny and resulted in the erosion of previously accumulated sedimentary cover. One of its most prominent results was the fracture network which defines the North African craton today.

1.B. Cambro-Ordovician Extension and the Development of the Sedimentary Cover

The extensional phase resulted in stretching of the continental crust which is associated with tectonic subsidence that later on developed thermal subsidence. Major volcanic rocks were important in evidencing the strength of this event.

1.C. The Taconic Compression Phase (Caradoc)

The time period of Caradoc marks the beginning of a compression phase after the extensional stage and the general marine transgression during the Arenig–Llanvirn. Regional uplift and subsequent erosion characterized the last compressional phase. Simultaneously, climatic changes gave rise to the development of an ice cap over the Central Sahara, from the Caradoc to the Ashgill.

1.D. Melting of the Ice Sheet and Eustatic Rebounds

During the Late Ordovician, the meltdown of the ice sheet was responsible for the rearing of ocean levels.

1.E. The Caledonian Compression Phase

The thrusting phase of the Eburnean Orogeny marked the end of the Silurian.

1.F. The Lower Devonian Extension Phase

An Emsian marine transgression initiated with the distention of the extensional movement.

1.G. Tectonic Movements of the Middle to Upper Devonian

These movements are marked by the Frasnian unconformity, with a north-south orientation.

1.H. Hercynian Movements

Chronologically, this includes the tectonic movements of the Upper Devonian and the post-Famennian movements. According to the BEICIP-Sonatrach studies (1975), the Hercynian cycle is divided into two major phases:

- Early Hercynian Movements (Conrad, J., 1984):

  These likely represent the initial uplift events at the present location of the Ougarta Mountains.

- Major Hercynian Movements:

  This was a very significant tectonic phase in the geological history of the region.

Table 1: : main tectonic events affecting the Saharan platform.(A.Boujemaa, 1987).

PERIODE MAX D'ACTIVITE	DIRECTION DE LA CONTRAINTE	EFFET SUR LE SYSTEME DE FAILLES	EFFET SUR LA SEDIMENTATION
PANAFRICAINE	E-W	Tectonique cassante créant des failles et des fractures conjuguées NW-SE&NE-SW	Compartimentage du craton du Sahara central.
CAMBROORDOVICINNE	NW-SE	Mouvement normal le long des failles N-S.	Les variations de l'épaisseur sont contrôlées par des failles. Basculement NW de la plate-forme saharienne. Volcanisme.
TACONIQUE (Caradoc-Ashgilien)	E-W	Mouvement inverse le long des failles N-S résultant. Formation des structures N-S	Soulèvement des boucliers Reguibat et Touareg.
CALEDONIENNE (Siluro-Dévonien)	E-W	Mouvement inverse ou décrochant le long des failles NS	Erosion le long des zones hautes d'orientation N-S&E-W (Tihemboka, Ahara)
FRASNIEN	NW-SE	Mouvement normal le long des failles NE-SW.	Non-dépôt et érosion locale(mole d'Ahara). Volcanisme.
VISEEN (Hercynienne précoce)	*N40°*	Mouvement inverse ou décrochant le long des failles NS. Début de formation de la chaîne varisque.	Erosion de Tihemboka etsoulèvement de l'Ougarta.
CARBONIFERE SUP,A PERMIEN (Hercynienne principale)	N120°	Mouvement inverse oudécrochant le long des faillesNE-SW (résultant de laformation de la pangée).	Erosion sur les axes NE-SW.
RIFTING TRIAS-LIAS (dislocation de la pangée)	NW-SE	Réaction des failles NE-SW se terminant au TAGS et S4	Contrôle de la sédimentation par des failles entraînant une variation rapide d'épaisseur le long desfailles NE-SW
CRETACE INFERIEUR (Autrichienne)	E-W	Réaction des décrochements des failles N-S&NE-SW résultant du mouvement différentiel de la plaque européenne et de la plaque africaine	Erosion des sédiments du Crétacé sous l'Aptien (l'arche d'Al biod& Illizi), effet léger sur le bassin de Berkine.
EOCENE (pyrénéenne)	N-S&NW-SE	Début de chevauchement auNord résultant de laconvergence de la plaque Africaine avec la plaqueEuropéenne. Décrochement de la faille SudAtlas.	
MIOCENE	NW-SE&N-S	Episode de compression majeur dans le domaine atlasique.	Sédimentation prédominante de flyshs au Nord.
POSTVILLAFRANCHIEN	N-S	Basculement et inversion deblocs. Période finale de compression dans le domaine atlasique. Evénement majeur de collision.	Soulèvement du Hoggar. Basculement du bloc d'El Borma

1.1.E. Structural Evolution of the Oued Mya Basin

The main structural features of the basin trend mainly north-south and northeast-southwest (Figure 04) (SH and Sch, 2007).

E. 1. Cambrian:

This period experienced significant erosion that leveled earlier structures and reliefs (Boeuf et al., 1971). The central area of Oued Mya was located on the flank of a major depression, corresponding to the present-day high zone of Hassi Messaoud (Benamrane, 1993).

E. 2. Ordovician:

The Ordovician began with a marine transgression during the Arenig-Llanvirn stages, accompanied by regional uplifts such as in the Eglab area. These uplifts caused erosion that sometimes reached down to the basement rocks (Boeuf, 1971). Towards the end of this period, glaciation developed, forming an ice cap over what is now the Hoggar region.

Following the Caledonian phase, the central Oued Mya area began to rise but remained submerged.

E. 3. Silurian:

The final melting of this ice cap led to a rise in sea level, causing a widespread transgression that reached southern Sahara, where black shales with graptolites were deposited (Boudjemaa, 1987). At this time, the central Oued Mya area was completely covered by the sea (Benamrane et al., 1993).

E. 4. Devonian:

Following tectonic uplift during the Caledonian phase, the sea regressed during the Gedinnian stage, followed by another transgression. The start of the Hercynian orogeny and the gradual uplift of the Hassi Messaoud area caused sediment deposits to shift westward, where Devonian deposits are well developed.

E. 5. Late Carboniferous:

The collision between Gondwana and Laurasia intensified the uplift of the Tilghermt dome region and contributed to the structuring of the Djemaa Touggourt area. The Oued Mya region stood as a high submerged plateau, preventing Carboniferous deposits from forming there (Benamrane et al., 1991). The formation of Pangaea occurred toward the end of the Hercynian orogeny, accompanied by intense erosion that locally reached the basement rocks.

In Oued Mya, the Devonian represents the youngest Paleozoic formation. During the Permo-Triassic, the region remained continental until the end of the Triassic, which prevented the Permian sea from reaching the area.

E. 6. Triassic:

The Oued Mya area was characterized by a fluvial system following the Hercynian paleovalleys trending NE-SW. The main sediment sources were elevated zones at the time—Hassi R'mel, Hassi Messaoud, and the Allal arch.

At the end of the Triassic, evaporitic deposits were followed by carbonates on this submerged land, then by a marine transgression in the Late Jurassic.

E. 7. Cretaceous:

The Alpine orogeny left its mark, along with a widespread marine transgression followed by a regression during the Albian. Subsequent widespread transgressions in the Cenomanian and Turonian, combined with Alpine tectonic movements, shaped the basin’s current structure.

Today, the Oued Mya area is characterized by a fairly complex structural pattern inherited since the Paleozoic.

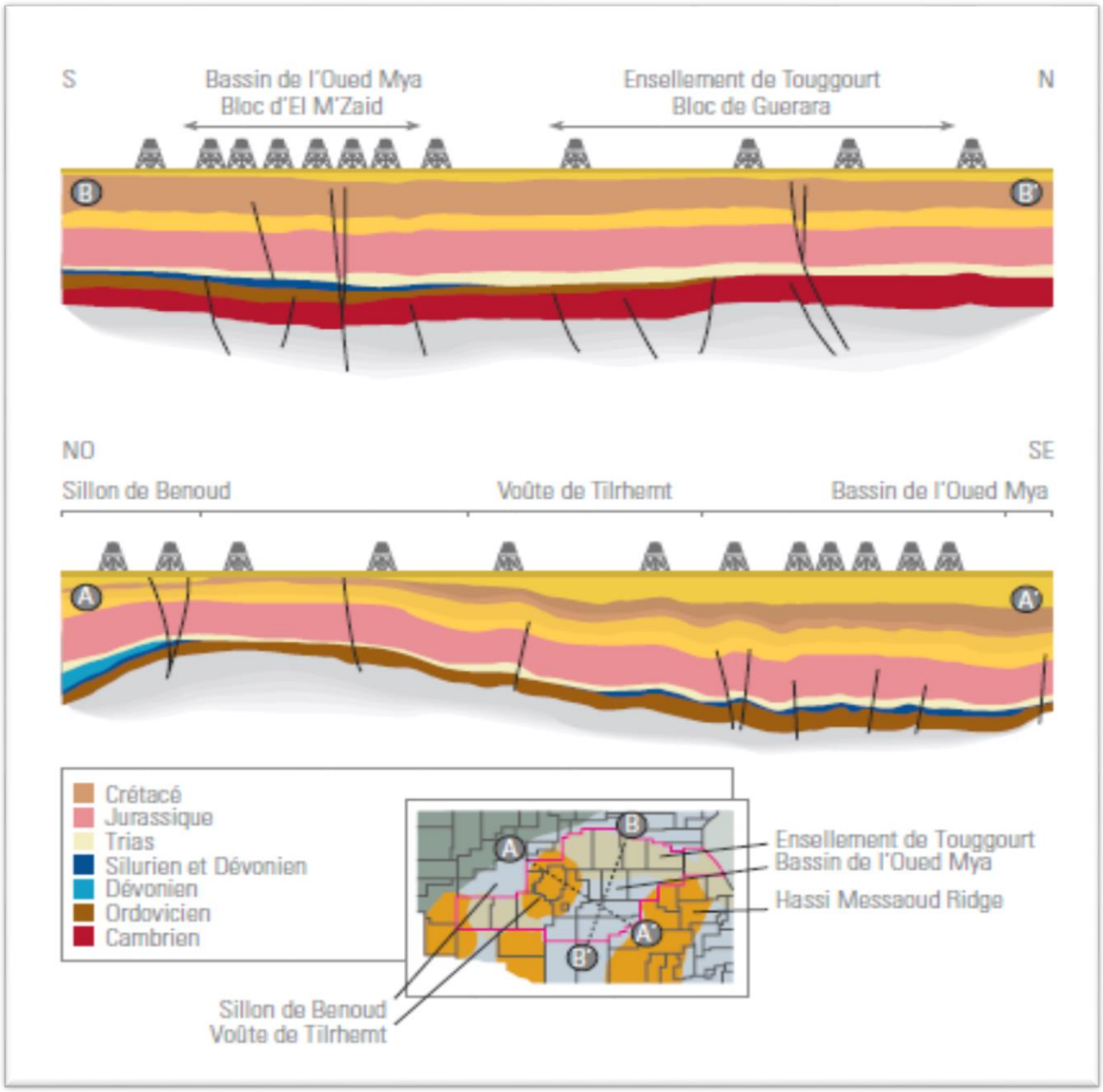

Figure 4: The N-S and Nw-Se Geological Cross-Sections in the Oued Mya Basin. (SONATRACH and SCHLUMBERGER, 2007).

1.1.F. Oil potential of the reservoirs of the Oued M'ya basin

In the Oued Mya basin, the petroleum system is fully represented in the Triassic, Ordovician, and Lower Devonian. Our study focuses on the Triassic reservoirs, mainly the lower series. The primary source rock for these reservoirs consists of the radioactive clays of the Silurian. The Ordovician clays (El Gssi clays and Azzel clays) are secondary rocks.

The regional cap rocks is provided by the thick evaporitic series of the S4 salt layer and the S3 and S1 levels of the Liassic. The clays intercalated between the Triassic reservoirs may from local cap rocks. Volcanic rocks, when sufficiently thick and not fractured, from a good local cap for the reservoir in the lower series.

The trapping is structural in type, purely stratigraphic (wedge of the lower series reservoirs and T1) or mixed (as in the case of the Benkahla structure).

F.1. Sourse Rocks

The importance of the Lower Paleozoic series is related to the presence of source rocks in the basin, the richest of which is made up of the radioactive clays of the Silurian. In connection with the sedimentary condensation of the entire Silurian in this basin, these clays exhibit excellent geochemical characteristic. Their shallow burial during the Paleozoic preserved their petroleum potential with their maturation and the generation of hydrocarbons occurring later during their subsequent evolution under the effect of Mesozoic subsidence.

The Silurian source rock is absent on the Hassi Messaoud and Talemzane domes. In the Oued Mya depression, the Silurian source rock currently has a maturation level favourable for oil generation. Its maturation degree is higher (gas zone) to the west of Haai R'mel and north of the Talemzane dome, where its burial increases towards the southern Atlas trough.

The current configuration of the basin and the extension of the Silurian source rock have been extremely favourable for suppling the overlying reservoirs(Triassic and locally Lower Devonian) in the Oued Mya depression.

To the west; the Hassi R'mel field, located in immediate proximity to the Silurian wedge, has been able to be supplied due to its highly favourable structural configuration.

F.2. Reservoirs Rocks

With the exception of a few reservoir levels located in the Lower Devonian at the heart of the Oued Mya trough, the Paleozoic reservoirs are limited to the Cambro-Ordovician sandstone.

These reservoirs generally have poor characteristics, especially in the M'Kratta slab and the Hamra Quartzites. The extension of the latter is limited to the eastern part of the basin, where is thickness is much thinner than on the western edge of the Berkine Basin.

The most significant reservoirs are those of the Cambrian is covered by the clayey-sandy series of the Ordovician, it is generally very deep and unfavourably positioned in relation to the source rocks. On the Talemzane dome, where it is partially eroded the Triassic sandstones, it is not covered. In contrast, on the El- Agreb-Hassi Messaoud dome, the Cambrian is covered by the clayey facies of the Trias, as good reservoir levels were not deposited in this sector.

In the Oued Mya depression, the Triassic reservoirs are similar, but the distribution and quality of these reservoirs vary significantly,. They can be distinguished as fallows :

F.2.1. Lower series

It rests on the Paleozoic substrate, with the best facies located in the Oued Mya depression, likely linked to the paleo-dome of Benkahla, Guellala, Houad Berkaoui, and much of block 438. This formation is considered the equivalent of the Lower Triassic clayey-sandy (TAG) series of the Berkine Bsin.

F.2.2. Unit T1

Very interesting reservoirs are developed in the western part of the basin. In contrast, in the Oued Mya trough, the reservoir levels of this unit are significantly reduced (Reservoir T1) above a very developed volcanic series in this sector, related to the extensional structures of the major structural trends. This units is the equivalent of the Triassic carbonates of the Berkine Basin and the Intermediate Triassic reservoirs in the Rhourde Nouss region.

F.2.3. Unit T2

Particularly important in the Hassi R'mel field, is developed in this unit, though it is rapidly degraded elsewhere, particularly by generalized salt cementation in block 438. This unit is the equivalent of the Upper Triassic clayey-sandy (TAGS) series, which reaches its maximum development in the Rhourde Nouss region.

F.3. Cap Rocks

The evaporitic series deposited at the end of the Triassic across the Benkahla field forms an excellent regional cap rock throughout the entire Triassic basin. This cap rock is composed of salts and anhydrites, with thickness exceeding one thousand meters.

In addition to this regional cap rock, there is a local cap specific to this reservoir :the volcanic rocks of the Triassic, which are well-developed and come from substantial lava flows. These volcanic rocks play an important role in ensuring good seal integrity between the Lower series and T2.

The reservoir of the Lower series is a lithostratigraphic wedge trap, limited to the west by a regional fault, which acts as a barrier, with a wedge-shaped seal to the south.

F.4. Megration

The hydrocarbons generated, especially in the northeast part of the Oued Mya basin, which is the most subsided, migrated toward the higher areas where trapping occurred. Migration took place from the west toward Hassi Messaoud and from the north toward the south, in the directions of Houad Berkaoui, Benkahla, Guelalla, and even Hassi Messaoud

The timing between the deposition of the salt cap at the end of the Triassic, early Jurassic, and the beginning of hydrocarbon generation in the Middle Cretaceous implies that all the hydrocarbons generated were accumulated and trapped within the same basin, in the absence of any leakage

F.**5. Traps**

Any geological anomaly, whether its origin is tectonic (anticlinal fold, flexure, fault), stratigraphic (wedge, reef), or lithological (loss of permeability), that gives the roof of the reservoir (the zone where porosity and permeability disappear) a concave shape, is likely to from a trap. This means the reservoir is sealed .generally , three types of traps are distinguished:

F.5.1. Structural traps

Their formation primarily involves tectonic factors. The main type include:

Trap formed by an anticline.

Trap formed by a fault or more often by a fault system folds (against faults).

Trap that encompass both of the previous structures.

F.5.2. Stratigraphic traps

These involve the combination of two different environments, corresponding to the transition from a permeable medium to an impermeable one. These are traps that allow hydrocarbons to accumulate in the absence of tectonic deformation. These traps are due to lithological

phenomena (loss of permeability), sedimentary phenomena (original wedges, lenses), and paleo-geographical phenomena (erosional wedges).

F.5.3. Mixed traps

These are a combination of both stratigraphic and structural factors.

1.1.J. Assessment of Block 438

It corresponds to the western part of the Algerian Triassic Basin and is the most explored region in the basin. This area is situated between the two Hassi R'Mel deposits to the north-west and Hassi Messaoud to the south-east.

The block stretches approximately 400 km in longitude and 300 km in latitude; the area covers some 120,000 km2. The Paleozoic and Triassic objectives are located at an appreciable depth of between 3,400 m to 4,000 m.

Within the Triassic, the primary target is the Lower Series, while the T1 reservoir is a secondary target over a large part of the block.

Lower Devonian targets are only present along the axis of the Oued M'ya trench; Ordovician targets are virtually marginal and of little interest.

From a structural point of view, except for the Haoud-Berkaoui structure, which possesses a vertical closure of the order of 300 m, the area is generally poorly structured. Further complication arises from the presence of thick evaporitic series within the Mesozoic overburden, which obscures the definition of structural traps by seismic methods. Substantial impacts on the definition of these low-amplitude closures are due to dramatic changes of velocities linked to the complexity in the distribution of the saliferous Senonian.

The structures that have been identified are organized along fault-related trends, oriented mainly in the north-south and northeast/southwest directions, with the most significant corresponding to the axis of the Oued M'ya trench (Haoud-Berkaoui/Guellala/Boukhezna-Sahane trend).

These trends were intersected by transverse east-west trends that acted during the late stage as detachments.

In the lower series are situated the three deposits of Haoud-Berkaoui, Guellala, and Ben Kahla.

The other accumulations developed in the block in a multitude of peripheral fields which are, in the order of importance: N'Goussa, Guellalanord est, Draa Tamra, and Mokh El Kebechs.

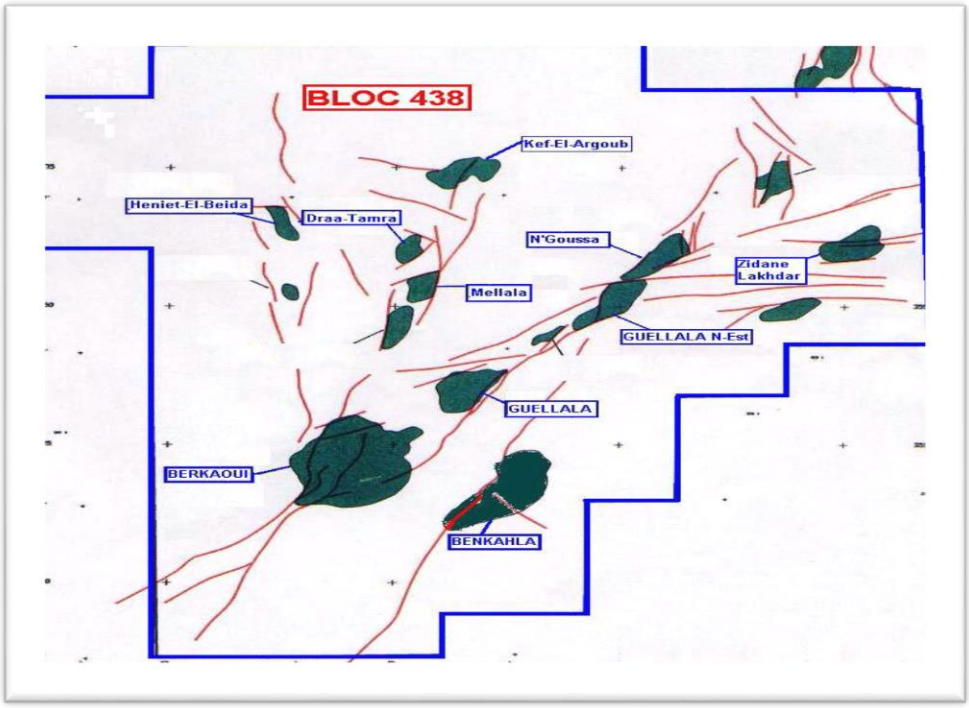

Figure 5: Map of the main accumulations on block 438BEICIP(BEICIP,1992).

1.2. Presntation of the Benkahla field

1.2.A. Geographical location of the Benkahla deposit

The Benkahla field is in the region earlier called Gara krima, about 80 km west of Hassi Messaoud, approximately 20 km south of the Guellala field and the same distance east of Haoud-Berkaoui. It covers an area of 83.5 km2 (Figure 06).The Benkahla zone is located in Ouargla wilaya between these two regions: Hassi Messaoud and HassiR'Mel, some 600 km from Algiers.

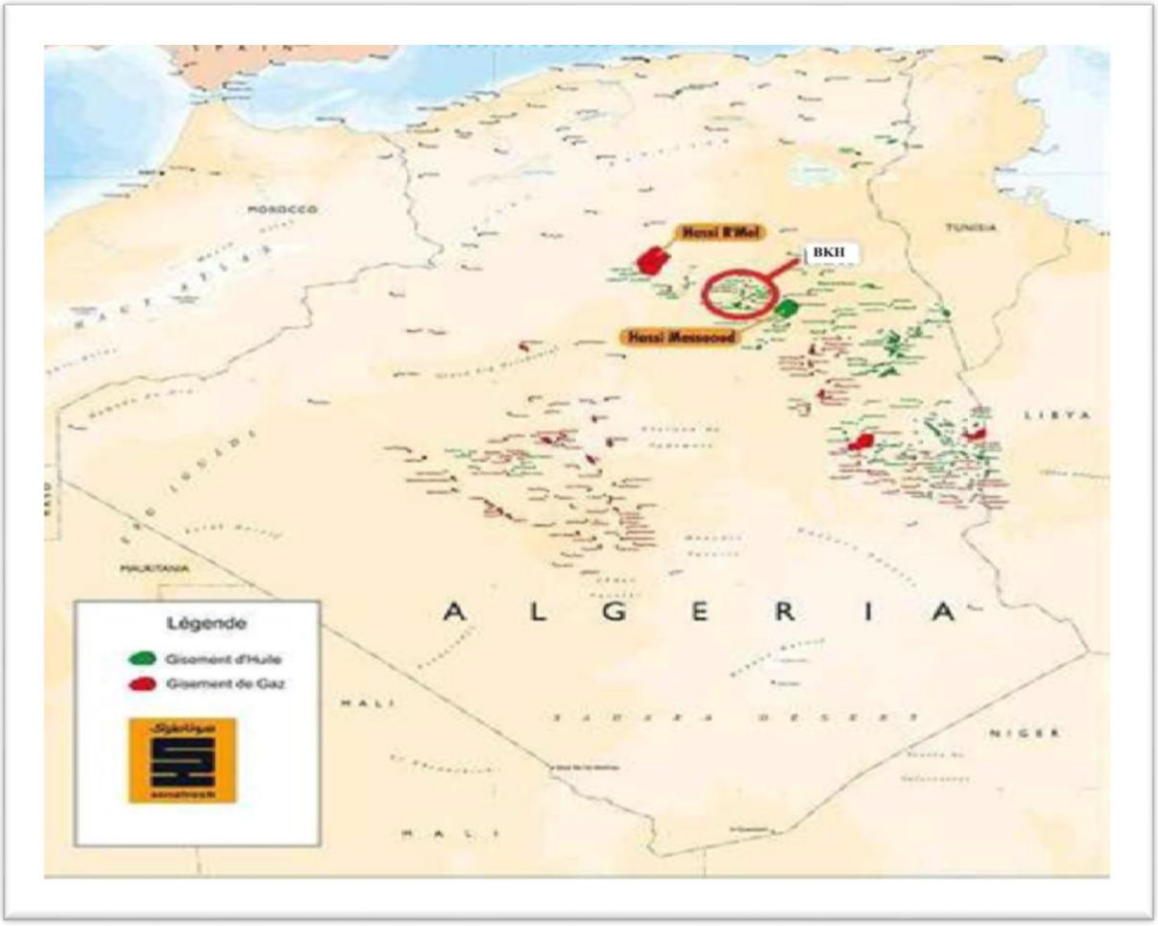

Figure 6: Geographical location of Benkahla.(SONATRACH/ EXPLOTATION,1995).

1.2.B. Geological location of Benkahla deposit

The Benkahla deposit is found in the Oued M'ya depression, centered in the Triassic province, wherein it is bordered on the west by the HassiR'Mel field, on the northwest by the Berkaoui deposit, on the northeast by the Galalla deposit, on the east of Hassi Messaoud field, and southward by the El-Gassi deposit.

1.2.C. History of the study region

The Haoud-Berkaoui area office is situated in the commune of Rouissat at a distance of 25 km from the capital city of the wilaya of Ouargla. The region used to be administered by Hassi Messaoud until 1977 when it became independent.

Geophysical research done in the area of Ouargla has discovered two (02) formations, namely Haoud-Berkaouiet Benkahla, both forming a small working surface of 1600 km².

The first well drilled in the Ouargla area was OA01 in 1963. In March 1965 the first drill hole OK101 was put down right at the crest of the Haoud-Berkaoui structure, putting on to light a discovery of light oil of density 43 °API (d = 0.8) in the lower Triassic clay-sandstone series (TAG), carried out by the Compagnie française de pétrole algérien (CFPA). At 3327.8 m, this bore hole pierced the Gothlandian (the first Paleozoic horizon met under the Hercynian unconformity). Following this borehole and seismic interpretations, a second OKP24 well was drilled on: 31/08/1966 in the Benkahla structure; here, also, oil was present in the T.A.G. Another well, OKS55, was also drilled to evaluate this new structure.

The production test conducted by CFPA yielded a flow rate of 11 m3/h at a reservoir pressure of 520 kg/cm2 and a GOR of 101 m3/m3. This successful test was promising, and persuaded producers to install other wells in the vicinity of the structure, which in turn led to another new peripheral deposit discovery.

At present, a total of thirty-eight wells are operating across the different fields, comprising twenty-seven producer wells and eight water injection wells for pressure maintenance. The remaining three wells are dry.

All recovered oil and gas are transmitted to the different production centers in the region. The main tasks in the region are :

* Oil and condensate production.

* Associated gas production (sales gas and lift gas).

* Water injection.

1.2.D. Benkahla stratigraphical column

In stratigraphy, the peculiarity of the Triassic province is that the Mesozoic is in Hercynian unconformity upon the Paleozoic, allowing us to point out that the Benkahla area has three complete, eroded sub-systems:

- Devonian.

- Carboniferous.

- Permian.

The stratigraphy starting with the Paleozoic is as follows:

1. Paleozoic

The stratigraphic data obtained from 32 boreholes at the deposit in this period are Silurian.

1.A. The Silurian

This stratigraphic unit, formerly known as the Gothlandian, was greatly affected by the Hercynian unconformity. It is composed of black, flaky, carbonaceous clays, sometimes carbonate-bearing, becoming highly fossiliferous at the top, with sandstone intercalations sometimes a few meters thick.

2. The Mesozoic

The Mesozoic is well developed in the Triassic province.

2.A. The Triassic

The Triassic is composed of a sandy-clay series of continental origin resting unconformably on the various terms of the Paleozoic, and terminating in a sandy-clay series of lagoon-marine origin, which provides excellent cover for the Triassic sandstone deposits, and is composed from bottom to top :

1. The Lower Series

This is the main reservoir in the Haoud-Berkaoui and Guellala fields, but the only reservoir at Benkahla (Sonatrach/ EP).

This geological series of clays and sandstones is unconformable with the Silurian (Hercynian unconformity), and is also overlain by andesitic outcrops. Its average thickness is around 40 {

50 m, consisting of a succession of coarse sandstones, fine { medium sandstones, very fine sandstones and frequently dolomitic clay (J.Thouvenienjan 1968).

These different constituents are generally arranged in sedimentary sequences, from the coarsest at the base to the finest at the top.

These clays are sometimes green at the top, sometimes grey. The intercalations of the clay joints are gray-green, on the order of centimeters, and finely laminated.

Less flattened pebbles are sometimes encountered, the probable cause being a sequential cessation of mud deposition. Towards the base, brown-red clays, sometimes brecciated sandstone and soft pebbles are deposited, with frequent pink dolomite concretions.

2. The Eruptive Series (Andesitic Series)

This is a series of volcanic outpourings within the lower series or towards the end of its sedimentation, ranging in thickness from 0 to 70 m at Haoud-Berkaoui, averaging 130 to 140 m at Guellala, and 0 to 80 m at Benkahla.

This series is sometimes intercalated with dolomitic or silty red clays (OKP12, OKP22 and OKP24).

Its thickness increases from south to north of Benkahla. The presence of intra-andesite sandstone intercalations, containing a pressure higher than that of the reservoir, seems to show that the eruptive forms the cover of the Benkaha deposit. A test carried out at the top of an intra-andesite detrital level at OKP22, recovered salt water at 320g/l. Virgin pressure was 477Kg/cm2, while in the lower series it was 210Kg/cm2.

Above the Andesite and in the southern part of Benkahla, a past of kinerite clay is encountered, varying in thickness from 1 to 6 m. However, some boreholes have not encountered the Andesite Series. According to J-Thouveninjan 1968, kinerite clays are the only manifestation of volcanism (PL2). These kinerite clays form a ferruginous armour (Paleosol).

3. Sandstone Triassic T1

This formation is a sandstone-clay sequence, varying between 20 and 30 m in thickness. At the top, there is a dolomitic and brecciated clay bank about 10 m high. The T1 level was deposited throughout the Haoud-Berkaoui and Guellala region, except at Benkahla, where it is very thinly deposited.

The presence of this weak deposit south of Benkahla leads us to believe that these deposits were interrupted by a volcanic phenomenon, or that the structure was much higher at the time of sedimentation. The T1 can be subdivided into two sub-layers:

- A clayey-dolomitic sublayer at the top, with a thickness of around 8m .

- A 12m-thick sandstone sub-layer.

4. Triassic sandstone T2

At the top is a reddish-brown silty-clay sub-layer, some ten meters thick. It is dolomitic with salt- and anhydrite-filled fissures. A sandstone underlayer lies at the base (medium to fine-grained, 8 to 10 m).

2.B. The Jurassic

It is made up of evaporitic (lagoon-marine) deposits, with a thickness of about 850m, and is subdivided as follows:

a. The Lias

Its thickness is around 340m-350m, subdivided into two lithological zones:

-At the base: massive salt (80m);

-At the top: massive anhydrite (260-270m).

The Jurassic wall is taken from the base of the marly bed, known as the “B” horizon, which forms a regional diagonal marker.

b. The Dogger

It is subdivided into two series:

b.1. The Dogger lagoon

120 m thick, composed of alternating grey-green and brown-red clays, grey marl and anhydrite.

B.2. The clayey Dogger

This series is composed of plastic clays and indurated clays, grey marls (sometimes dolomitic) and intercalations of fine sandstones.

c. The Malm

This 234 m-thick clay-sandstone-limestone complex is composed of alternating plastic clay, often silty, clay-dolomitic limestone and gray marl, with sandstone intercalations.

2.C. The Cretaceous

2.C.1. The Neocomian

The Neocomian is composed of brown red clays and gray marls, often dolomitic with intercalations of fine sandstone and dolomitic limestone, 181m thick.

2.C.2. Barremian

Composed of fine to very coarse sand and fine beige to reddish-brown sandstone, with occasional intercalations of reddish-brown silty clay and clayey limestone, 372m thick.

2.C.3. Aptian

A carbonate, dolomitic microcrystalline series, about 20 to 30m thick.

2.C.4. Albian

This is a series of sandstones and clays with some dolomitic intercalations, and alternating marl and clay at the top of the layer. It is around 460 m thick.

2.C.5. The Cenomanian

161m thick, with alternating white anhydrite, limestone, dolomitic marl and grey clay at the top, and grey dolomitic clay and marl at the base, with dolomitic limestone, grey-green and brown-red clay.

2.C.6. Turonian

A series of marine deposits 70 m thick, carbonated with beige to white chalky limestone, with clayey and dolomitic limestone at the top.

2.C.7. Le Sénonien

Il est subdivisé en :

a. Le Sénonien salifère

Il est formé de sel massif translucide avec des intercalations d'anhydrite cristalline dure, d'argile grise tendre, légèrement dolomitique et salifère, et à la base, il constitué d'anhydrite massive de 220 m d'épaisseur.

b. Anhydritic Senonian

It consists of alternating microcrystalline white anhydrite, sometimes crystalline, grey dolomite, beige limestone and brown-red dolomitic clay, 250m thick.

c. Carbonate Senonian

Affected by erosion and marked by the Alpine unconformity at the summit, this is a carbonate series of white fossiliferous limestone, often dolomitic and vacuolated, with marl layers 225 m thick.

3. The Cenozoic

Only the Miopliocene represents the Cenozoic terranes in the region, resting unconformably on the Mesozoic; its thickness varies from 30 to 70 m. It is made up of fine, coarse, sub-angular to rounded yellow sand, with layers of fine to medium-grained, friable sandstone with carbonate cement and soft white limestone, sometimes dolomitic sandstone.

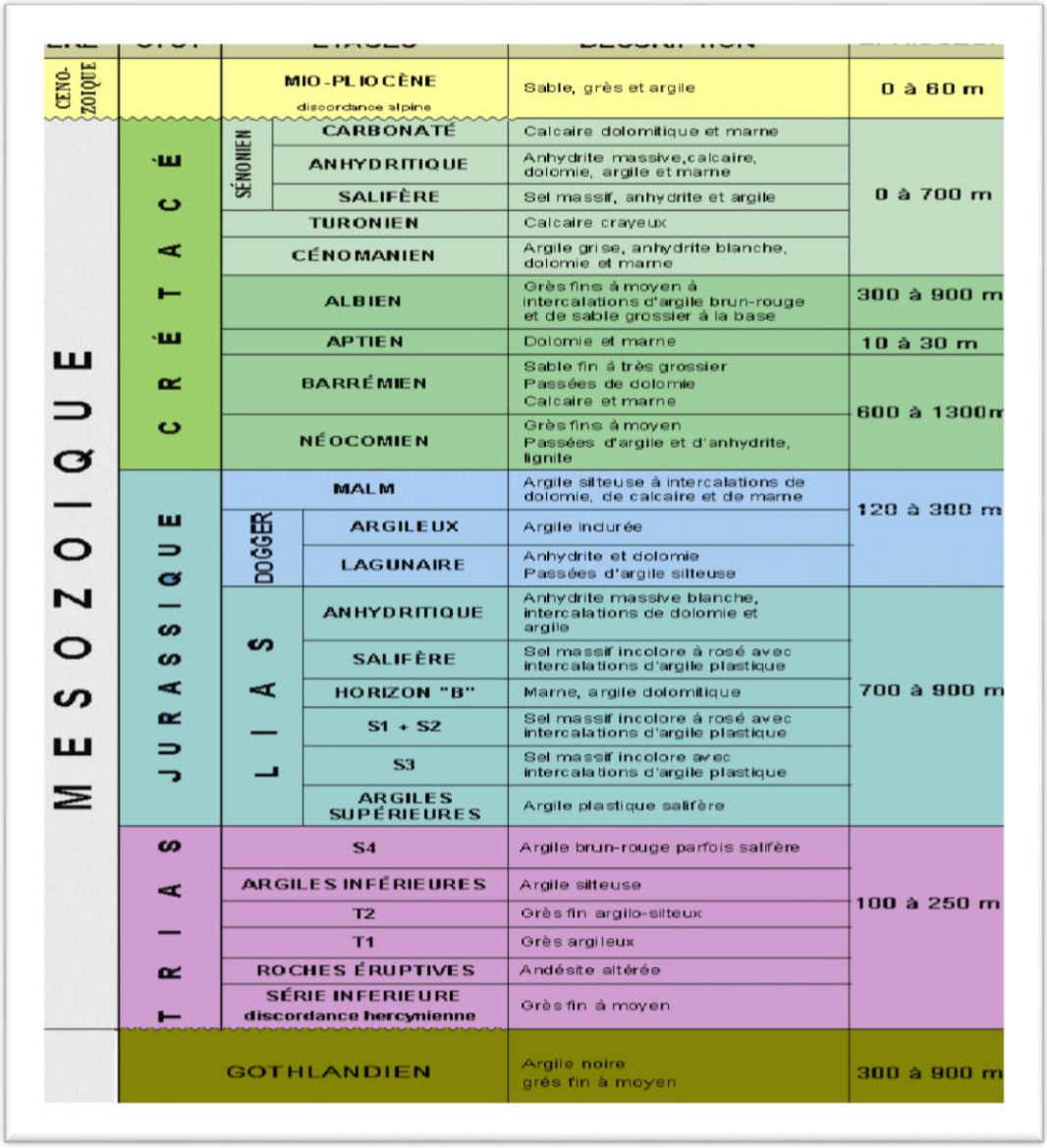

Figure 7: Typical Benkahla stratigraphic column.(Document Division Production/ SONATRACH 2007).

1.2.E. Structure of the Benkahla deposit

1. Source rocks

The importance of the lower Paleozoic series is linked to the presence of the basin's source rocks, the richest of which are the Silurian radioactive clays . Linked to the sedimentary condensation of the entire Silurian in this basin, these clays have excellent geochemical characteristics. Their shallow burial during the Paleozoic preserved their petroleum potential, as their maturation and hydrocarbon genesis took place during their subsequent evolution under the influence of Mesozoic subsidence. Silurian bedrock is absent from the Hassi Messaoud and Talemzane moles.

In the Oued M'ya depression, the Silurian bedrock currently shows a degree of maturation favorable to oil generation. Its degree of maturation is higher (gas zone) to the west of HassiR'Mel and to the north of the Talemzane mole, where its burial increases towards the South Atlasic trench.

The current configuration of the basin and the extension of the Silurian bedrock have been extremely favourable for feeding the overlying reservoirs (Triassic and locally Lower Devonian) in the Oued M'ya depression.

In the west, the HassiR'Mel reservoir, in the immediate vicinity of the Silurian wedge, was able to be fed, given its highly favorable structural configuration .

2. Reservoir rocks

With the exception of a few reservoir levels located in the Lower Devonian at the heart of the Oued M'ya furrow, Paleozoic reservoirs are limited to Cambro-Ordovician sandstones. These reservoirs are generally of poor quality, especially in the M'Kratta slab and the Hamra Quartzites. The extension of the latter is limited to the eastern part of the basin, where its thickness is much lower than on the western edge of the Berkine basin.

The most important reservoirs are those of the Cambrian age, present throughout the basin. However, in areas where the Cambrian is covered by the Ordovician clay-sandstone series, it is generally very deep and in an unfavorable position relative to the source rocks. On the Talemzane mole, where it is partially eroded beneath Triassic sandstones, it is not covered.

On the other hand, on the El Agreb-Hassi Messaoud mole, Cambrian cover can be provided by Triassic clay facies, as the good reservoir levels were not deposited in this sector.

In the Oued M'ya depression, the Triassic reservoirs are similar, but in which the distribution of reservoirs and their quality vary markedly :

a. The lower series

This is underlain by Paleozoic bedrock, the best facies of which are located in the Oued M'ya depression, probably in connection with the Hassi Messaoud paleo-mole. This series is the main reservoir for the Benkahla, Guellala and Haoud-Berkaoui deposits, as well as for a large part of Block 438. This formation is considered equivalent to the Lower Clay-Sandstone Triassic (TAG) of the Berkine Basin.

b. Unit T1

In which very interesting reservoirs are developed in the western part of the basin (reservoirs B and C). In contrast, in the Oued M'ya furrow, the reservoir levels of this unit are greatly reduced (T1 reservoir) above a highly developed eruptive series in this sector, in relation to the distensional plays of the major structural trends. This unit is equivalent to the carbonate Triassic of the Berkine Basin and the Intermediate Triassic reservoirs of the Rhourde-Nouss region.

c. T2 unit

In which the "A" reservoir is developed, particularly important in the HassiR'Mel deposit, and rapidly degraded elsewhere, in particular by widespread saliferous cementation at Block 438.

This unit is equivalent to the Upper Clay-Sandstone Triassic (TAGS), which is at its most developed in the Rhourde-Nouss region.

3. Cover rocks

The evaporitic series deposited at the end of the Triassic across the Benkahla field constitutes an excellent regional cover over the entire Triassic basin. This cover consists of salts and anhydrites with thicknesses exceeding a thousand meters.

In addition to this regional cover, there is a local cover specific to this reservoir: the Triassic eruptive rocks, which are well developed, originating from fairly considerable lava flows, play an important role in ensuring a good seal between the lower series and the T2 .

The reservoir of the lower series is a litho-stratigraphic wedge-shaped trap bounded to the west by a regional fault that forms a screen and wedge to the south.

4. Migration

The hydrocarbons generated, especially in the most subsided northeastern part of the Oued M'ya basin, migrated towards the high zones where the trapping took place. Migration took place from the west towards Hassi Messaoud, and from the north towards the south in the directions of Haoud-Berkaoui, Benkahla, Guellala and even Hassi Messaoud.

The timing between the establishment of the saliferous cover at the end of the Triassic, beginning of the Jurassic, and the start of hydrocarbon generation in the Middle Cretaceous, implies that all the hydrocarbons generated are accumulated and trapped in this same basin in the absence of leakage. (Document Division Production/ SONATRACH).

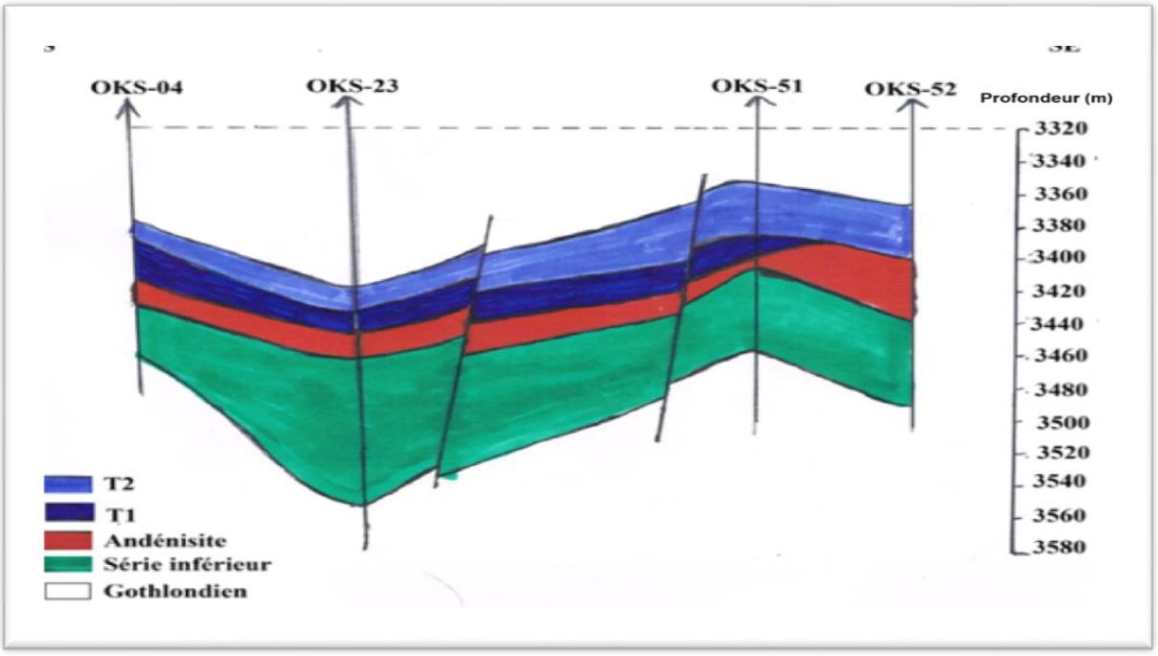

(Echelle : H : 1/ 500 00, V : 1/ 2000 m)

Figure 8:The S-SE geological section.

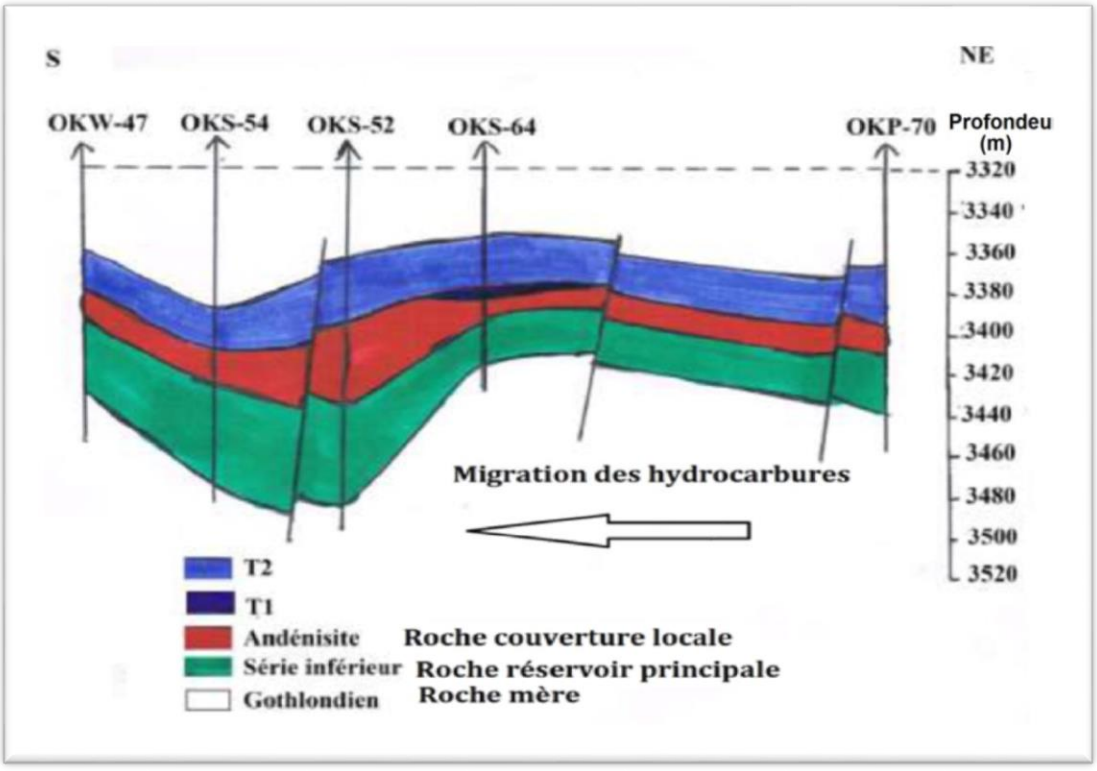

(Echelle : H : 1/ 500 00, V : 1/ 2000m)

Figure 9: S-NE geological section.

Exploration efforts in the Oued M'ya basin have gained momentum over the last five years, culminating in several oil discoveries. Particular interest has been focused on the possible extension of the Triassic deposits, notably Berkaoui and Benkahla, and on the development of the open fracture network in the deep objectives (Hamra quartzites: Ordovician). Several recent discoveries have been made in the basin:

An oil deposit, Benkahla est, was discovered in the lower series reservoir (Triassic) to the east of the Benkahla deposit

An oil discovery in the Ordovician Hamra quartzite reservoir in the Berkaoui area .

An oil discovery in the Triassic T1 reservoirs and lower series west of the Berkaoui deposit.

Two oil discoveries, between the Berkaoui and Benkahla deposits and north of Berkaoui, in the Lower Series reservoir (BKRE-1 well, 2005), and the Hamra quartzite reservoir.

Modelling and geochemical balances in the Oued M'ya basin show that a very large volume of hydrocarbons (around 3 { 4 times the total discovered to date) remains to be discovered in different types of traps (structural, mixed, stratigraphic, reservoir extension and deep targets).

Chapter 2: METHOD OF WORK

CHAPITRE 2

METHOD OF WORK

1. Introduction

It is developing a 3D geological model for the reservoir in the Benkahala field to evaluate key parameters including porosity, permeability, net pay thickness, and oil-water contact. The dataset collected during an internship at Sonatrach forms the basis of interpreting reservoir quality and fluid content via well logging geophysical techniques. Log measurements are used in the determination of porosity and permeability for better understanding the reservoir's properties. A geostatistical analysis on the processed data follows to produce iso-probability maps identifying zones with the highest potential for drilling and production. Such maps become vital for well placement and field development strategies optimization. This study, in general, highlights the role geostatistics plays in reservoir characterization with well-integrated decision-making in the oil and gas field.

1.1. Determining general and fundamental parameters

General and fundamental parameters are those that apply to a study as a whole or to a series of levels making up an interval:

A. Determination of Resistivities

A precise knowledge of Rw is essential for correctly determining the water saturation of a reservoir.

There are three main methods for determining Rw :

- From production tests.
- From regional data or databases.
- From delayed logs.

If we take the method of delayed logs:

1) **From PS** (Spontaneous Potential): The ratio Rw/Rmf is one of the factors controlling the development of the SP curve. This phenomenon allows the calculation of Rw from the SP.
2) **From the Resistivity Ratio**: This method is independent of porosity. The following equations can be written:

✧ In the virgin zone : $Rt = F \bullet \frac{Rw}{Sw}$

✧ In the invaded zone : $Rx0 = \frac{Rmf}{Sx0^2} \Rightarrow \frac{Rx0}{Rt} = \frac{Rmf}{Rw}\left(\frac{Sw}{Sx0}\right)^2$

✧ In a aquifer we have : $Sw = Sx0 = 100\%$ we can solve for Rw :

$$\frac{Rx0}{Rt} = \frac{Rmf}{Rw} = \max \Rightarrow RW = \left(\frac{Rt}{Rx0}\right)Rmf$$

$$Rw = \frac{Rdeep}{Rmsfl} \bullet Rmf$$

B. Determination of the parameters a, m, n

It was Archie (1942) who first proposed an empirical relationship linking the formation factor, derived from resistivity, to porosity and saturation, expressed by the well-known equation:

$$Sw = \left(\frac{F \bullet Rw}{Rt}\right)1/2 \qquad \text{with } F = a/\phi \wedge m$$

For Archie, a = 1, and m varies dependi$_n$g on the size and distribution of grains, and also on the complexity of the pore channels connecting the pores.

Following the work of the Humble Oil Company, it is generally accepted that a = 0.62 and m = 2.15 in unconsolidated sands.

In consolidated sands, the commonly used values are a = 0.81 and m = 2.

In carbonates with medium to good porosity, the typical values are a = 1 and m = 2.

Other researchers have proposed linking the values of a and m to the nature and age of the reservoir (clayey sands, calcareous sands, etc.) using the following equation:

$$m = 1.87 + 0.019/\phi$$

The saturation exponent n varies betwee$_n$ 1.8 and 2.5, but is commonly taken as 2.

C. Determination of Porosity and Lithology

The determination of porosity cannot be separated from that of lithology, as these two parameters are very closely related.

The apparent porosity of a clean formation can be obtained from:

- Sonic log: Φs
- Density log: Φd
- Neutron log: Φn

The neutron log is more influenced by clay or hydrocarbons than the density log.

In the most common clean reservoirs (such as sandstone, limestone, dolomite, and anhydrite), the easiest and most practical method is to overlay the density and neutron curves. This is even easier when both logs are recorded on the same (limestone) scale. To do this, the neutron log is directly calibrated in limestone porosity, and we get:

$$\Phi\,\mathbf{T} = \Phi\,\mathbf{1} + \Phi\,\mathbf{2}$$

Φ **T**: Total porosity, from (neutron and density)

Φ **1** :Intergranular and intercrystalline porosity

Φ **2:** Secondary porosity interfissure, interfracture

It is important to note that lithology determination from well logs is only possible if there are at least two measurements (typically porosity and resistivity) for a simple lithology, or three measurements (including two porosity measurements) for more complex lithologies.

1. **Single-mineral reservoirs**: These correspond to pure sandstones or limestones. In this case, a crossplot of Rhob or Δt vs $1/\sqrt{Rt}$ may be sufficient to determine the lithological nature using the matrix values ρma or Δtma.
2. **Two-mineral reservoirs**: These include clayey sandstones, limestones, dolomites, or sandstones with calcareous cement.

allow determination of the nature of the two minerals present (ρb , Φn), (Φn , Δt), (ρb , Δt) .

D. Determination of Clay Parameters

Within a given interval corresponding to the same depositional environment, it is reasonable to assume that the nature of the clay does not vary significantly.

In this case, for an interpretation in terms of sand–silt–clay, the clay parameters for that interval are determined:

(ρsh, Δtsh, GRsh, Pesh, Nsh), which are necessary for quantitative interpretation.

E. Determination of Saturation

of the hole and a high-resistivity one further down. So a simple comparison of resistivities read by one deep resistivity tool with another shallow one can detect hydrocarbons.According to Archie's formula:

$Sw = \sqrt{F \bullet \frac{Rw}{Rt}}$ .....porosity-resistivity combination.

$Sw = \left[\left(\frac{Rx0}{Rt} \right) \left(\frac{Rt}{Rmf} \right) \right]^{\frac{5}{8}}$ .....resistivity ratio method with (Rw constant, $Vsh \langle 5\%$, $Sx0 = Sw^{1/5}$).

And according to Simandoux's formula:

$$Sw = \left[\left(\frac{1}{Rt} - \frac{Vsh}{Rtsh} \right) \left(F \bullet \frac{Rw}{1 - Vsh} \right) \right]^{\frac{1}{2}}$$

F. Determining the nature of the hydrocarbons

Once the hydrocarbon zones have been delimited, it is important to determine the nature of the hydrocarbon.

Several methods can be used:

1) comparison of porosity curves :

In gas tanks. The porosity deduced from density measurements is significantly higher than that deduced from neutron measurements, since gas is lighter and has a lower hydrogen concentration than water.

2) Graphical plotting method:

By plotting the density ρb as a function of Φn or, better still, Pe as a function of ρb or (ρma) as a function of Uma , the effect of the gas is manifested by a shift in the points corresponding to a decrease in density and Φn .

G. Determining hydrocarbon mobility

This is assessed by comparing the two saturations Sw and Sx0. The greater the difference, the higher the mobility, although it should be remembered that sometimes hydrocarbons return very easily to the hole wall (in the case of gas) and therefore have high mobility, whereas Sx0 may be closer to Sw .

H. Fracture detection

This is carried out by determining secondary porosity, as follows:

$$\Phi t = \Phi 1 + \Phi 2$$

$\Phi 1$:Primary porosity (intercrystalline, intergranular).

$\Phi 2$:Secondary porosity (interfracture, interfissure).

1.2. Corrections to raw data

In addition to the signal coming from the formation, there are signals due to the borehole and the type of measurement itself. The measurement is therefore tainted by noise, and it's obvious that if this parasitic noise becomes too great, the measurement will no longer be usable, so it's not advisable to interpret the raw log data, but to correct them for these parasitic influences. As we have seen, these influences are of several kinds.

A. Borehole effects

The influence of the borehole is itself linked to several factors, analyzed below:

1) **drilling fluid**

We know that different drilling fluids can be used: air-foam, water more or less loaded with solid particles (bentonite - baryte, oil).

The composition of the drilling fluid will determine its density (and therefore its ability to absorb gamma rays), salinity, resistivity, radioactivity (bentonite or K40 salt content), the quantity of free water and therefore the invasion diameter, and finally the thickness, composition and density of the mud-cake.

2) Volume of drilling fluid around the tool

This will depend on the hole diameter and cross-section, the nature of the hole wall (smooth or rough), but also on the tool diameter, its position in the hole (centered or eccentric), and its type (skid-mounted or not).

B. Tool-related effects

There are several types of effect

1) Vertical tool resolution

We know that when the benches are too thin, compared with the vertical resolution of the device, the measurement is not representative of these benches, as it is influenced by those around them in abacuses, supplied by service companies, allow these effects to be corrected manually. No automatic program for truck computers yet exists.

2) Statistical variations

Nuclear parameters are measured and subject to statistical fluctuations due to the random nature of the phenomena. These variations can sometimes be so great that they require filtering prior to any use of the measurement, as is the case, in particular, for NGS natural gamma ray spectrometry.

1.3. Quantitative interpretation of delayed logs

Interpretation of delayed logs is the art of selecting the most appropriate model, based on the data available, to obtain results that are as close as possible to reality.

An interpretation model is a combination of different sub-models relating to

the following areas:

- Tool response or, in other words, the relationship between the actual measurement made by each tool and its conversion into logging parameters (ρb , Φn , Δt).
- The geology, which can be subdivided into.

A. **Mineralogy**: specifying the nature of the main and accessory minerals present and making up the grains or particles, crystals, cement or clay, with an idea of the geologically possible percentage limits.

B. **Texture**: giving an idea of grain size, grading, distribution of grains and clay, type of porosity, connection between pores.

C. **Structure**: indicating the internal organization of electro-banks: massive, heterogeneous, laminated.

D. **Petrophysics**: follows on from the previous field and enables us to specify parameters such as (ρma , ρf , Rsh , Δtsh , Rmf , Rw ...); necessary for quantitative interpretation.

E. **Mathematics**: choice of equations linking logging parameters to the parameters sought: porosity - saturation, permeability and choice of constraints and levels of uncertainty on measurements.

1.4. Locating reservoir zones

The interest in locating these zones is twofold: they are the only ones of any real economic interest, and it is therefore on them that the analysis should be concentrated to avoid wasting time.

Reservoir zones are characterized by specific logging responses, linked to their petrophysical properties (porosity, permeability), which most often lead to filtrate invasion, with the formation of mud-cake, at least if the pressure of the mud column is higher than the pressure of the formation, and hence an annular zone in the reservoir containing fluids that are generally different from the original fluids, resulting in more or less coaxial rings with different characteristics (resistivity, density, hydrogen index). A reservoir zone can therefore be distinguished by the simultaneous presence of some or all of the following features:

A. **Radioactivity**

The GR curve is generally presented on range1 at the same time as the PS and Diameter, if they exist, the scale is generally from left to right from 0 to 150 API. In clays, radioactivity often comes mainly from potassium K 40 , with contributions from

contributions from Thorium and Uranium contained in plant processing products.

Reservoir zones often have low radioactivity or very low levels of K 40. However, it should not be forgotten that there are radioactive sands or silts with high levels of potassium feldspars, mica or heavy minerals carrying Thorium and Uranium.

Furthermore, non-radioactive zones are not necessarily porous and permeable (e.g. anhydrite, gypsum, halite).

B. Presence of Mud-cake

Mud-cake is usually deposited on the hole wall as a result of invasion, reducing its nominal diameter. However, if the formation is slumping (sands) or crumbling (fractured carbonates), it will not be possible to observe this deposit as the hole widens.

C. Resistivity separation

The micro normals and micro inverses of the microlog most often show a positive separation due to their difference in depth of investigation. However, it should be remembered that a positive separation can occur in cavitated areas, or a negative separation in areas with mud cake deposits, especially in the case of Rmf < Rs .

On macrodevices such as DLL or DIL-LL8, due to invasion and differences in the depth of investigation of the devices, separation between the resistivity curves is observed, at least if the formation is permeable and if the contrast between the resistivities of the filtrate and formation water is sufficient.

Lode, LL3, LL7, LL8, I'd, AIT.....determination of virgin zone resistivity Rt.

LLs, I'm, PL, ML, MLL, AIT, MSFL....determination of resistivity of washed zone

Rx0 .

D. **Method (Rx0 / Rt)**

We can also calculate the ratio Rx0 /Rt, which will be close to 1 in clay or compact zones and close to Ruff /Rs in aquifer zones, and much lower than Mr /raw in hydrocarbon zones.

E. **Porosity method**

In the vicinity of reservoir zones, these tools should each have a reading which, once converted into porosity according to lithology, highlights the porosity, which should be more or less the same for each tool unless the reservoir contains gas.

But don't forget that some rocks have a low density and a high hydrogen index, which can be mistaken for reservoir rocks (as in the case of gypsum).

1.5. **Characterization of fluids in place**

The aim is to determine whether any of these reservoirs contain hydrocarbons, and if so, what type.

A. **Resistivity method**

If the formation water remains the same (same salinity, hence same resistivity) when moving from a hydrocarbon zone to a water zone, reservoirs containing hydrocarbons will be characterized by consistently higher resistivities compared with those of aquifer reservoirs.

In addition, due to the invasion of the filtrate and therefore the change in fluid and hydrocarbon saturation in the invaded zone, and the difference in depth of investigation between micro- and macro-devices for measuring resistivity,the ratio Rx0 /Rt decreases in hydrocarbon zones compared to its value in water zones; consequently, to detect water zones, it is necessary to look for the highest values of this ratio, the maximum deviation between the curves of microdevices (MLL, MSFL, PL, etc.),and macrodevices (LLd, ILd,...), if R(MLL or MSFL)>R(LL or IL) and, conversely, the minimum deviation if R (MLL or MSFL)<R (LL or IL).

Hydrocarbon zones can be detected by looking for the min deviation in the 1st case and the max deviation in the second.

The resistivity curves of micro and macro devices can also be superimposed on water zones, with hydrocarbon zones appearing when there is a gap between the curves.

These methods are not recommended if the salinity of the formation water varies frequently, and are not very effective if the invasion is zero or very deep.

According to Archie's relation, the ratio Rx0 /Rt is equal to Rx0 /Rt.

$$\frac{Rx0}{Rt} = \left(\frac{Rmf}{Rw}\right) \bullet \left(Sx0 \diagup Sw\right)$$

In water zones Sw and Sx0 are equal to 1

In hydrocarbon zones Sw < Sx0 .

B. Graphical plotting method

This method involves plotting ρ b , Φ n or Δt, in linear scale, as a function of $\left(1 \diagup \sqrt{Rt}\right)$

The points representing water zones are aligned along a straight line enveloping the points with the lowest value of Rt for the same value of ρb , Φn or Δt.

To ensure that the points represent clean zones, the gamma ray or PS values can be plotted in Z. Points representative of hydrocarbon zones will be clearly below this line.

These same plots can be used to determine saturation S w . To do this, simply construct straight lines of equal saturation.

These lines all start from the point representing the matrix (Pma, Φ=0, Δtma) on the line corresponding to Rt=∞. The lines S=50¨% and S=25% are constructed by joining the matrix point at 4 and 16 times the value of Rt of the water line (which corresponds to R0).These points can be easily obtained using the computers fitted to modern trucks.

This method gives the best results when the following conditions are met: presence of a saltwater zone, little or no clay, constant lithology, constant formation water salinity, moderate invasion.

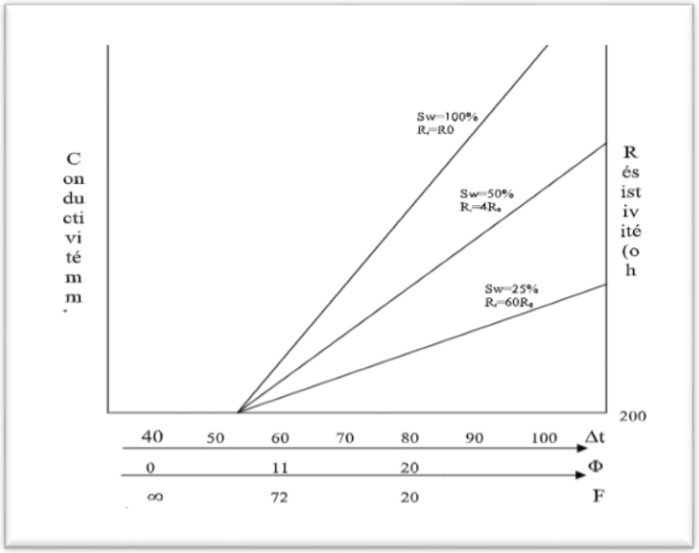

Figure 10: Graphical reporting method.

C. **Formation factor method**

Using a combination of density (FDC-LDT), neutron (CNL) and macro resistivities (MLL or MSFL, LL or IL). Apparent formation factors can be calculated and compared.

This gives :

$$F_{DN} = a / \phi_{DN}^{\,m} \qquad F_{Rt} = Rt / Rw \quad \text{and} \quad F_{x0} = Rx0 / Rmf$$

The calculation of these formation fact rs is carried out automatically at the drilling site using o

the truck's computers and reproduced in logarithmic scale as a function of depth, this method is known as “F-overlay”.

In clean formations ΦDN is very close to the true porosity of the formation .in water-bearing formations the three F values are more or less identical and equal to the real F factor, provided Rw and Rmf have been well chosen.

In formations containing displaceable hydrocarbons, we have Sw <Sx0 <1 and therefore FRt <FRx0 <FDN .

If the formations are clayey, this method does not give excellent results, as Archie's relationship no longer applies in this case.

D. **Rwa method**

Rwa is the apparent resistivity of formation water as calculated from Archie's relation, assuming a “clean”, aquifer formation. Rwa is defined by the following relationship:

$$R_{wa} = \frac{R_{IL}}{F_{DN}} ou \frac{R_{LL}}{F_S}$$

In clean aquifer zones, R wa takes on its minimum value, which corresponds roughly to Rw , whereas in hydrocarbon zones this value is much higher, since in reality we have :

$$R_w = \frac{R_t}{F} \bullet S^n{}_w$$

Sw: being much less than 1. If therefore we plot the value of Rwa as a function of depth in log form.

As hydrocarbon zones are characterized by high Rwa values, this representation is representation is carried out on site and is known as a “merged quick look”.

This technique can be used to determine the resistivity Rw .

A similar technique can be applied to calculate Rmf

$$R_{mfa} = \frac{R_{MLL}}{F_{DN}} ou \frac{R_{MSFL}}{F_{x0}}$$

1.6. The geostatistical methods used

The two geostatistical methods used are:

A. **Sequential Indicator Simulation (SIS)** is a geostatistical technique commonly used to represent how categorical variables—like rock types, geological facies, or the presence or absence of resources such as oil, water, or minerals—are distributed across a given area. It helps create realistic models of the subsurface by capturing spatial patterns and uncertainty in the data.

1. Steps of Sequential Indicator Simulation (SIS)

a) **Indicator Transformation** is a way to prepare categorical data—like lithofacies or rock types—for geostatistical analysis. Since these types ofbinary indicator variables .

In this process, each category (for example, sandstone, shale, or limestone) is turned into a separate variable. This new variable takes the value 1 if that category is pre0 if it's not. By doing

this, we make it possible to apply geostatistical methods—which typically work with numerical data—to datasets that contain discrete.

b) **Indicator Variogram Modeling** For each indicator variable, a variogram is computed to quantify spatial continuity. Experimental variograms are calculated and then fitted with theoretical models (e.g., spherical, exponential). These models describe how the presence of a category varies with distance, forming the foundation for spatial interpolation.

c) **Sequential Simulation Process** The simulation proceeds by visiting each grid node in a random order. At each location:

- Conditional probabilities of each category are estimated using indicator kriging, based on known and previously simulated data.
- This captures the local uncertainty for each category at that point.

d) **Assignment of Simulated Values** a category is randomly selected based on the estimated conditional probabilities.This is done through a weighted random draw, ensuring that the selected category reflects the estimated local uncertainty.

The newly simulated value becomes part of the data for simulating the next point.

e) **Post-Processing** after multiple realizations are generated, the results are analyzed. This includes:

- Creating probability maps (e.g., sand probability map).
- Measuring spatial uncertainty.
- Computing summary statistics.
- Selecting representative realizations for further modeling (e.g., flow simulation in reservoir studies).

2. Techniques used in SIS

a) **Indicator Kriging :**Kriging is applied to the indicator variables in this method to derive conditional probabilities. Models of the covariance (or variogram) structure pertaining to the indicator data are constructed first, and kriging is then used to estimate, at each site, the probability that a value belongs to a given category, given the data around it.

b) Sequential Simulation Algorithm : At random sequence, each point in the spatial domain is simulated one by one, mostly for eliminating bias. In each step, a value is simulated based on the knowledge of the data and the values simulated in the nearby points. This helps generate a more coherent spatial realization.

c) Using Conditional Distributions : For every simulation point, a conditional distribution is calculated based on the observed data and the previously simulated values in the

neighborhood, thus accounting for uncertainty while preserving the dataset's spatial structure.

d) Validation and Calibration : The simulation results would be compared to the real data for validation. This phase of validation could entail a comparison of descriptive statistics (for instance means, variances, histograms) and adjustment of possible variogram models or simulation parameters to have an end result that closely resembles reality.

3. Application in the oil industry

Sequential Indicator Simulation -- is an effective geostatistic methodology widely applied in petroleum exploration and production for reservoir characterization, property prediction, and uncertainty assessment. It is capable of such simulations of the facies or lithologies (for instance, sand, shale, limestone) distribution based on well data together with their spatial continuity and allows building realistic 3D subsurface models even in poorly or inaccessible data areas. This is done by producing multiple statistical realizations of the reservoir, which are used to evaluate geological uncertainties related to field development risk assessment. These realizations are employed to guide decision making with respect to well locations, production plan, and recoverable volumes. Finally, SIS may be applied in combination with other simulations, such as porosity and permeability, to create more complete reservoir models applicable to dynamic flow simulation.

4. SIS Method Advantages

a) **Efficiently handles spatial variability** :SIS is a great simulator for highly variable properties in even the most complex geological environments.

b) **Captures sharp geological boundaries**: It represents distinct breaks in the subsurface, such as faults and fractures, via binary indicators, thus giving more realistic models.

c) **Adequate quantification of uncertainties**: This can help manage risks and visualize alternative scenarios before decision-making by creating multiple possible scenarios with SIS.

d) **Flexibility with complex geological models**! The method is easily adapted to complicated cases where many geological variables are interacting, thus enhancing simulation accuracy.

e) **Supports planning and decision-making**: By offering credible probabilistic results, SIS helps engineers in planning drilling better, optimizing production, and reducing operational risks.

f) **Provides realistic and trustworthy simulations**: Outputs appear closer to real than other methods due to better representation of spatial variability and geological distributions.

B. **Sequential Gaussian Simulation (SGS)** is one of the primary geostatistical techniques for modeling the spatial distributions of continuous subsurface properties such as porosity and permeability, with applications to the oil-and-gasinspired industries. It generates many equally probable realizations that reproduce statistical data patterns and the spatial continuity of the variable imaged. This enhances knowledge about natural variability and uncertainty, enabling geoscientists and engineers to make informed decisions.

1. Methodological in SGS

a) **The transformation of scores:** Before running the simulation, we must standardize the data.The SGS method assumes that the data is normally (Gaussian) distributed. So we transform the original values (that may be skewed/irregular) into the standard normal distribution (mean 0, variance 1).

b) Grid Definition : we create a grid over the area of interest, as if putting a mesh over a map. Each square or cell or node is a place where we will simulate a new value.

c) **Random Path Generation:** To avoid any bias in the simulation (like favoring one direction over another), we randomize the order in which we visit the grid nodes.

d) Kriging estimation is a geostatistical technique used to predict the value of a variable at an unsampled location by considering the spatial correlation with nearby known data points and, in simulation contexts, with already simulated values. For each grid node, kriging provides a local mean, which represents the best linear unbiased estimate based on the surrounding data, and a local variance, which quantifies the uncertainty of that estimate. This dual output makes kriging especially powerful, as it not only predicts a likely value but also indicates how confident we can be about that prediction, allowing for more realistic and data-consistent spatial modeling.

e) Value Simulation: using the kriging mean and variance, we randomly pick a value from a normal distribution that matches that mean and variance.
That value is assigned to the current node**.**

f) Iteration: We add the simulated value to our dataset and move to the next node (following the random path).This process repeats until every grid node has a value.

g) **Back-Transformation:** we convert the simulated values back to the original data scale (undoing the initial normal score transformation).

2.Techniques Used in Sequential Gaussian Simulation (SGS)

SGS relies on a combination of smart geostatistical tools to create realistic and reliable simulations of geological properties. Here's how each technique plays a key role:

a) **Kriging** is like a highly informed guess — it's a statistical method that uses surrounding data to predict unknown values as accurately and fairly as possible. In SGS, kriging helps estimate what the value at each point should look like, along with how uncertain that estimate is.

b) **Variogram Modeling** acts like a fingerprint of the spatial data — it shows how values change with distance and helps define how connected or continuous geological features are. It's essential for making sure the simulation respects the natural flow and variability of the subsurface.

c) **Sequential Simulation** is the heart of SGS it builds the model step by step, visiting one point at a time. Each new simulated value is influenced by both real data and the values already simulated, allowing the model to capture natural spatial patterns and dependencies.

3.Applications in the Oil and Gas Industry

In the oil and gas industry, Sequential Gaussian Simulation (SGS) is widely used to better understand and model subsurface reservoirs. Its strength lies in generating multiple realistic versions of how reservoir properties—like porosity or permeability—might vary in space. This helps engineers and geoscientists assess uncertainty, since they can explore the range of possible scenarios rather than relying on a single model. With SGS, reservoir models become more detailed and geologically accurate, capturing natural variability that's crucial for predicting fluid flow. As a result, companies can make smarter decisions about where to drill, how to produce, and how to maximize recovery while minimizing risk.

4.Advantages of the SGS

a) **Incorporation of Uncertainty:** SGS offers a solid, science-based way to deal with uncertainty in subsurface predictions. By creating multiple possible versions (realizations) of how reservoir properties might vary, it helps geoscientists and engineers explore a full range of realistic scenarios. This makes it easier to estimate the risks and confidence levels tied to each prediction—an essential part of planning wells and managing reservoirs, where decisions must account for both geological and petrophysical uncertainty (Journel, 1974; Matheron, 1971).

b) **Flexibility:** SGS is a highly adaptable method that works well across different spatial scales—from detailed local studies to full-field evaluations of large petroleum reservoirs. It can also incorporate various types of data, such as well logs, seismic data, core samples, and even surface measurements. This flexibility allows experts to combine diverse sources of information into one strong, reliable geostatistical model (Jean & Pierre, 2012).

c)

2.Reservoir Modeling Methodology

2.1. **Introduction**

Geologists have always imagined underground environments in 3D in their minds, using the data and interpretations they had. But to make these mental images more concrete and useful, we create real models that represent the geology in a simplified but understandable way.

Modeling is about building these simplified versions of reality to focus on what's important. In this context, we talk about static models — meaning models that show a system at a single point in time without considering changes over time. Maps, models, and even data diagrams are examples of this.

In this work, when we mention "model," we're always referring to a static, three-dimensional spatial model. Before diving into geological modeling itself, it's important to understand the idea of a "dimension." Here , dimension means measurable aspects like length, width, and depth.

This modeling helps address a key challenge: making geological predictions — especially useful when planning drilling locations and for monitoring by field geologists.

2.2. **Petrel Software Overview**

n the past few years, integrated workstations have transformed the oil industry, thanks to dvances in microelectronics and computing.

These powerful systems have made many tasks, especially seismic data interpretation (2D and 3D), easier and faster for geologists, geophysicists, and reservoir engineers.

Among the leading tools developed for this purpose is Petrel by Schlumberger — a high-performance Windows-based platform for 3D visualization, mapping, modeling, and reservoir simulation.

2.3. **Key Advantages of Petrel**

Everything is integrated into one platform, making collaboration easier and eliminating data transfer issues.

Its powerful 3D visualization tools provide instant quality checks on the data.

Models can be updated instantly with new data, allowing faster and more confident decision-making.

Results are easy to export and share using regular Windows applications.

Familiar features like undo/redo and model saving make it user-friendly and efficient.

2.4. **Modeling the OKS Area in the Benkahla Field**

Using Petrel's modules, we could build various types of models for our reservoir, whether in 3D or 2D views like maps and sections.
In this project, we focused on three main types of modeling:

a) Structural modeling
b) Facies modeling
c) Petrophysical modeling.

2.5. **Starting a New Project and Loading Data**

To get started with Petrel, a minimum set of essential data must be loaded. This includes:

a) Well locations (X, Y coordinates)
b) Deviation data (for deviated or horizontal wells)
c) Formation tops
d) Seismic data (if available)
e) interpreted log data (from well logging)

Seismic data is very valuable, but if it's not available — as was the case for us — it's important at least to have fault information in 3D, or in 2D that can be adapted for 3D use.

2.6. **Structural Modeling**

Structural modeling lays the groundwork for the entire geological model. It defines the geometry of the subsurface, guides the placement of horizons and properties, and ensures the model reflects the actual structure of the field. Since it forms the backbone of the 3D model, getting it right is crucial.

A. **Structural Data and Sources**

Because we didn't have access to full 3D seismic volumes, we had to rely on a combination of available resources:

Interpreted 2D and 3D seismic data from earlier surveys.

structural map at the Top Triassic level, which we used to manually digitize the main faults.

Well tops picked from log data, which helped us define key stratigraphic horizons and tie everything to real depth control.

Even though this approach came with limitations (like no dip info from seismic), the integration of seismic interpretation with well data allowed us to create a workable structural framework.

B. **Fault Digitization and Integration**

We imported fault traces into Petrel, originally as 2D polylines, then turned them into full 3D fault planes using the "cut-and-extend" tool. This step allowed us to extend faults into depth and integrate them with the grid.

Most of the faults were modeled as vertical to sub-vertical, which fits with the extensional tectonic setting of the area. Each fault was carefully oriented to follow the dominant NE–SW trend, matching the regional structure.

In places where existing data didn't fully explain the geometry, we added a few interpreted faults. These were mainly technical — they helped stabilize the grid during construction but didn't change our geological interpretation.

C. **Structural Gridding (Pillar Grid)**

Once the faults were in place, we moved on to building the structural grid — the actual 3D skeleton of the model. We used a pillar gridding method, where vertical lines define the structure of the grid and help connect the horizons and faults.

The grid was divided vertically into three main layers:

- Top boundary,
- Middle surface (often the reservoir),
- Bottm boundary.

This setup allowed us to slice the model into volumetric cells that can hold lithological and petrophysical information later on. We paid close attention to fault behavior during gridding, making sure throws and offsets were properly captured.

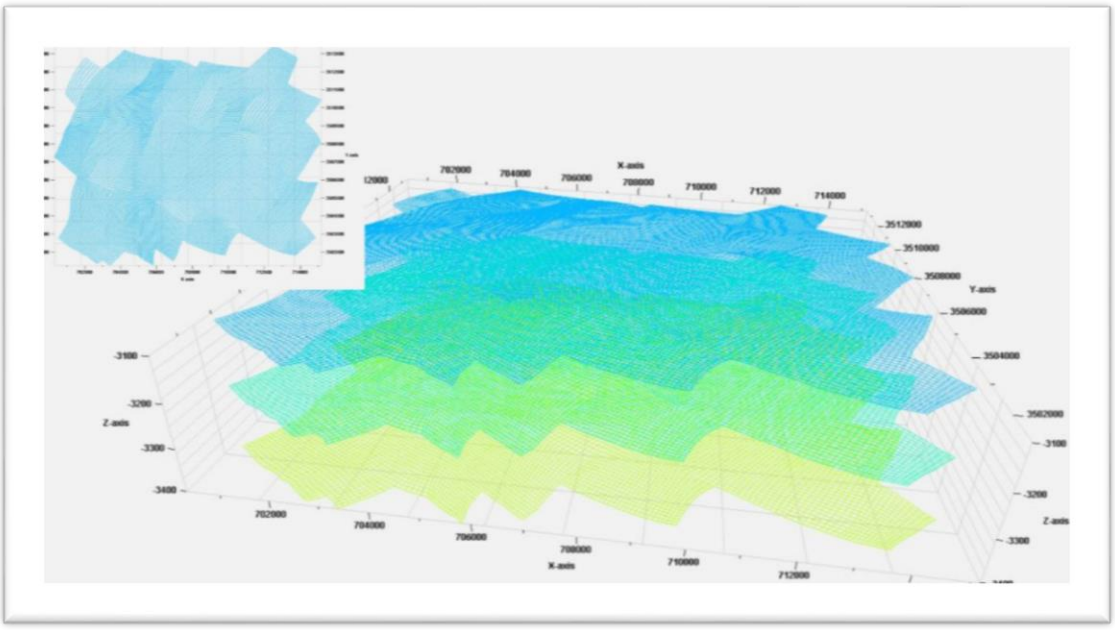

Figure 11: structural of gridding (Petrel 2018).

D. **Horizon Insertion**

Next, we inserted the main horizons into the grid. These came from the well tops and represent the major geological boundaries in the field. We selected five key horizons, each marking a change in lithology or reservoir quality.

Because we didn't have throw values from seismic, Petrel calculated them automatically based on elevation differences across fault blocks. We reviewed and adjusted them to keep faults consistent and make sure horizons stayed geologically realistic.

In areas with poor control, we interpolated surfaces between wells while respecting regional dips and structural trends. This kept the geometry smooth and geologically plausible, even where data was sparse.

2.7. **Property Modeling**

Once the structural grid was in place, the next step was to fill it with actual geological and reservoir information. Property modeling brings the model to life — assigning both facies (rock types) and petrophysical properties like porosity, permeability, and water saturation to each grid cell.

This step turns a geometric skeleton into a usable reservoir model that can be simulated, analyzed, and used to make operational decisions.

A. **Facies Modeling**

We modeled the distribution of lithological facies using Sequential Indicator Simulation (SIS), which is well-suited for categorical variables like facies. This method works by turning each facies into a binary indicator and simulating them one by one, using well data and spatial continuity rules. (Geostatistics Lessons. (n.d.). Sequential Indicator Simulation).

Here's how we approached it:

1) **Facies Classification**: Since we had no core data, we generated electrofacies using cluster analysis on wireline logs (mainly GR, NPHI, and RHOB). These clusters acted as proxies for real depositional facies.
2) **Upscaling**: The electrofacies were upscaled from log resolution to grid resolution, ensuring consistency with the structural model
3) **Variogram Models**: For each facies, we built variograms to control how far the influence of each facies could extend in 3D space, honoring geological trends.
4) **Proportion Curves**: We used vertical proportion trends to preserve realistic facies stacking and layering.
5) **Search Ellipsoids**: Parameters were tuned to balance lateral spread and vertical continuity of each facies.

SIS also allowed us to create multiple realizations, helping us assess uncertainty in facies distribution — especially important when dealing with sparse data and transitional environments.

B. **Petrophysical Modeling**

For continuous properties like porosity (ϕ), permeability (K), and water saturation (Sw), we used Sequential Gaussian Simulation (SGS). This geostatistical approach is widely used for reservoir modeling because it captures spatial variability while staying true to real data values. (Geostatistics Lessons. (n.d.). Sequential Gaussian Simulation).

Our workflow was as follows:

1) **Upscaling Logs**: Raw log data was upscaled to the grid scale to match cell resolution.
2) **Variogram Analysis**: We modeled variograms for each property to define how they vary in space — both laterally and vertically.
3) **Gaussian Transformation**: Property values were transformed into a normal (Gaussian) distribution, simulated using SGS, then back-transformed to retain their original data

characteristics.

4) **Simulation**: The simulation honored well data, variogram structure, and geostatistical parameters, giving us a property model that reflects the true heterogeneity of the reservoir.

SGS provided us with a continuous and realistic distribution of reservoir properties, which is essential for later phases like volumetric calculation.The overall structure was based on the internal training guide (Practical Guide for Petrel at HMD by SLB).

2.7.C. Final Integration

By combining facies and petrophysical simulations, we produced a fully populated 3D static model that honors both geological constraints and reservoir property distributions. This model now serves as a robust foundation for advanced geological and petrophysical interpretation, with the goal of refining reservoir understanding, characterizing heterogeneities, and supporting more informed exploration and development decisions.

2.8. Quality Control (QC)

Quality control was applied throughout the reservoir modeling process to ensure geological coherence, accuracy, and data integrity at each stage. Despite limitations such as the absence of seismic cubes and core data, we implemented practical QC measures using available well data, regional analogs, and careful visual inspection to reduce uncertainty and validate our model of the Benkahla field.

A. Well Data QC

Well headers, formation tops, and log data were verified for consistency before import. Depth units were standardized, and logs were visually reviewed for missing values or anomalies. Wells with incomplete curves were flagged and treated with caution during modeling.

B. Fault and Horizon QC

Fault and horizon interpretations—based on well data and limited seismic sections—were checked for geological plausibility. Fault connectivity, throw continuity, and horizon smoothness were visually inspected in both map and 3D views to avoid unrealistic geometries or structural mismatches.

C. Grid QC

The structural grid was reviewed to ensure accurate alignment with faults and layering. Fault gaps, distorted cells, and structural inconsistencies were corrected to maintain model integrity, particularly around complex fault zones.

D. Facies Modeling QC

Due to the lack of core data, facies were interpreted from log responses and regional analogs. Electrofacies clustering was validated through crossplots (e.g., GR vs. NPHI) and checked for continuity between wells. Vertical proportion curves and 3D views helped verify reasonable facies distribution and layering trends.

E. Petrophysical Modeling QC

Log-based porosity, permeability, and water saturation were compared with their upscaled versions in the grid. Simulated property distributions were cross-checked against well data using histograms, crossplots, and variograms to ensure realistic variability and consistency with lithology and facies.

F. Final Model QC

A final integrated check was performed across the structural, facies, and property models. The overall model was assessed in 3D to confirm alignment between input data and simulation results, and to detect any remaining anomalies or inconsistencies before export

2..9. Model Validation

To ensure the reliability of the 3D geological model constructed using Petrel, a validation phase was conducted in accordance with common industry practices. This process involved the exclusion of three wells from the simulation dataset during the modeling phase. These wells were intentionally withheld from the simulation in order to serve as independent control points for validation.

After completing the simulation, the petrophysical outputs generated by the model—specifically porosity and water saturation—were compared with actual measured values obtained from core data in the excluded wells. The model was considered valid if the differences between simulated and measured values remained within an acceptable error margin, typically less than 10%. This comparative analysis helps assess the predictive accuracy of the model and ensures its robustness for further use in reservoir evaluation and decision-making processes.

Chapter 3 : Reservoirs modeling

CHAPITRE 3

RESERVOIR MODELING

Introduction

The 3D geological model of the southern zone of the BenKahla (BKH) field, presented in Figure N°, was built using Petrel software, based on a rigorous integration of all available data. This model represents a coherent volumetric representation of the subsurface, aimed at better understanding the distribution of reservoir units, the geometry of structures, and petrophysical properties at field scale.

The model is based on results supplied directly by Sonatrach's geological department, including estimated porosity and water saturation values for each well. These data, derived from the petrophysical and electrofaciological interpretation of the recorded logs, have been used in the IP (Interactive Petrophysics) software to also identify the electrodiagraphic facies. These results form the basis for the construction of the property model, enabling their spatial distribution in the reservoir to be represented.

The spatial distribution of these parameters was determined by applying geostatistical laws, in particular through the use of variograms, to interpolate values between wells and restore a realistic model of the reservoir environment. This approach captures the reservoir's lateral heterogeneities, while respecting the structural geometry determined by seismic interpretation and geological cross-sections.

In addition, the integration of 35 wells located in the study area (Figure 16) provided sufficient coverage to produce a robust model. Electrical, nuclear and acoustic logging data have been used to characterize the different stratigraphic levels and estimate lateral and vertical variations in petrophysical properties.

In this way, the model provides an essential basis for understanding reservoir behavior, assessing volumes in place, and helping to make decisions on field development and production.

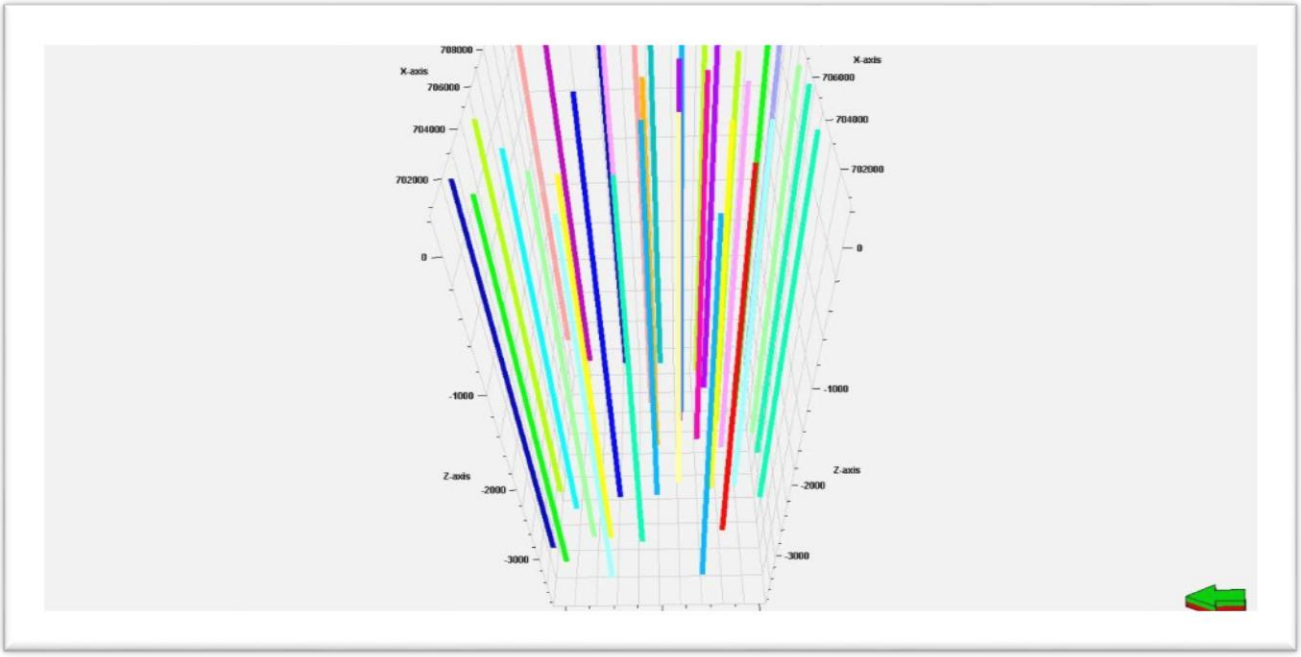

Figure 12: 3D Well positions.

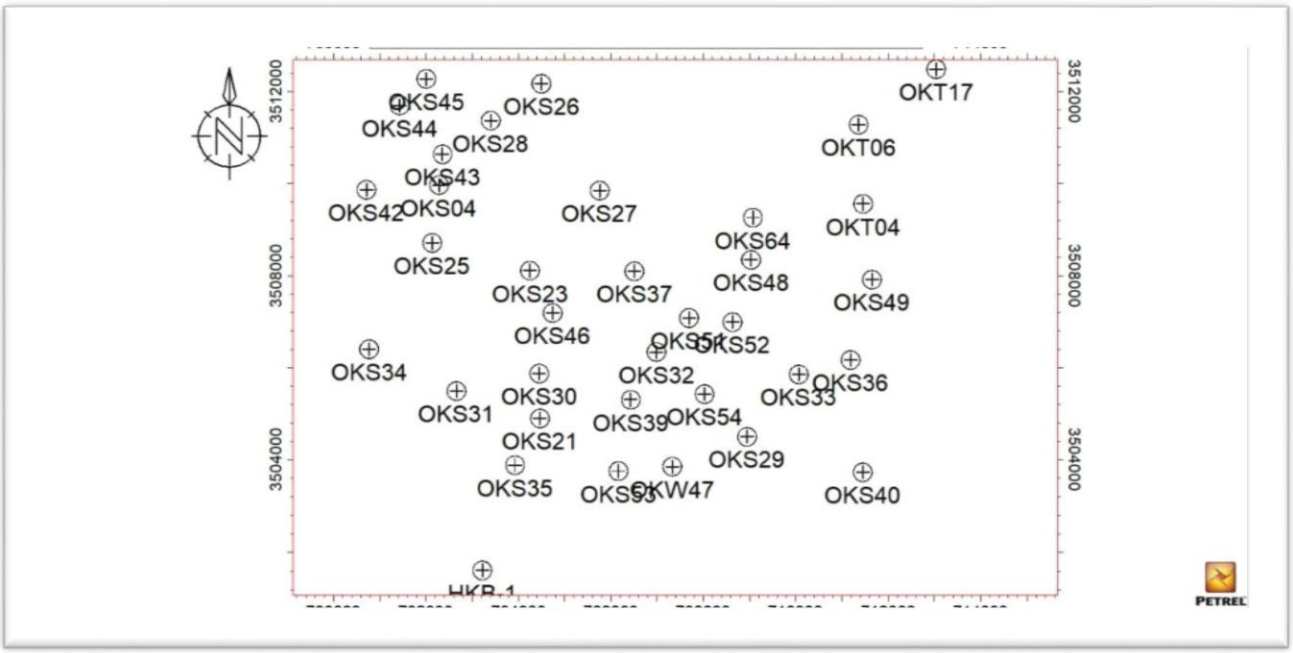

Figure 13: 2D Well positions.

1. Well correlations

This study presents methodologies of correlations applied to Benkahla oilfield. In fact, the main objective is to characterize the facies and reservoir architecture of the lower series using stratigraphic cutting and inter-well correlation techniques for identifying petrophysical properties and heterogeneities in the reservoirs.

2. Principle of Division

ratigraphic units are divided by the methodical recognition of sedimentary discontinuities and regional boarders. These discontinuities manifest in abrupt granulometric variations and localized erosive surfaces compensating the absence of continuous regional markers. This makes it possible for the recognition of grano-decreasing (fining-up) sequences identifiable by their specific log signatures of bell shape (MEBROUKI N. (2015)). Yet, the complex structure of basin within its fault networks constitutes a limit to the continuity of correlation.

3. Different Correlations Performed in the Benkahla Field

3.1. Lithological correlation

Lithological correlation uses the Hercynian unconformity as a major stratigraphic landmark. It reveals a remarkable uniformity of the lower series over the entire field, with thicknesses ranging from 43 to 48 meters. At the same time, it demonstrates significant variability in volcanic deposits, the distribution and amplitude of which are directly controlled by proximity to existing fault systems.

3.2. Lithofacies correlation

Lithofacies correlation is based on a model of fluvial deposition in a braided regime. It integrates macroscopic well descriptions and log data to establish five distinct sequential units.

These units exhibit lithological transitions marked by textural and granulometric variations, changes in clay/sandstone ratios, changes in cementation, and differential diagenetic processes. Intensive erosion is identified as a potential limiting factor for the complete preservation of facies successions (MEBROUKI N. (2015)).

3.3. Log correlation

The study involves wells OKS-26, OKS-23, OKS-21, OKS-64, OKS-52; OKS-54; OKT06; OKT-17 of Benkahla field (according to intersection figure design). The depositional units in this part of the study have been defined through log interpretations and sedimentological analyses of core samples. The following are some of the main conclusions:

Boundaries of sandstone are correlatable from well to well and observation of the lenses of sandstones suggest that they have probably been cut at cross-section, confirming ancient sedimentation and flow directions.

Also, sonic logging was used for determination of the genetic independence of the units (MEBROUKI N. (2015)).

3.4. Electrofacies correlation

The base of the lower series is clearly identifiable in all boreholes thanks to a typical Gamma Ray signature: a radioactive peak (>120 API). Combined with the Sonic response, this association reveals a characteristic profile opposite the greyish laminated clays of the reservoir, precisely at the lower series/Silurian roof contact.

The top of this series corresponds to reddish clayey silts punctuated by patches of greenish clay.

The analysis reveals floodplain deposits characteristic of an arid climate, identifiable by their sawtooth-shaped Gamma Ray curves.

This study exploits two logging methods (Gamma Ray and Sonic) to :

- ✧ Établir correlations between units
- ✧ Relier petrophysical parameters
- ✧ Déterminer bench thickness (MEBROUKI N. (2015)).

3.5. Interpretation of the Triassic clay-sandstone correlation

The correlation has been made according to three profiles (A, B, C) in order to better understand the lateral behavior of the units. This approach allows thickness variation and its spatial evolution to be observed among the various wells.

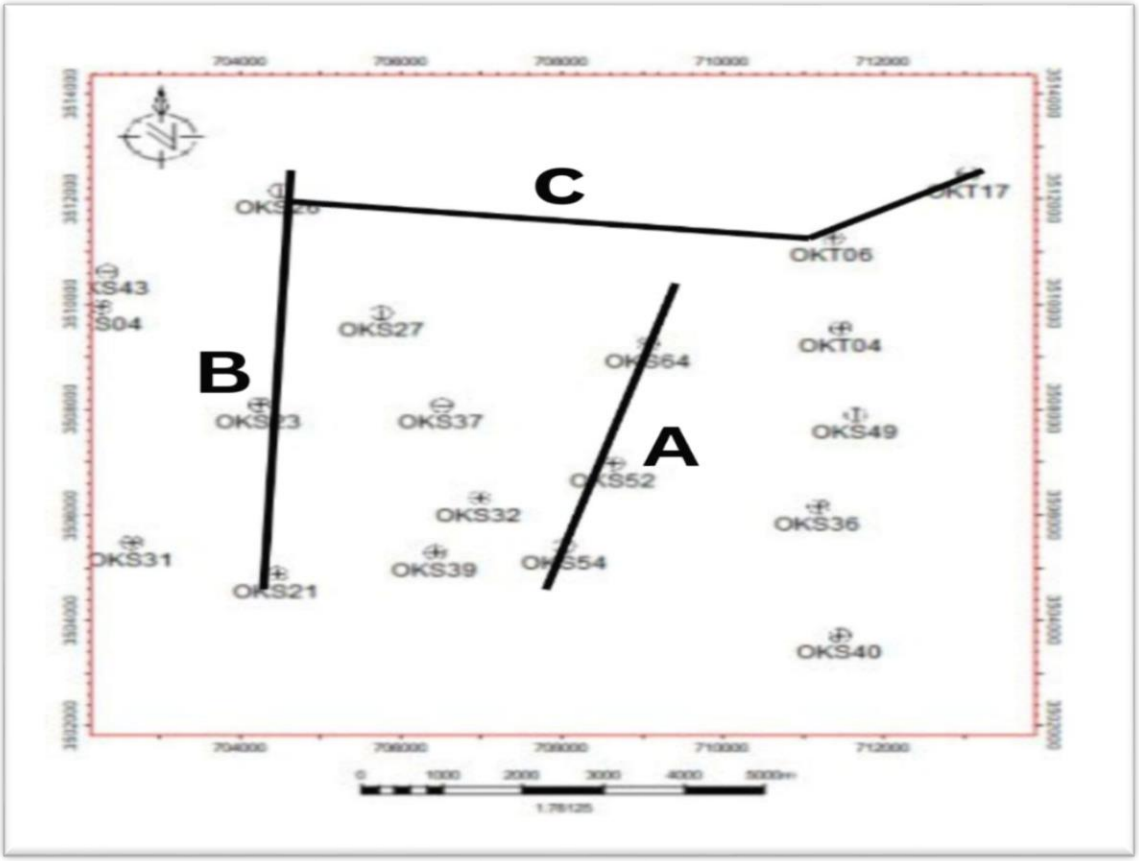

Figure 14: Profile position A,B,C.

A. OKS64-OKS54-OKS52 Profile

Unit T2, T1, and the Andesites show a progressive thickening from OKS64 to OKS52. Also, there is a sinking of the roofs of each unit, reflecting the tendency to deepen eastwards or according to the orientation of the profiles for every unit. This indicates subsiding or tectono-sedimentary control more towards this direction.

Unit01:

Very lateral variation is scored by Unit01 concerning its thickness; it registers 3.0 m at OKS64, achieves a maximum value of 22.0 m at OKS54, and then returns to a value of 11.4 m at OKS52. This is indicative of the clear thickening towards OKS54, which is followed by a thinning trend towards OKS52.

Unit02:

Unit02 remains relatively constant from OKS64 (3.0 m) and then thickens significantly at OKS54 (11.0 m), but KBIS gradually becomes thinner to only 1.4 m at OKS52. This indicates a heterogeneous deposit, probably controlled by conditions at the locality.

Unit03:

This unit has a rising thickness from 2.0 m at OKS64 to 9.03 m at OKS54 and then a considerable thickening to 19.6 m at OKS52. This is indicative of increasing sedimentary filling on the way to OKS52, although the intermediate stage is more moderate.

Unit04:

This thickness exhibited progressive changes in Unit 04 as: 2.0 m at OKS64; 4.42 m at OKS54; and 11.0 m at OKS52. This gradual increase in thickness may be indicative of the progressive deepening of the basin or itself towards OKS52.

Unit05:

From 3.0 m thick at OKS64, Unit05 rises moderately to 7.55 m at OKS54 only to decline to below that value again at 4.0 m at OKS52. Probably indicative of a maximum deposition zone centered around OKS54.

OKS54 is characterized by the greatest thicknesses in several units, denoting a depositional zone. In fact, OKS52 exhibits a more heterogeneous distribution, with some units thick and others very thin, while OKS64 is the shallowest overall, suggesting a marginal or stable position in the basin.

at deposits were not distributed evenly laterally.

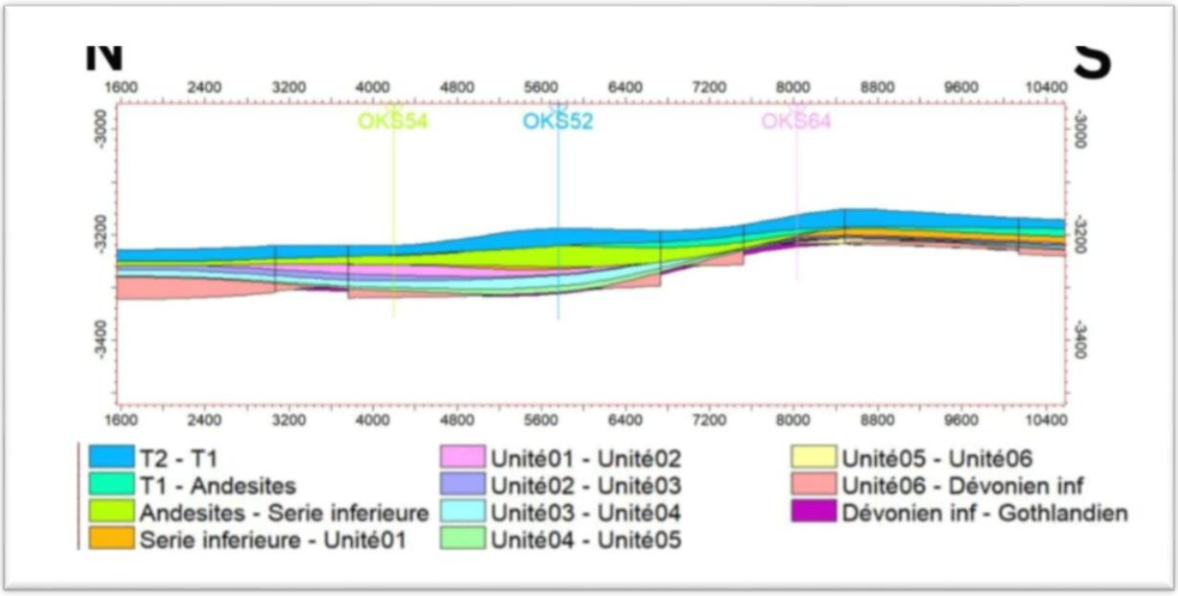

Figure 15: profile A geological section.

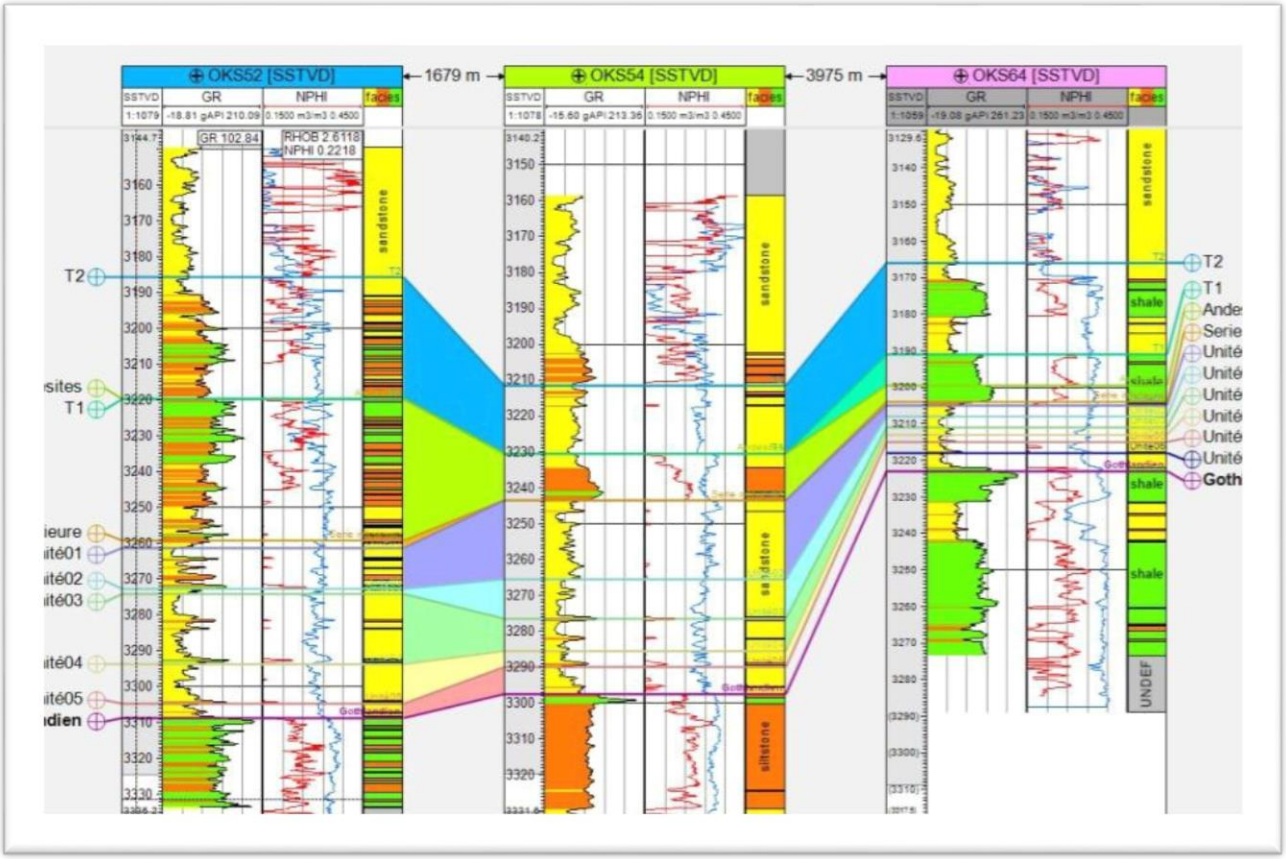

Figure 16: correlation profile A .

B. Profile OKS21 - OKS23 - OKS26

Between OKS21, OKS23 and OKS26, the thicknesses of **units T2, T1 and the Andesites** increase overall towards OKS26. T2 varies from 18 m to 21 m, T1 from 18 m to 22 m, and the Andesites, absent or confused with T1 in the first two shafts, reach 11 m at OKS26. This evolution reflects a thickening of the layers towards the east (or depending on the orientation of the wells), suggesting progressive subsidence and a more active depositional environment in this direction.

there is a general increase in unit thickness towards the deeper OKS23 shaft.

Unit01 increases from 9 m (OKS21) to 14.8 m (OKS23), then decreases slightly to 1.5 m (OKS26).

Unit02 increases from 11 m (OKS21) to 5.7 m (OKS23), then falls back to 3 m (OKS26).

Unit03 has a more constant thickness: 11 m (OKS21), 8.5 m (OKS23), 3 m (OKS26).

Unit04 remains relatively thin and stable, at around 3 m in all wells.

Unit05 varies little: around 4 m in all cases.

We note that some units show a thickening towards the deepest well (OKS23), which may reflect greater deposition towards the center of the basin, or local tectonic or sedimentary control. Then, the thickness seems to decrease slightly towards well OKS26, suggesting a non-regular lateral distribution of deposits.

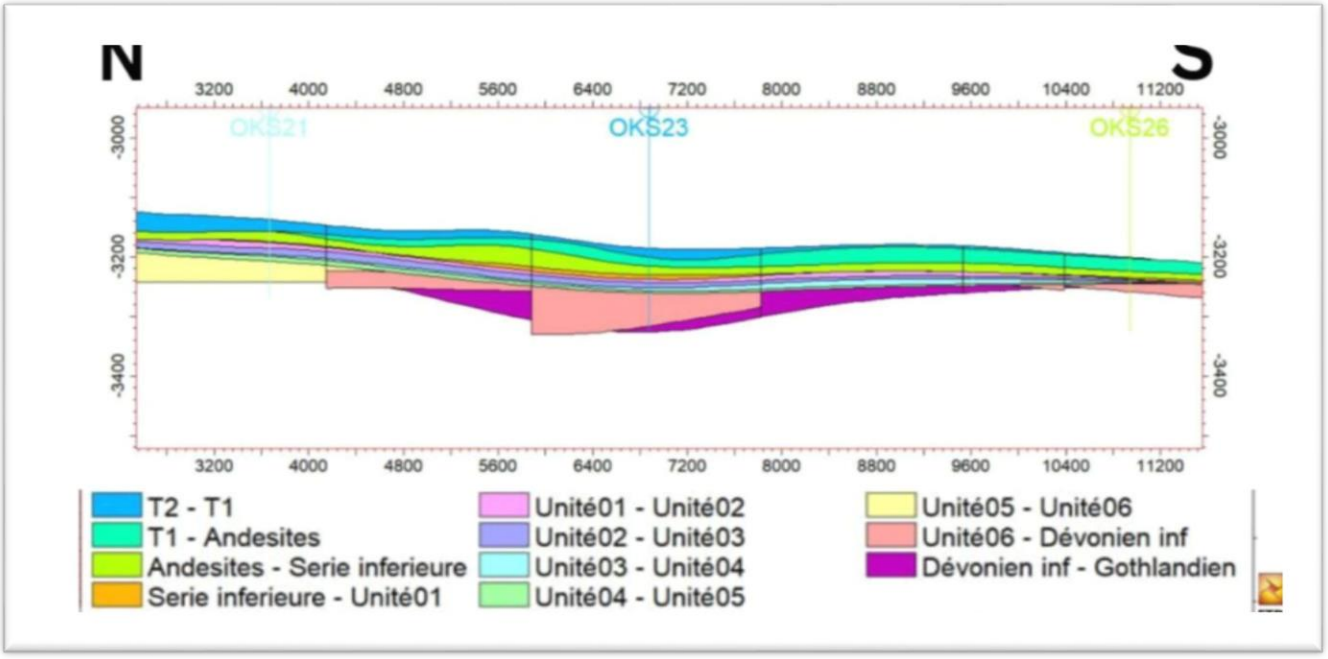

Figure 17: profile B geological section.

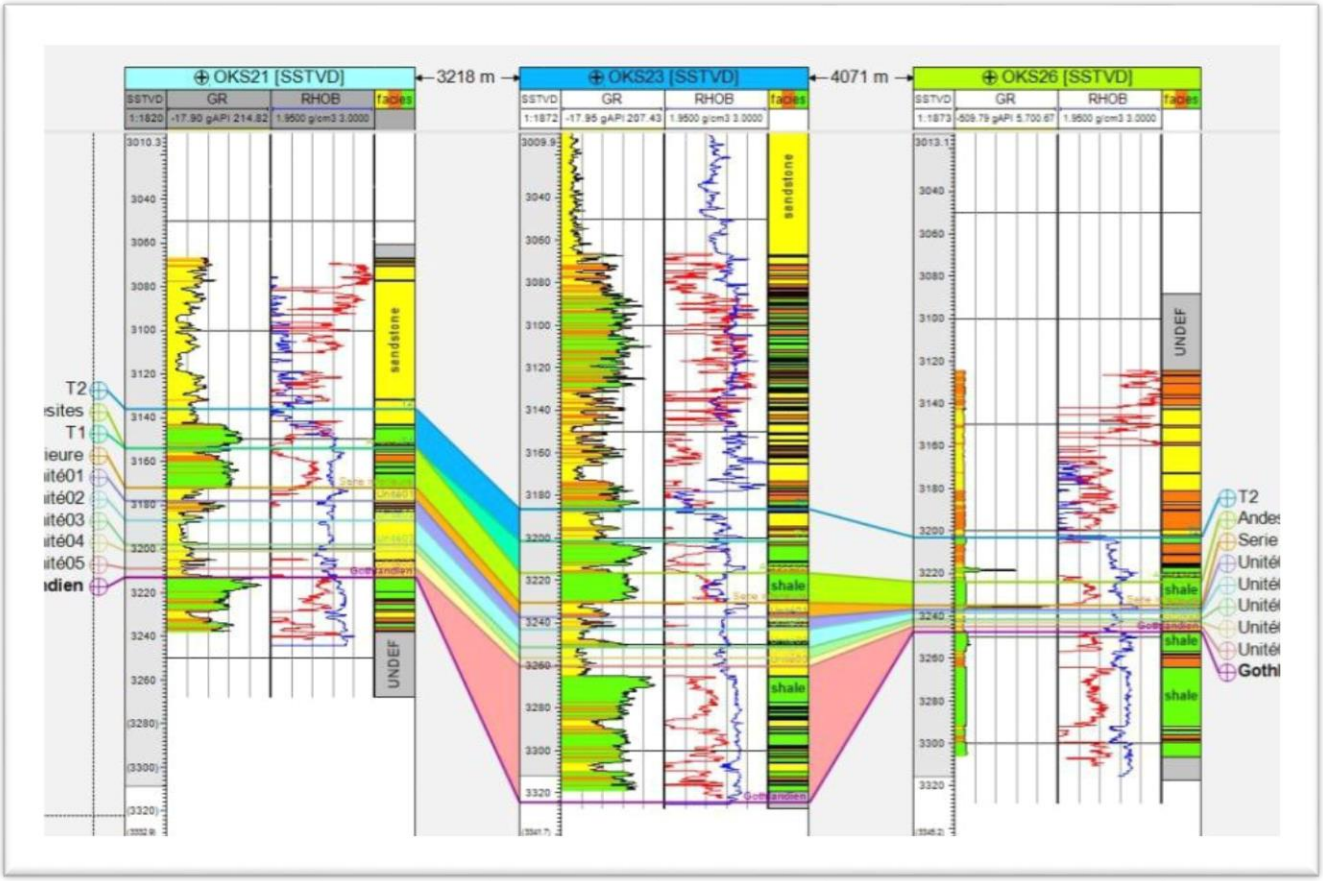

Figure 18: correlation profile B.

C. Profile OKS26 - OKT06 - OKT17

UnitT2 shows uniform thickness of 21 m in all three wells from profile OKS26 to OKT17, indicating that the deposition of sediments has continued. **UnitT1** shows a marked increase in thickness from 22 m at OKS26 to 28 m at OKT06, being 41 m at OKT17; thus, there is a gradual thickening towards OKT17, that is deeper down. As for the **andesites**, they were also thickening, rising from 11 m at OKS26, to 14 m at OKT06, and reaching up to 22 m at OKT17. High variations thus indicate a further increase in subsidence or accumulation towards OKT17.

Unit01 shows a thickness that has relatively constant values from 1.5 m at OKS26, 4.5 m at OKT06, and 8 m at OKT17, that shows an overall increase towards OKT17.

The thickness of **Unit02** grows from 3 m at OKS26 to 6 m at OKT06, and its last value at 11 m is at OKT17. This indicates that there is thicker sediment at the latter location.

Unit03 continues to develop in an even more gradual manner, with 1.5 m at OKS26, 5 m at OKT06, and 6 m at OKT17.

Unit04 increases its thickness from 2 m (OKS26) to 5 m (OKT06), then to 6 m (OKT17).

Unit05 shows changes of depth, for example, 2.5 m at OKS26; 3.5 m at OKT06; and reaches up to 9 m at OKT17.

There is clear and progressive increase of unit thicknesses from OKS26 to OKT17. Such trend indicates higher accumulation of sediments towards OKT17, probably due to a more passive or favorable topography or subsidence for sedimentation in this direction.

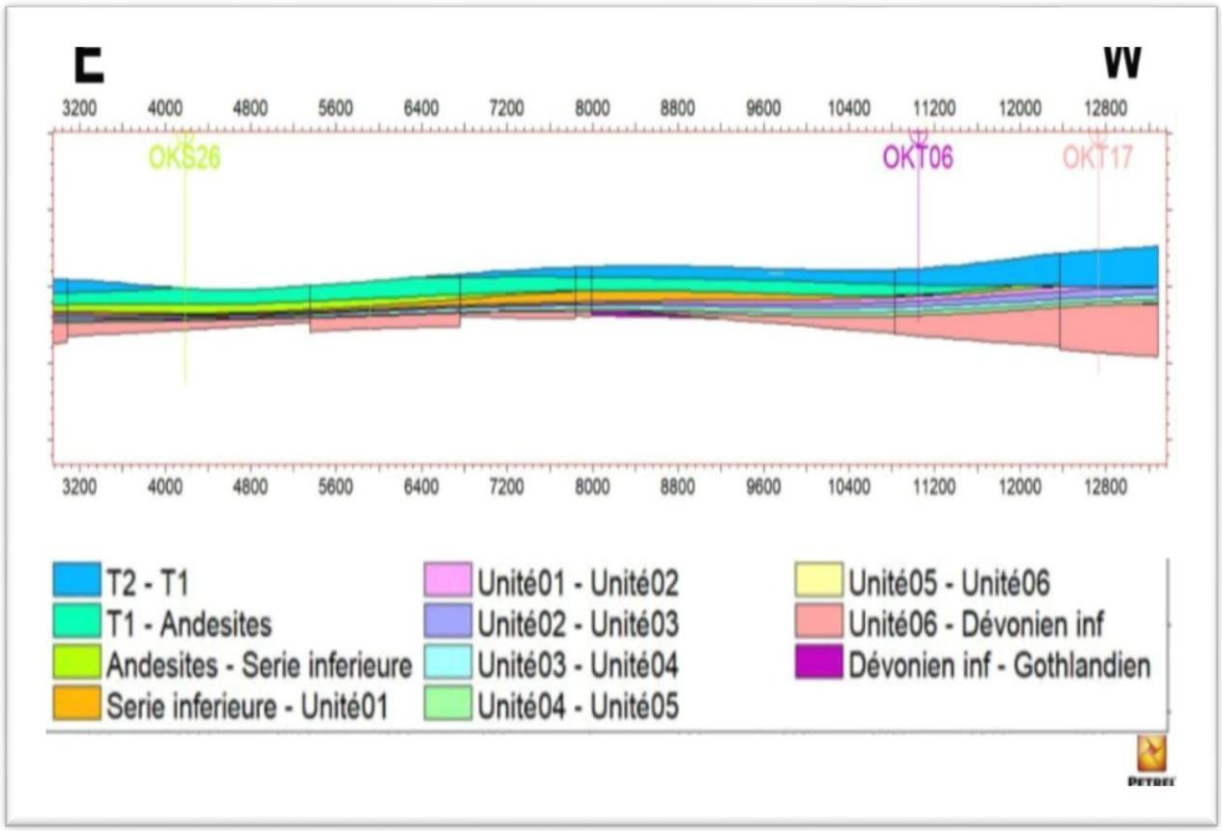

Figure 19: profile C geological section.

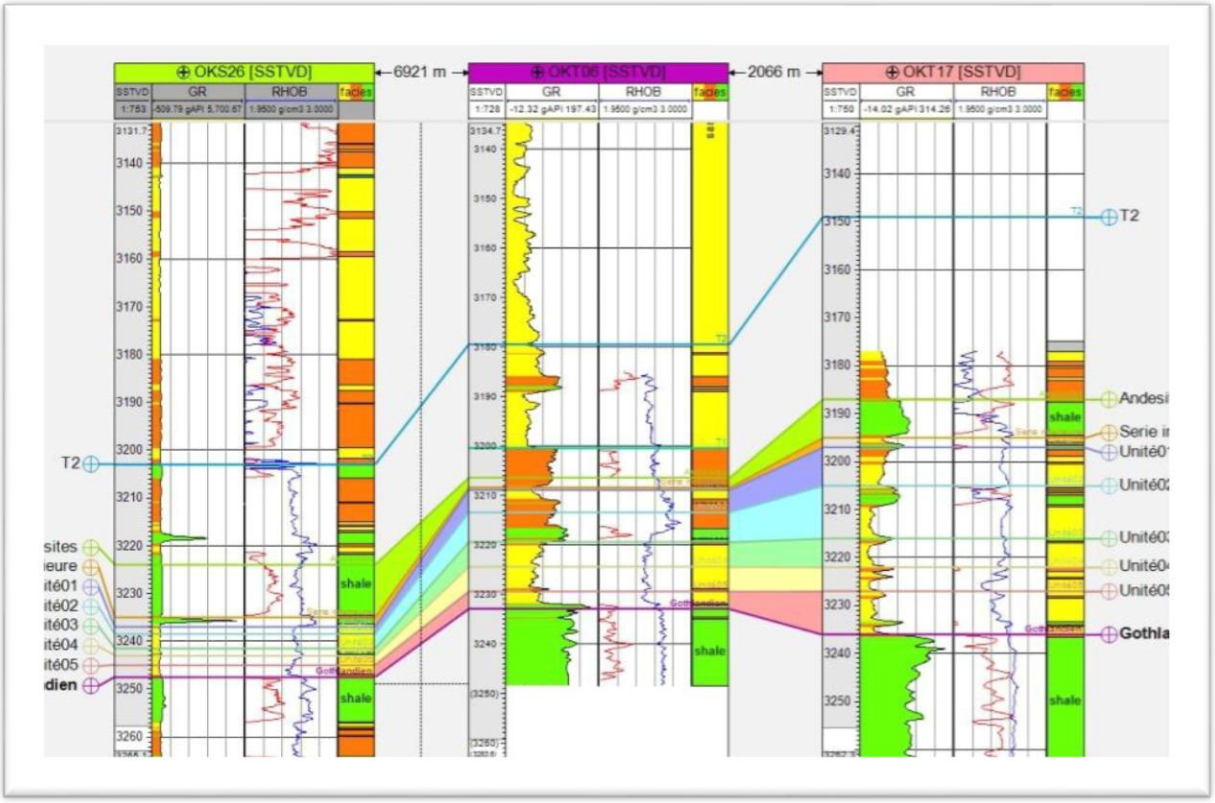

Figure 20: Correlation profile C.

By analyzing the three profiles: OKS21-OKS23-OKS26; OKS64-OKS54-OKS52; and OKS26-OKT06-OKT17, it can be seen that thickening of the sedimentary units and the depression of stratigraphic roofs (T2, T1, Andesites) are taking place in different structural directions along progressive time, all of which reflect the differential subsidence which takes place across the Ben Kahla basin.

Moderate but continuous increase in thickness is evident across the central area of the wells OKS21, OKS23 and OKS26 and can be interpreted as the influence of stable sedimentation dynamics linked to ongoing subsidence. In contrast, marked lateral variability exists within the OKS64-OKS54-OKS52 profile, with maximum thickness at OKS54, then defined contrasts with OKS64 (more stable zone) and OKS52 (localized thickening). The same can be said or observed in the OKS26-OK-06-OKT17 profile found in an explicit sedimentation accumulation bias towards OKT17, which suggests a topographic dip or better structural trapping.

The longitudinal and cross-sections of the whole OKS zone confirm an average reservoir thickness of 50 m with superimposed sandstone units and clay levels separating the two. This configuration, together with the blocky structure, separated by normal faults showing low to medium rejection (mostly between 0 and 30 m), suggest that there are moderate lateral variations in most areas, except in specific zones affected by major faults (e.g. OKS52 well).

Thickening variations, sinking of the roofs and active tectonics within the OKS zone demonstrate a strong interplay between structural and sedimentary factors controlling the geometry, distribution and reservoir potential of the lower Triassic series.

4. Structural Model Interpretations

The Benkahla oilfield, encased in the Oued M'ya depression (melghir sillon on the east and Allal vault to the west), showcases a neotectonic architecture inherited from varying tectonic phases. Seismic surveys depict an elongated NE-SW monoclinal structure toward the west (-3136 m at OKS-21 well), subdivided into compartments by two major fault systems represented by 35 faults divided according to their dip:

A dominant NE-SW network (Pan-African/Hercynian orientation);

A subordinate NW-SE network.

Moreover, there are two regional faults:

- Fault I (NNE-SSW direction, 110 m throw): Watertight western limit of the reservoir (discharge > reservoir thickness).
- Fault VI (NW-SE, strike 10 m): Contributes to internal compartmentalization.

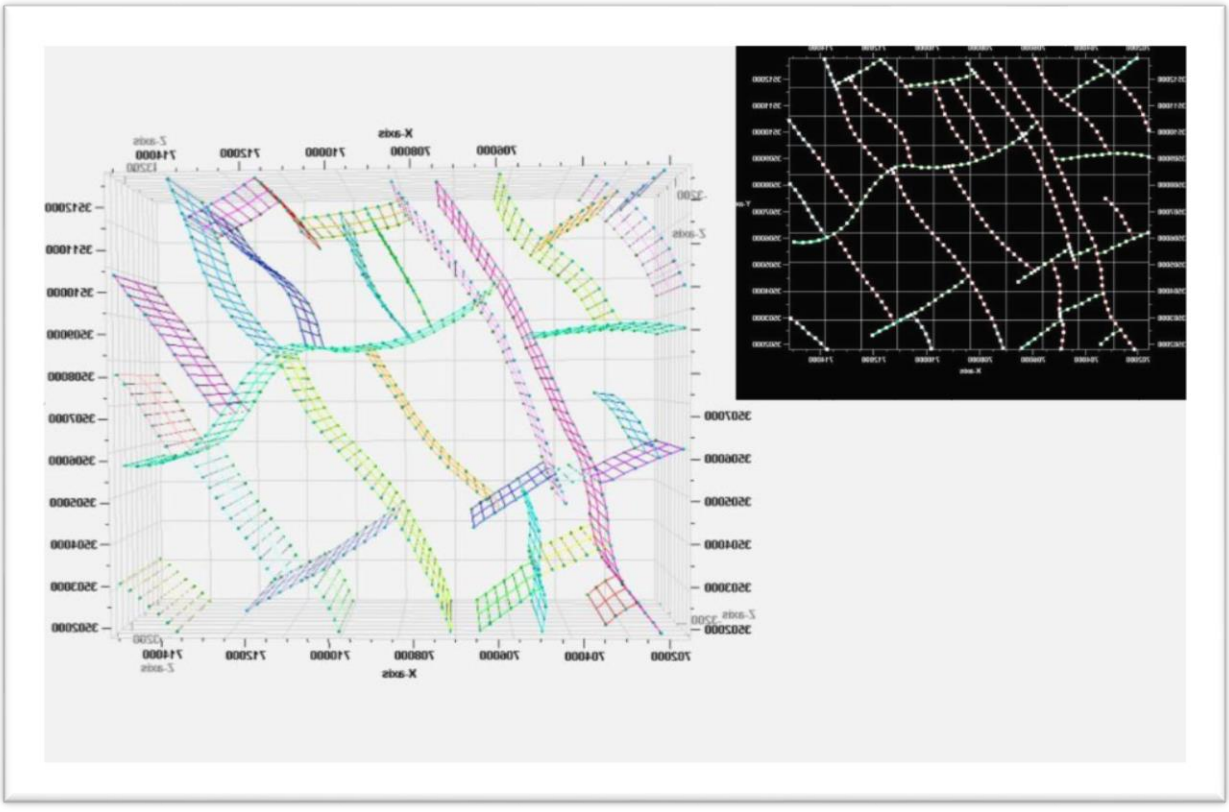

Figure 21: the 3D, 2D fault network .

Confirmation comes from the 3D model for a horst and graben morphology with an anticline located around HKB-1, OKS-21, and OKS-53 wells. They have a direct relation with facies distribution.

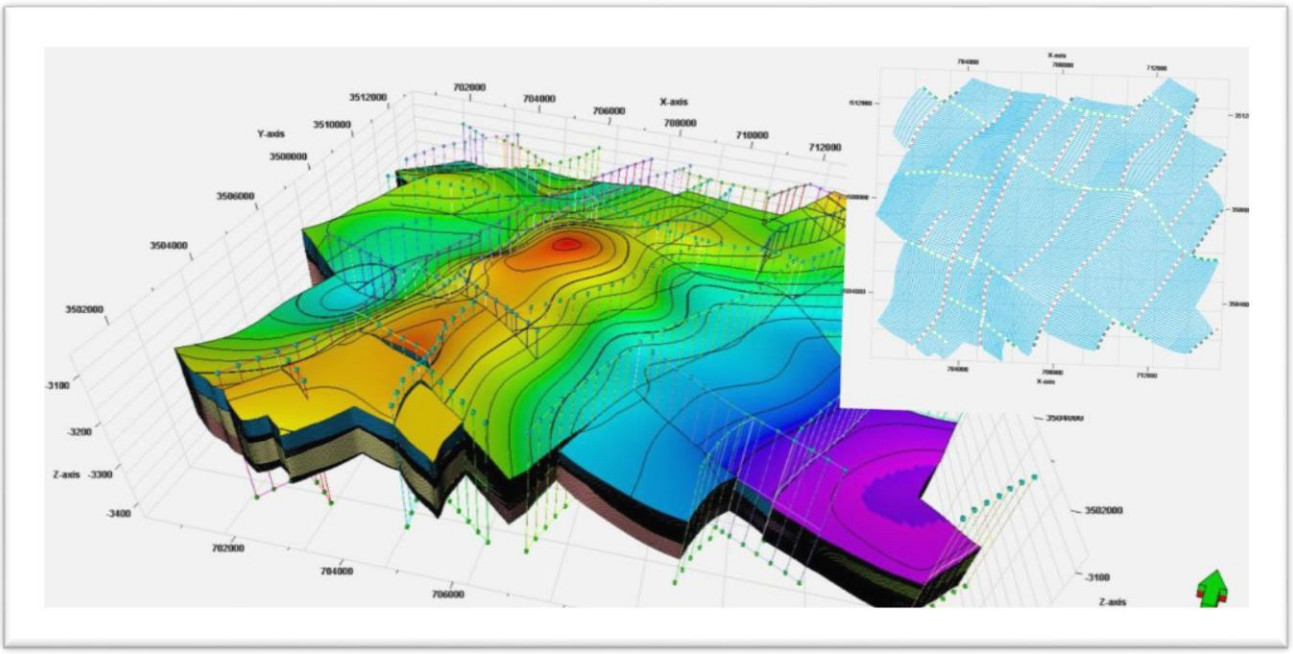

Figure 22: 3D,2D structural model .

4.1. Facies Model

A. Reservoir T2

Facies modelling (Figure 28) indicates that the three components of sediment are sands (51.37%), silts (30.72%) and clays (17.91%). Majority is represented by sands, but they appear in isolated lenses without continuity laterally. This indicates low-energy distal river channels where branching channels (NE-SW) deposit sand sporadically but floods overflow and spread silts and clays which quickly isolate these sandy lenses. These channels can be described as unstable and often change course during floods which in turn disperse the sands. They are mostly dry in-between floods during semi-arid conditions. These channels have collected silts and clays (48.63% in total), sealing up the sandy bodies and laterally limiting their extension. Thus, apparently, contradictory: even though it has so high volume, the silts remain dispersed, very typical in flood plains where the channels are ephemeral (Ait Bali & Sadoun; Truc et al., 1989).

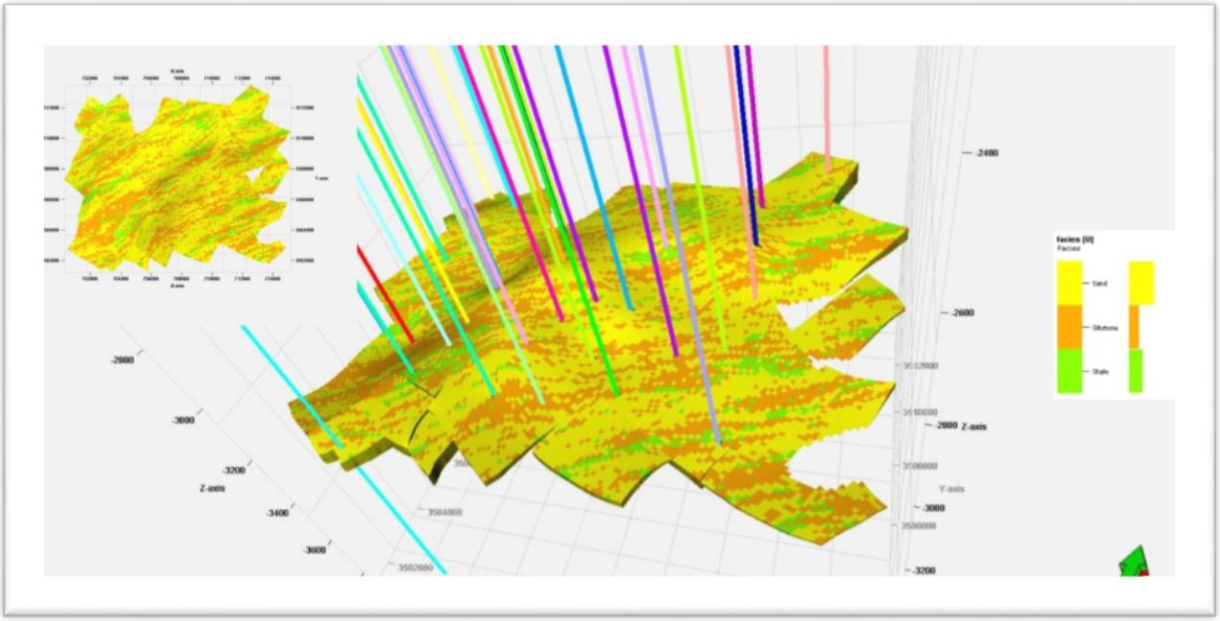

Figure 23: 3D ,2D facies distribution in T2.

B. Resevoir T1

Almost the entire Reservoir T1 site (Figure 29) is beneath clays and silts, with only a small fringe of sands found at the edges. This would suggest a broad floodplain where fine deposits are dominant and sand appears only occasionally and in specific places. According to composition, the unit consists roughly of 41.67% clays and silts, 32.62% silts, and 25.71% sands. Channels, if ever formed in such a semi-arid climate with well-defined seasons, would infrequently carry sand (Ait Bali & Sadoun). This vertical and lateral homogeneity is consistent with calm and continuous sedimentation with perhaps no major channel reactivation.

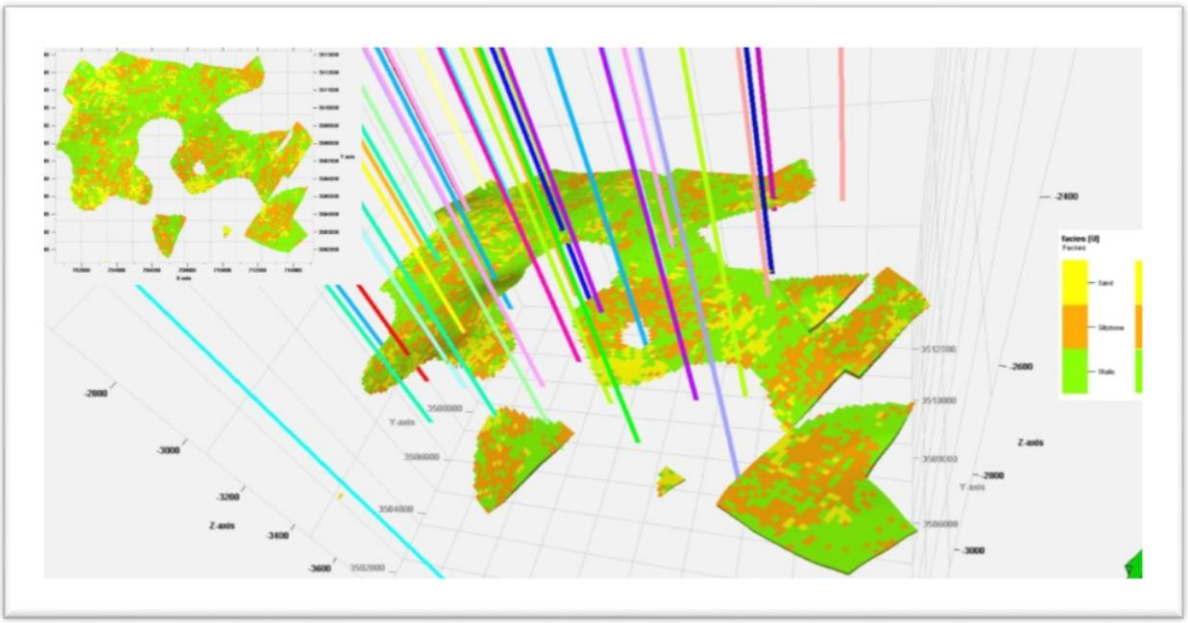

Figure 24: 3D,2D facies distribution in T1.

C. ANDESITE RESERVOIR

This unit is predominantly composed of clays and silts, totalling 82%, with less than 18% randomly dispersed sand. It acts as a regional blanket, sealing off the reservoirs below.

The scarcity of sandy beds and their irregular distribution indicate very low-energy deposition, probably in distal alluvial plains or marshy areas where channels have only limited influence. This corresponds to a distal alluvial fan environment or a temporary lake, where the semi-arid climate and intermittent flows (NE-SW) mainly favor fine sedimentation. This dominance of clays and silts explains its role as an impermeable cover.

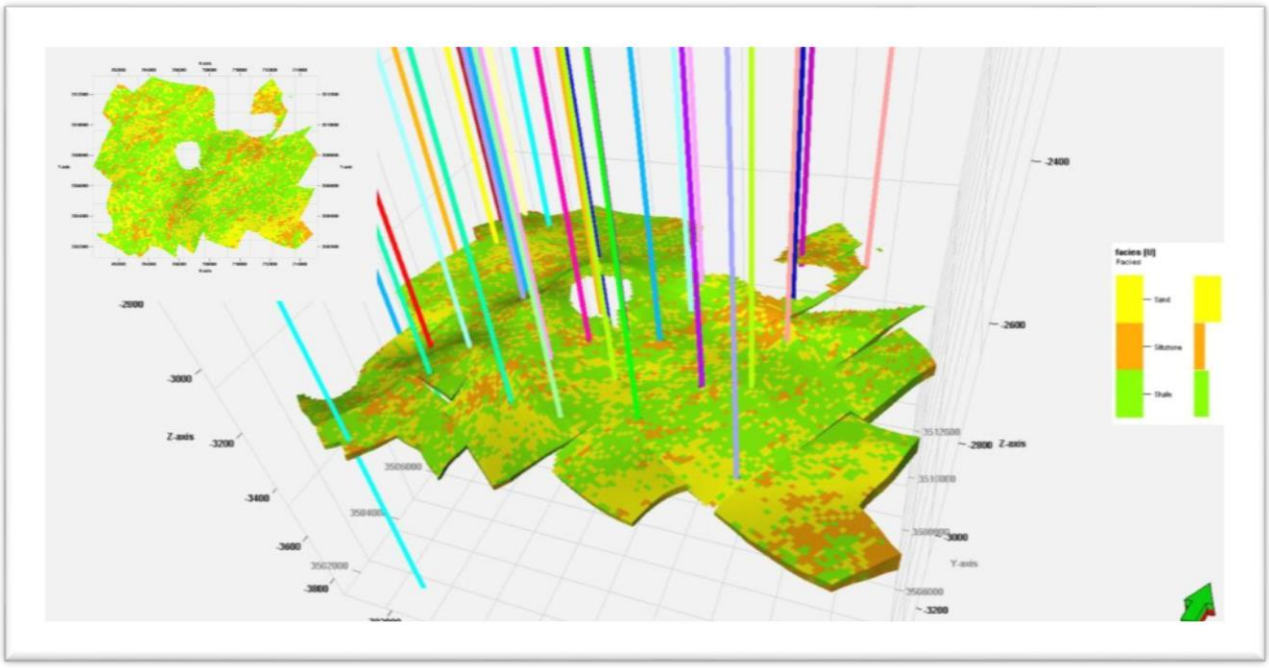

Figure 25: 3D, 2D distribution in Andisite.

D. LOWER SERIES

The main target for drilling, this unit shows a vertical succession of 4 to 5 fairly thick sandy bodies (approx. 40-50 m each), separated by clay levels. Their distribution shows active channels oriented NE-SW, forming continuous sandy corridors with good lateral connection, characteristic of a branched channel system.

This pattern can be explained by seasonal flooding in a climate with marked seasons: floods deposit coarse sands first, then when the water level drops, clays and organic matter are deposited in calmer waters.

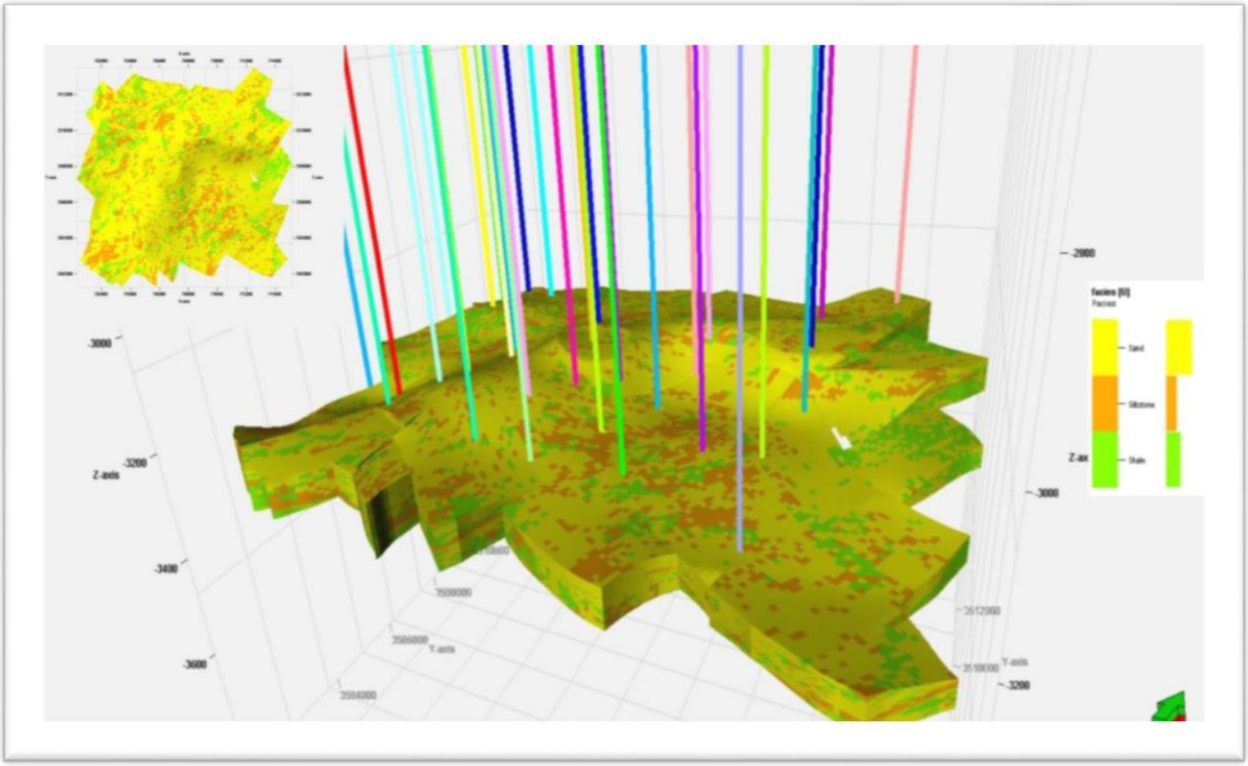

Figure 26: 3D, 2D distribution in lower series.

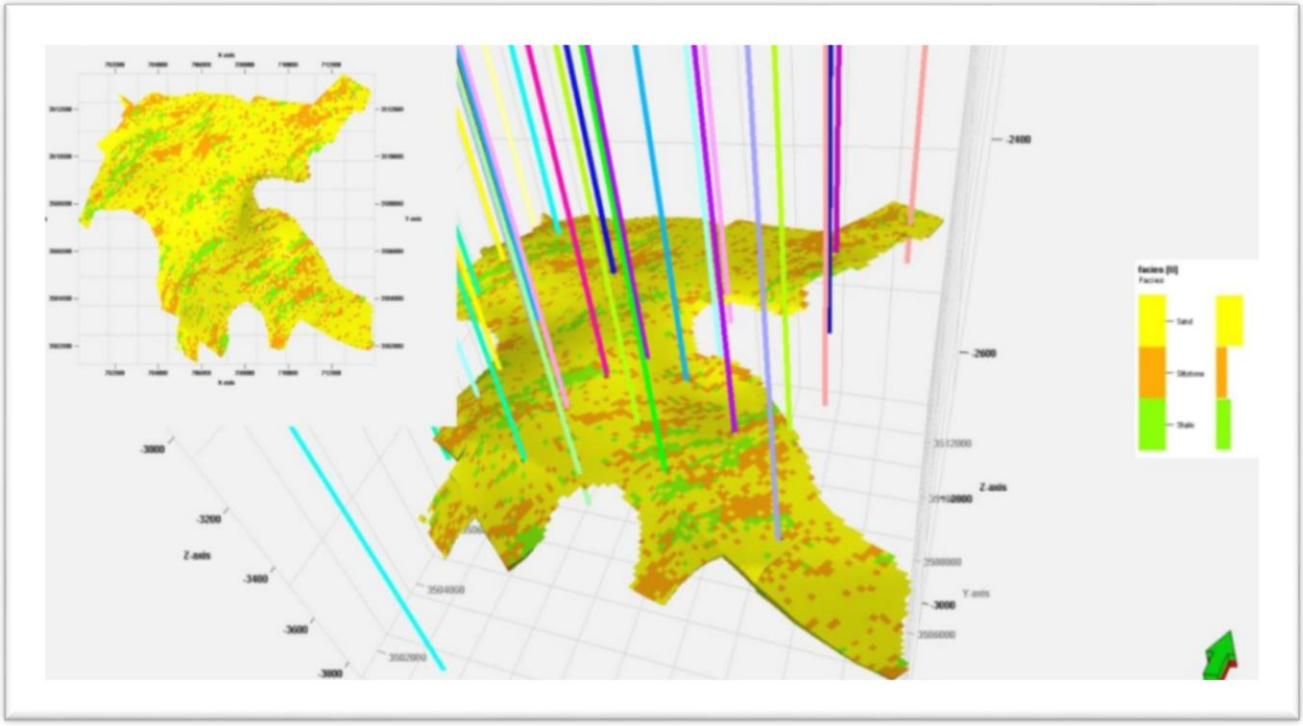

Figure 27: 3D,2D distribution in U1

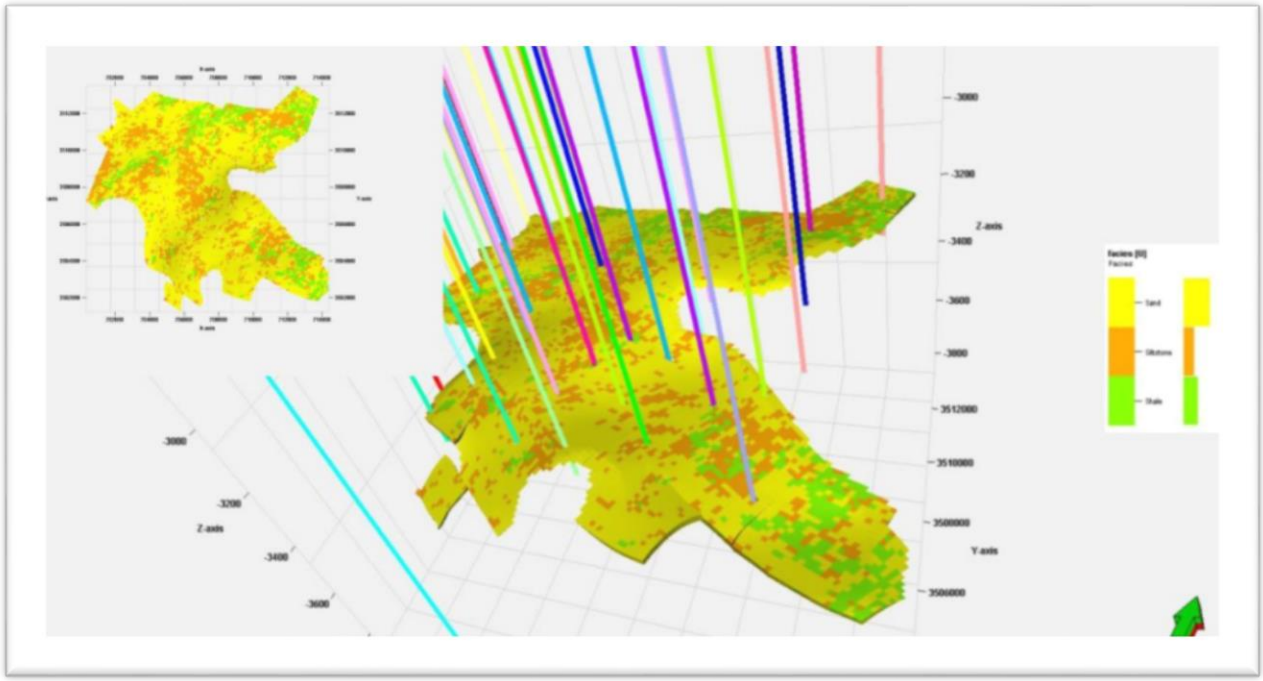

Figure 28: 3D,2D distribution in U2.

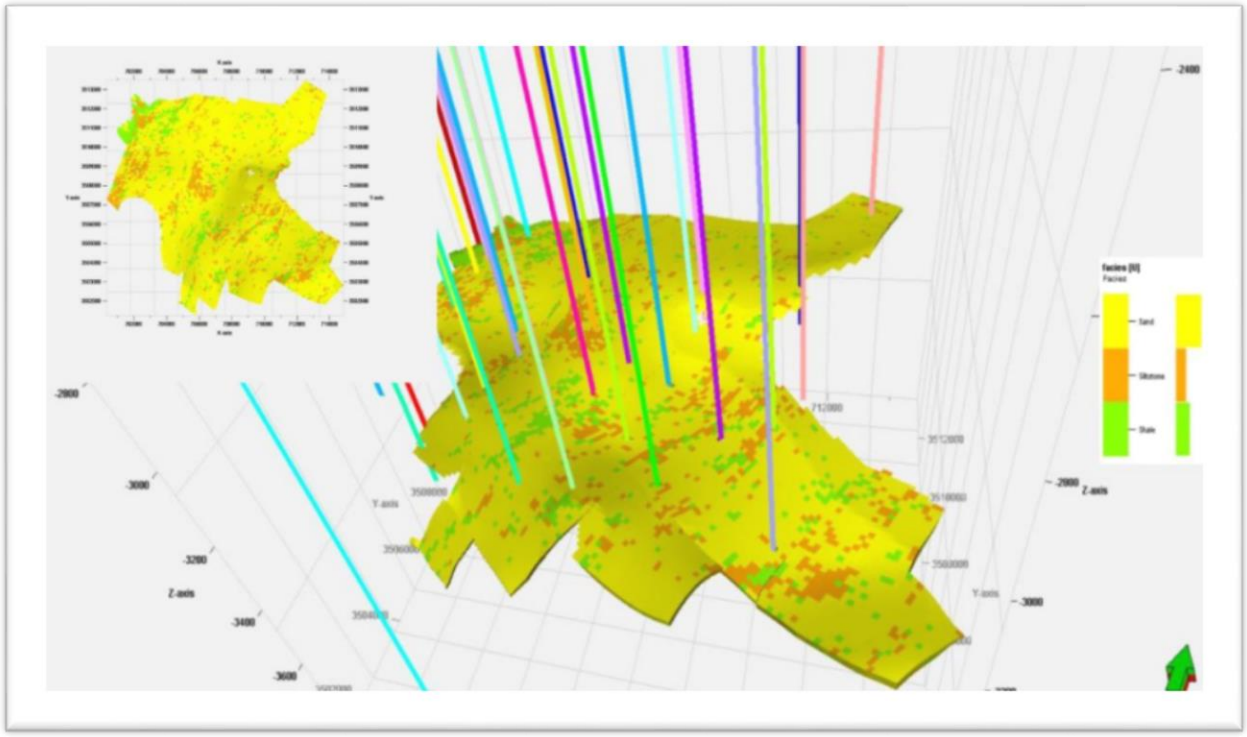

Figure 29: 3D,2D distribution in U3.

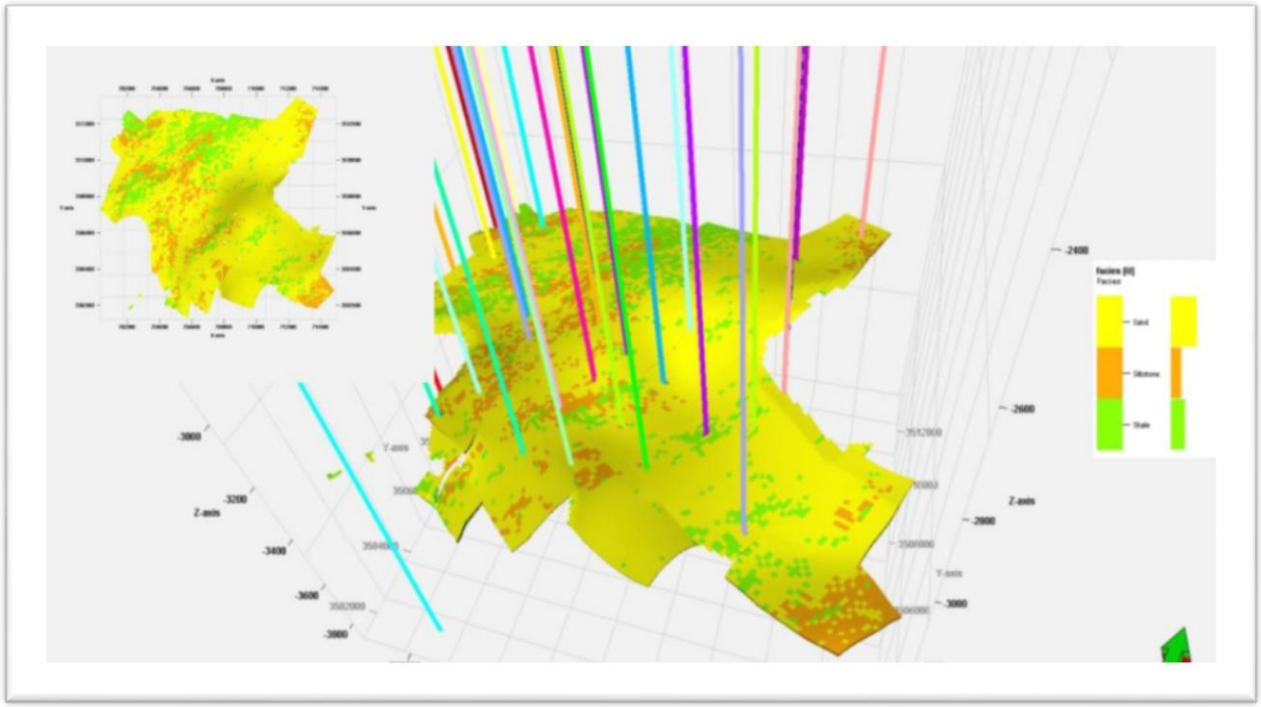

Figure 30: 3D,2D distribution in U4.

4.2. Petrophysical model

a. variograme Analysis

In a five-layer fluvial-channel system oriented NE–SW according to paleogeographic reconstructions, we modeled the spatial continuity of porosity (Φ) and water saturation (Sw) using an anisotropic spherical variogram—chosen for its ability to capture both submetric variability (nugget) and longer-range autocorrelation (range) along the principal paleoflow axis (Journel & Huijbregts, 1978). After fitting this model to experimental variograms calculated for each layer in both major and minor directions, we ran Sequential Gaussian Simulation (SGS) to produce multiple equally probable 3D realizations of Φ and Sw. SGS not only honors the anisotropic spatial structure but also quantifies uncertainty through pixel-wise standard deviations, thereby delineating zones of high reservoir potential and guiding operational decision-making (Deutsch & Journel, 1998).

We selected two representative layers with contrasting petrophysical properties to illustrate the spatial variability and anisotropy behavior. The corresponding variogram models are shown in the figures, highlighting the directional continuity and heterogeneity patterns.

EXEMPLE 01

Variogram for the 45° direction:

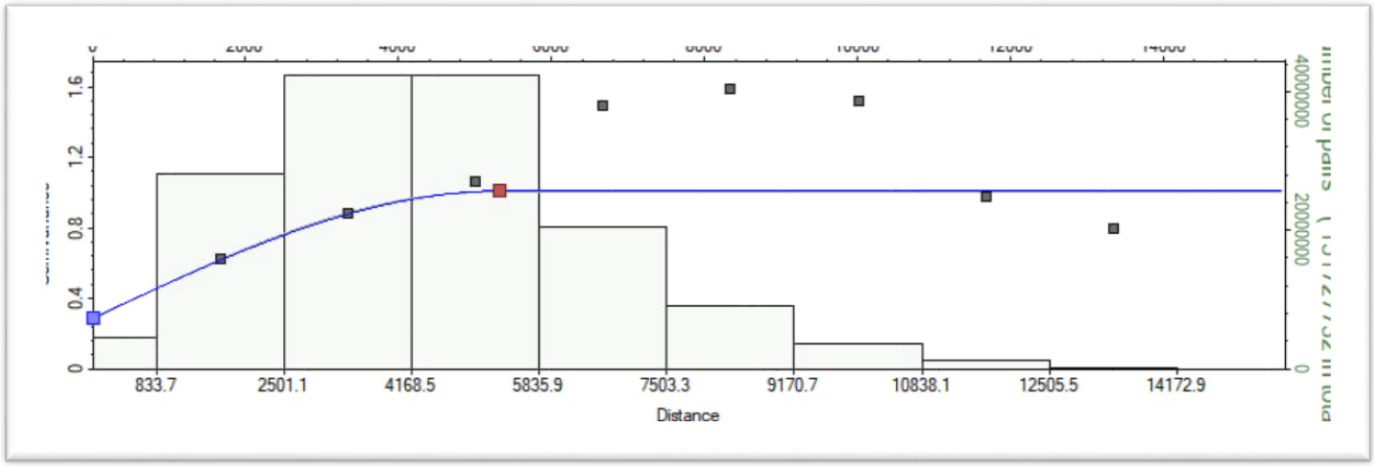

Figure 31 : Spherical Sw variogram of the 45° direction unit 1.

$$\gamma_{45}(h) = 0.283 + 0.717 * [1.5 \cdot (h/5093.1) - 0.5 \cdot (h/5093.1)^3]$$

Variogram for the 135° direction:

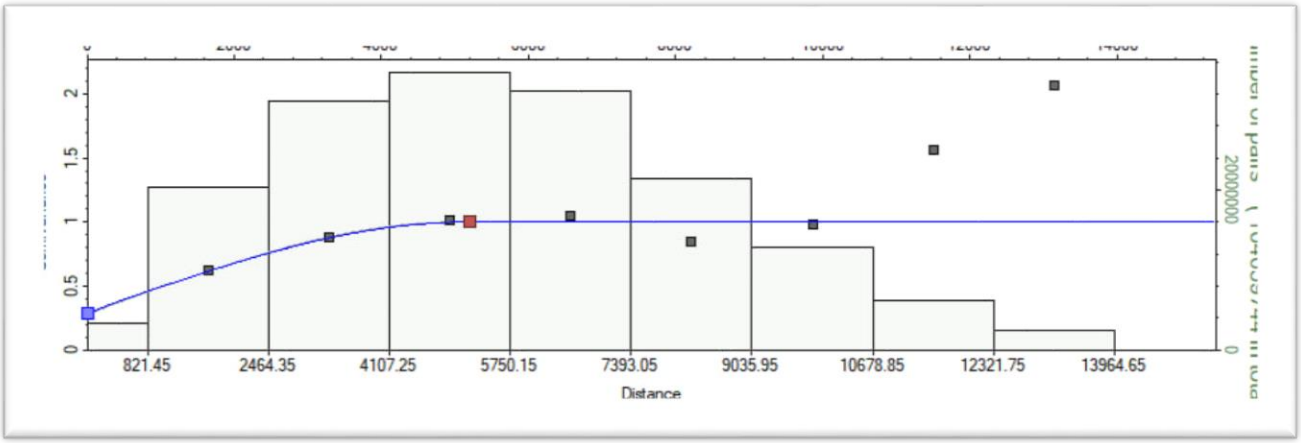

Figure 32 : Spherical Sw variogram of the 135° direction unit 1.

$$\gamma_{135}(h) = 0.276 + (0.724 - 0.276)*[1.5\cdot(h/5066.2) - 0.5\cdot(h/5066.2)^3]$$

Interpretation:

The nearly five-kilometer correlation in both the 45° and 135° directions shows that U1's channel bodies are exceptionally broad and laterally continuous. A nugget effect of roughly 0.28–0.276 (≈40 % of the sill) highlights moderate small-scale heterogeneity—likely from bar-scale facies shifts or minor microfaults. Finally, the almost identical ranges (anisotropy ratio ≈ 0.3) indicate a near-isotropic connectivity pattern, suggesting overlapping or multidirectional channel stacking in U1.

EXEMPLE 02

Variogram for the 45° direction:

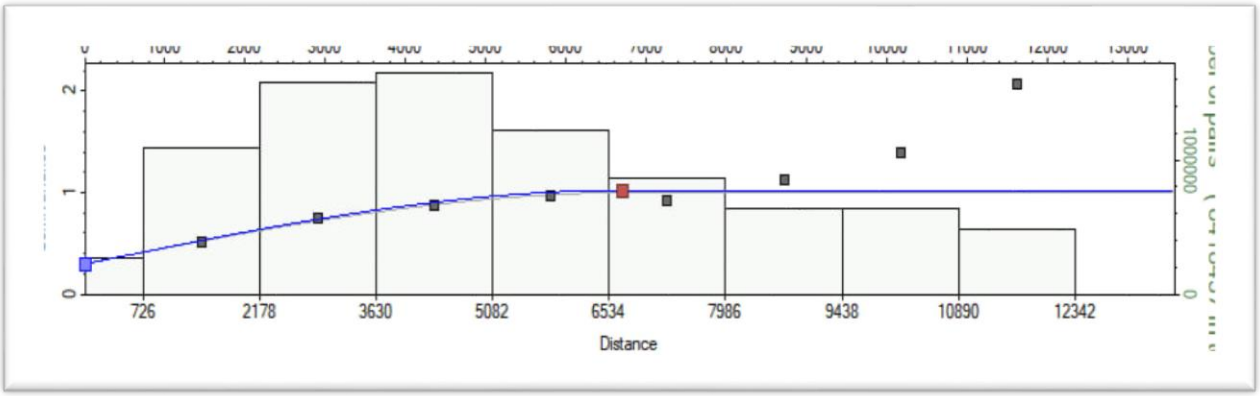

Figure 33: Spherical Porosity variogram of the 45° direction unit 4.

$$\gamma_{45}(h) = 0.3 + (0.7 - 0.3) *[1.5\cdot(h/6798.7) - 0.5\cdot(h/6798.7)^3]$$

Variogram for the 135° direction:

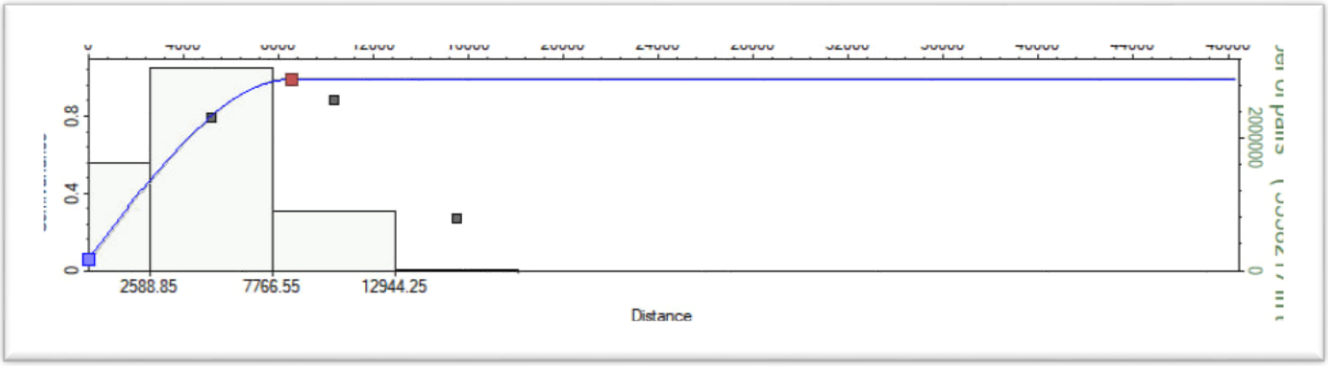

Figure 34: Spherical Porosity variogram of the 135° direction unit 4.

$$\gamma_{135}(h) = 0.039 + (0.96 - 0.039)* [1.5\cdot(h/8742) - 0.5\cdot(h/8742)^3]$$

Interpretation

In this U5 configuration, the 135° direction presents a longer correlation range and a much lower nugget effect, suggesting highly continuous facies bodies with minimal small-scale variability across the channel belt. Conversely, the 45° direction—presumably aligned with paleoflow—shows more short-range variability and a higher nugget, possibly reflecting internal complexity within channels or erosional surfaces. The reversal of anisotropy here (range ratio ≈ 0.77) may imply that lateral accretion or stacking patterns dominate, enhancing continuity perpendicular to the main flow axis.

Tableau 2 :Directional Variogram Porosity and Anisotropy Coefficients by Variable and Azimuth .

Direction	Equations	Anisotropy
45° T2	$\gamma_{45}(h) = 0.181 + (0.819 - 0.181)*[1.5\cdot(h/9148.1) - 0.5\cdot(h/9148.1)^3]$	0.22
135° T2	$\gamma_{135}(h) = 0.18 + (0.82 - 0.18) \cdot \backslash[1.5\cdot(h/8742) - 0.5\cdot(h/8742)^3]$	0.21
45° T1	$\gamma_{45}(h) = 0.315 + (0.685 - 0.315)*[1.5\cdot(h/4212.9) - 0.5\cdot(h/4212.9)^3]$	0.45
135° T1	$\gamma_{135}(h) = 0.193 + (0.807 - 0.193) \cdot \backslash[1.5\cdot(h/3624.2) - 0.5\cdot(h/3624.2)^3]$	0.23
45° Andisite	$\gamma_{45}(h) = 0.244 + (0.756 - 0.244)*[1.5\cdot(h/3587.3) - 0.5\cdot(h/3587.3)^3]$	0.32
135° Andisite	$\gamma_{135}(h) = 0.192 + (0.808 - 0.192) \cdot \backslash[1.5\cdot(h/2926.8) - 0.5\cdot(h/2926.8)^3]$	0.23
45° U1	$\gamma_{45}(h) = 0.003 + (0.996 - 0.003)*[1.5\cdot(h/5997.6) - 0.5\cdot(h/5997.6)^3]$	0.003
135° U1	$\gamma_{135}(h) = 0.034 + (0.965 - 0.034)*[1.5\cdot(h/6226.7) - 0.5\cdot(h/6226.7)$	0.004

Tableau 3: Directional Variogram Sw and Anisotropy Coefficients by Variable and Azimuth.

Direction	Equations	Anisotropy
45° T2	$\gamma_{45}(h) = 0.38 + (0.62 - 0.38)*[1.5\cdot(h/3585.9) - 0.5\cdot(h/3585.9)^3]$	0.61
135° T2	$\gamma_{135}(h) = 0.043+(0.956-0.043)*[1.5\cdot(h/3741.7) - 0.5\cdot(h/3741.7)^3]$	0.044
45° T1	$\gamma_{45}(h) = 0.164 + (0.836-0.164)*[1.5\cdot(h/1620.2) - 0.5\cdot(h/1620.2)^3]$	0.19
135° T1	$\gamma_{135}(h) = 0.042+(0.957-0.042)*[1.5\cdot(h/4962.1) - 0.5\cdot(h/4962.1)^3]$	0.043
45° Andisite	$\gamma_{45}(h) = 0.1 + (0.9- 0.1)*[1.5\cdot(h/4586.1) - 0.5\cdot(h/4586.1)^3]$	0.11
135° Andisite	$\gamma_{135}(h) = 0.1 + (0.9 - 0.1)*[1.5\cdot(h/4586.1) - 0.5\cdot(h/4586.1)^3]$	0.11
45° U4	$\gamma_{45}(h) = 0.12 + (0.88- 0.12)*[1.5\cdot(h/1055.5) - 0.5\cdot(h/1055.5)^3]$	0.13
135° U4	$\gamma_{135}(h) = 0.121 + (0.879 - 0.1)*[1.5\cdot(h/1511.8) - 0.5\cdot(h/1511.8)^3]$	0.13

b. 3D Mode analysis

A. Layer T2

Overall, T2 reservoir is characterized by low porosity values and relatively low water saturation. However, pressure measurements provide evidence of considerably compacted zone. Interestingly, near to faults, porosity reaches its mean; this indicates that these fracture zones have higher void volume storage. This data indicates that generally porosity is low in mst of T2, but faulted areas may be searched in future for improved porosity and hydrocarbon storage volume.

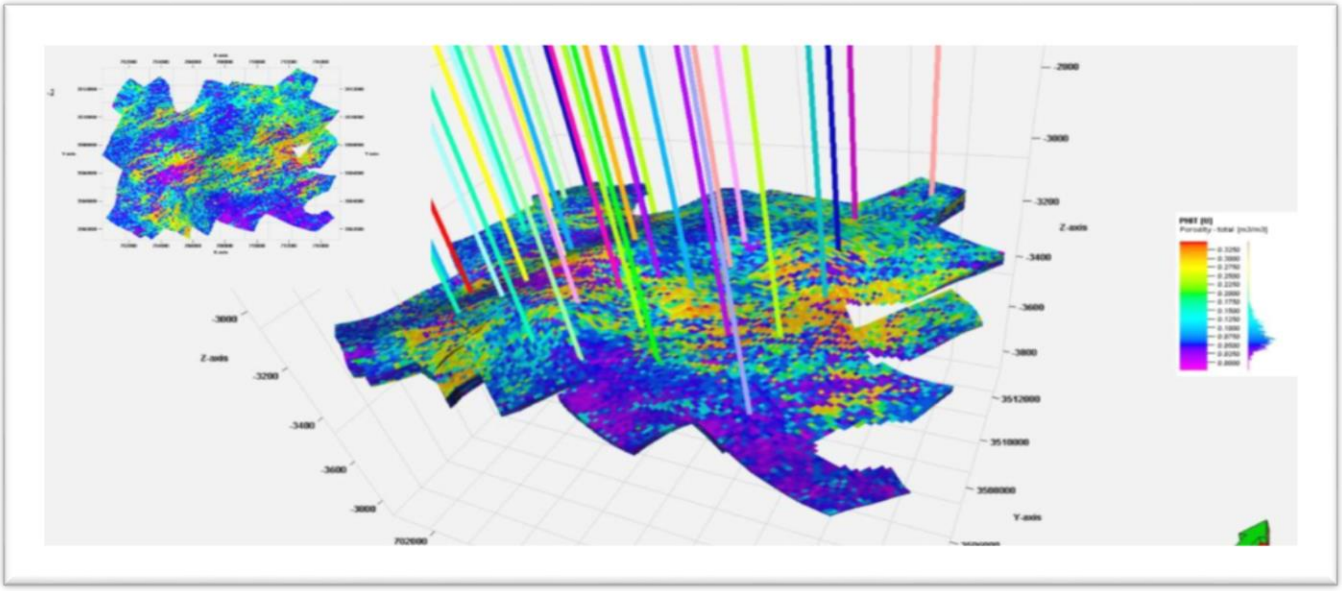

Figure 35: 3D,2D Porosity distributions in T2.

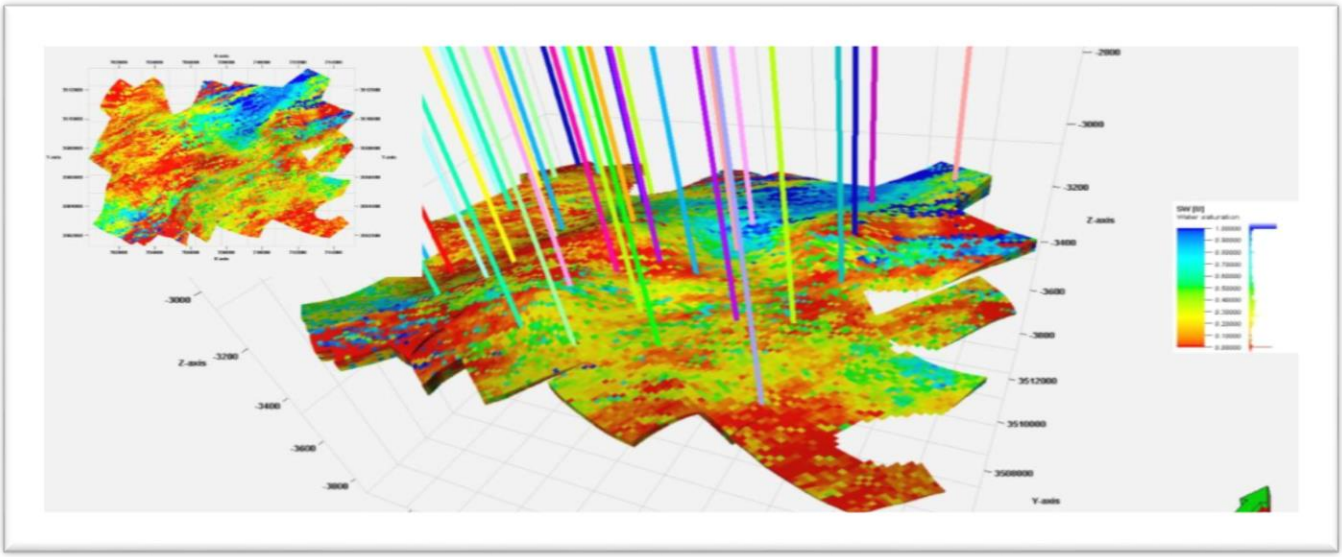

Figure 36: 3D,2D water saturation distributions in T2.

B. Layer T1

This main layer is composed primarily of clays and silts, which have low porosity; thus, the layer is characterized with low reservoir quality. Modeling shows the unit consisting of very low porosity values and very high water saturation within its limits, with no portions showing any higher tendency towards hydrocarbon accretion. Thus, T1 is not among the foremost targets for new wells, given the low petrophysical potential it harbors.

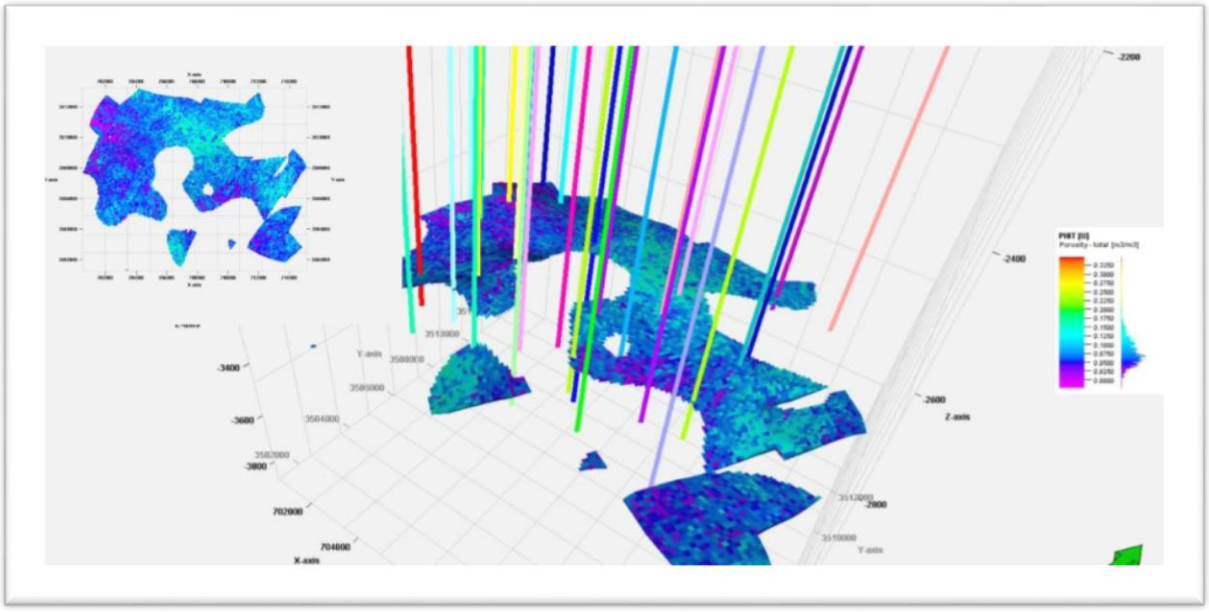

Figure 37: 3D,2D Porosity distributions in T1.

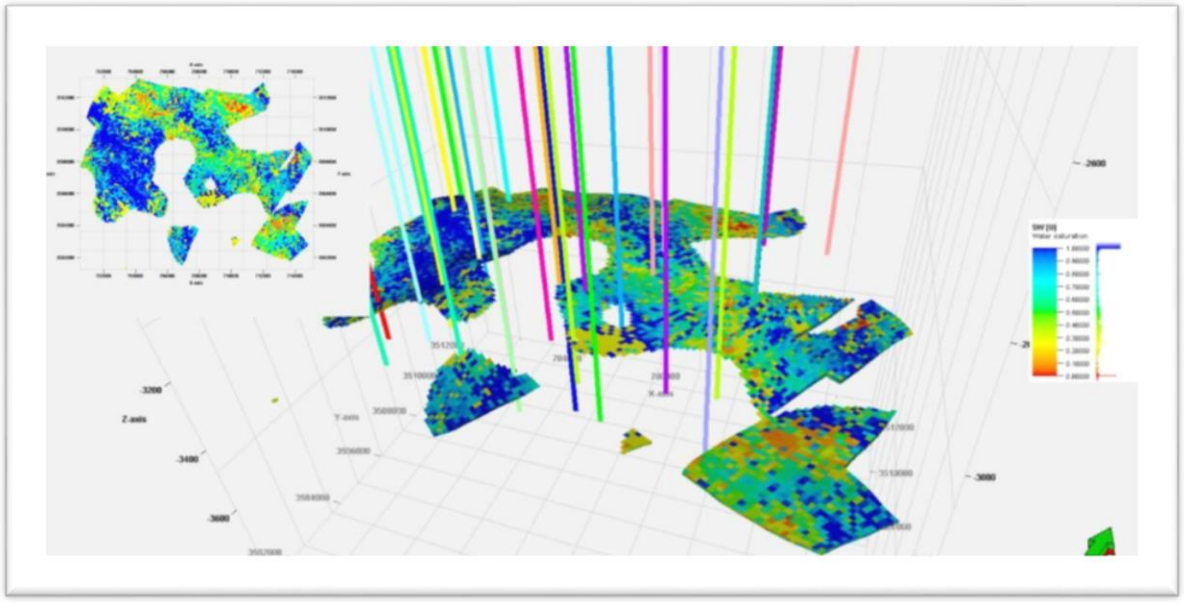

Figure 38: 3D,2D Water saturation distributions in T1.

C. Andesite unit

shows generally low porosity values consistent with its dominantly clayey nature. Log porosity is sometimes overestimated due to the microporous nature of shales. Water saturations vary widely (0.2-1.0) because clays can retain water very well by capillary and adsorption. This variation, although very considerable, confirms the non-reservoir role of this unit that acts as an impermeable cap overlying the reservoirs beneath.

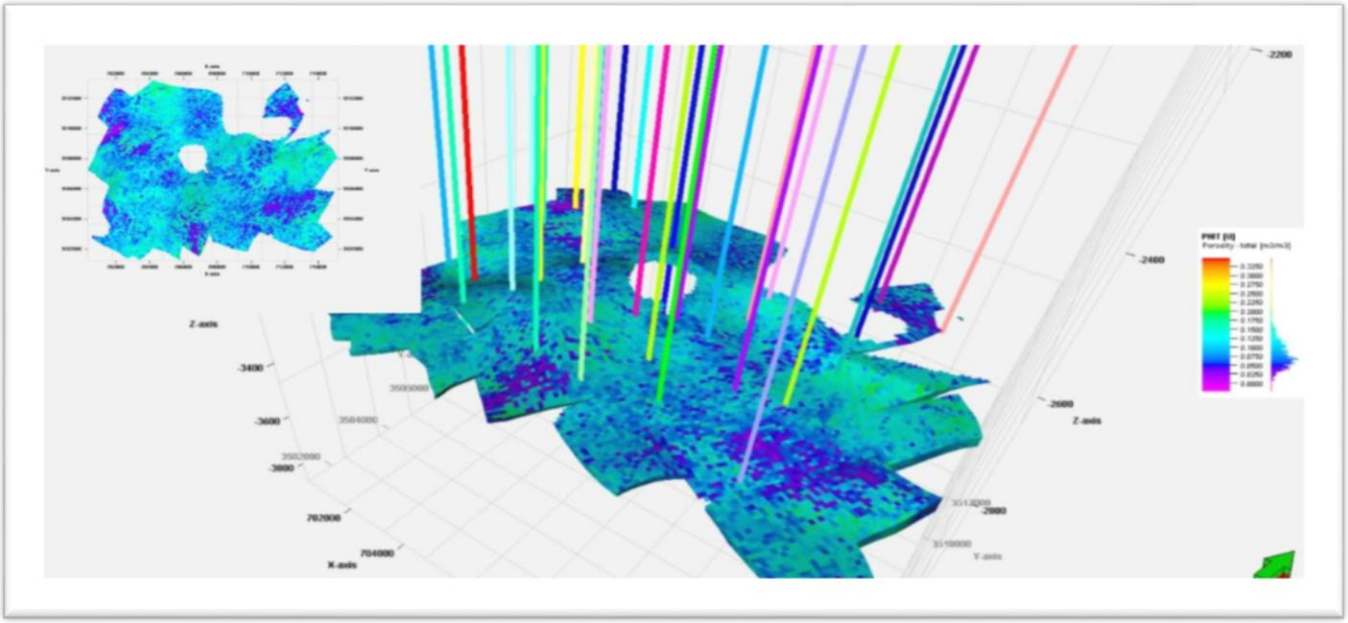

Figure 39: 3D,2D Porosity distributions in Andiste.

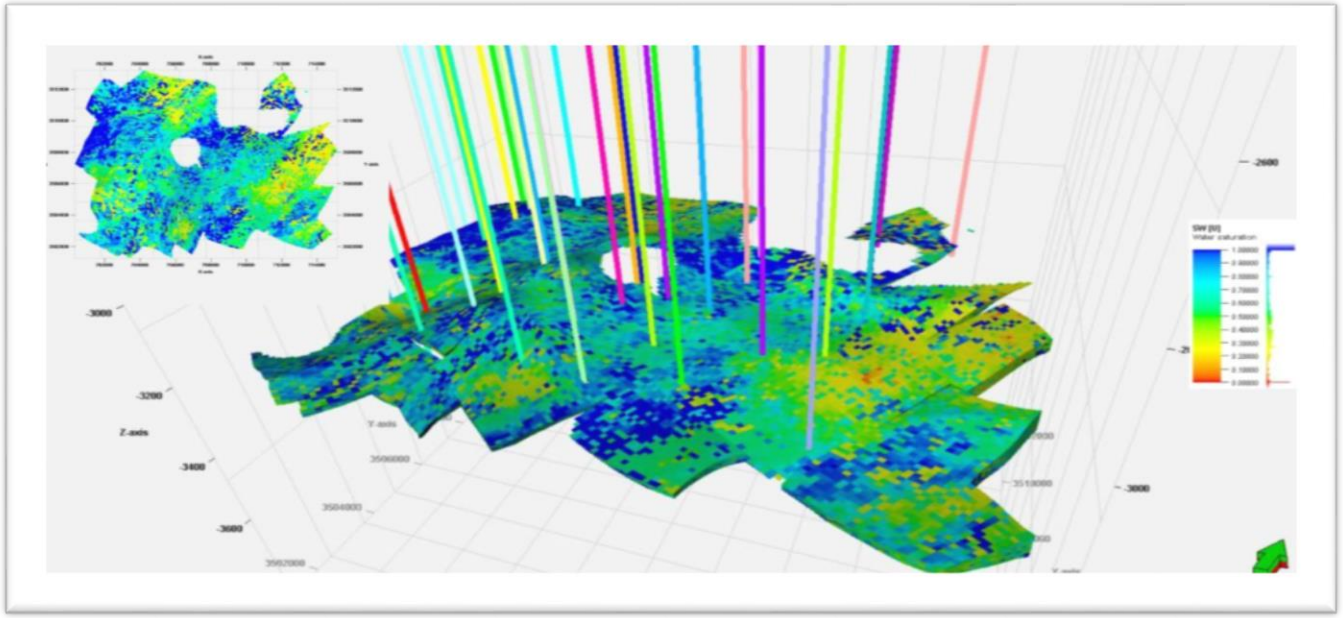

Figure 40: 3D,2D water saturation distributions in Andisit.

D. Lower Series

Lower Series are the main target of drilling. They have an average thickness of 40-50 m and consist of 4-5 vertically stacked units. Modelling suggests that lodged porosities average about 12-14% over much of the field, with maximum values at the top of the anticline.

In the southwestern region, where argillosity is present in large amounts, it has been noted that most of the regions have fracture networks which in them accommodate substantial volumes of high porosity. The distribution of porosity and water saturation observed rather hints to a preferred direction which is actually perpendicular to the structural axes; the latter exceedingly attempts to identify their influence in reservoir quality.

Analysis of the petrophysical model shows that the Triassic clay-sandstone reservoirs are extremely heterogeneous both laterally and vertically. The lower series sandy units perform the best as reservoirs, holding fairly high porosities combined with a distribution suitable for upcoming drilling. Conversely, the T1 and Andesite units do not provide much conducive property for fluid circulation since they play a covering function. Finally, the T2 unit is compact overall, yet locally it shows interesting potential around faulted zones where porosity becomes average. These outcomes will arm us with information to target better zones of high potential, and therefore pursue optimal strategies for field development.

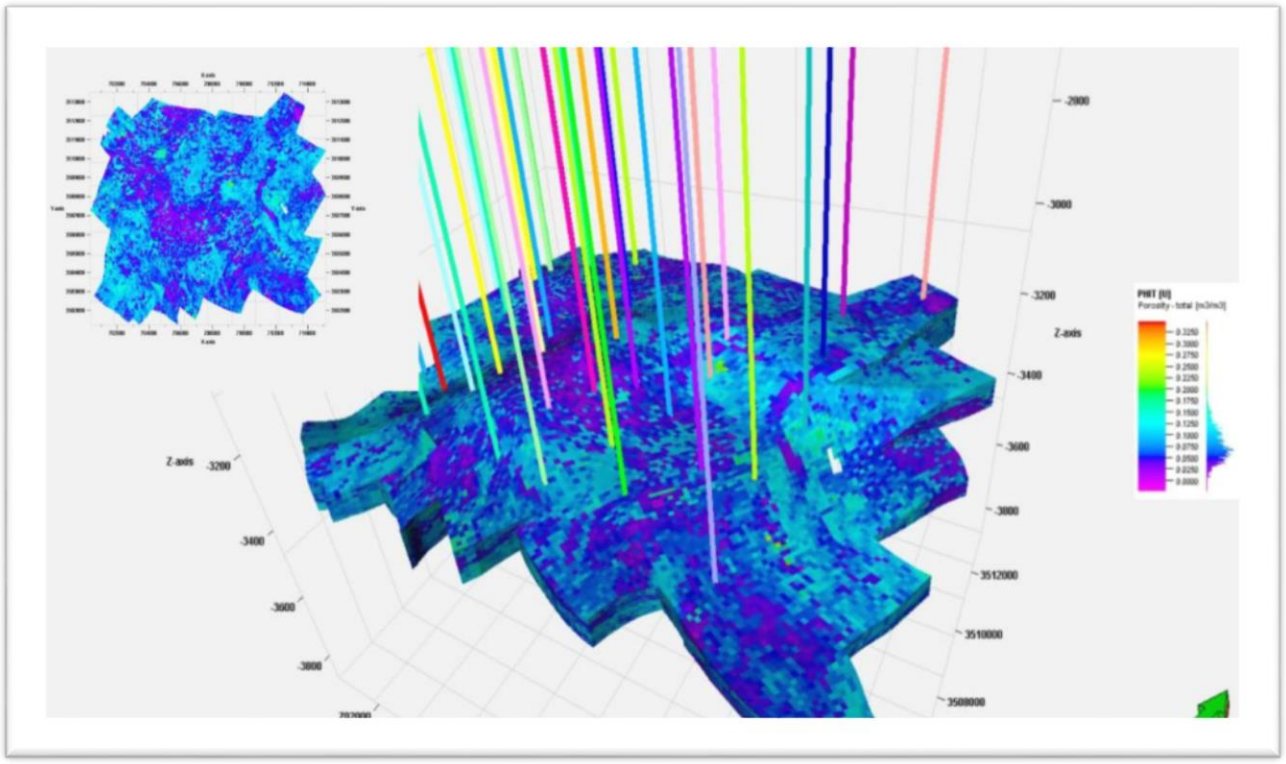

Figure 41: 3D,2D Porosity distributions in Lower Series.

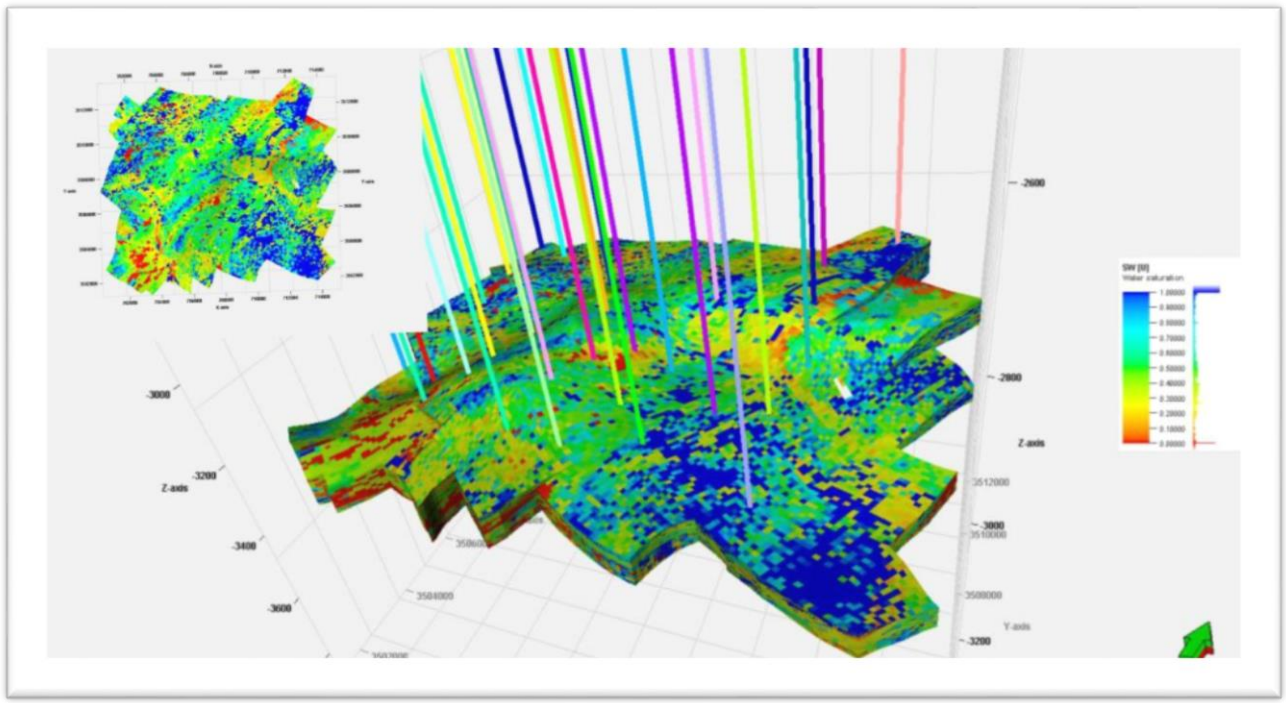

Figure 42: 3D,2D water saturation distributions in Lower Series.

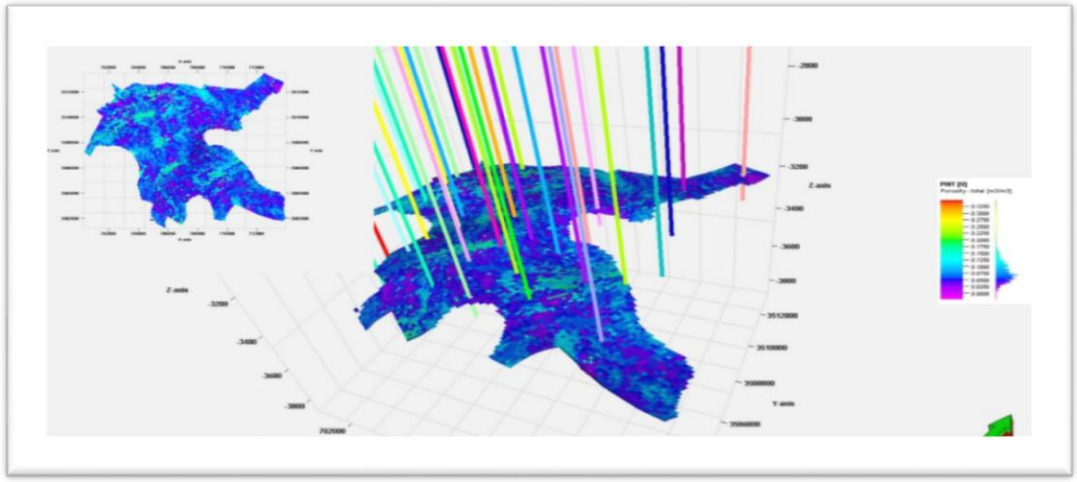

Figure 43: 3D,2D Porosity distributions in U1.

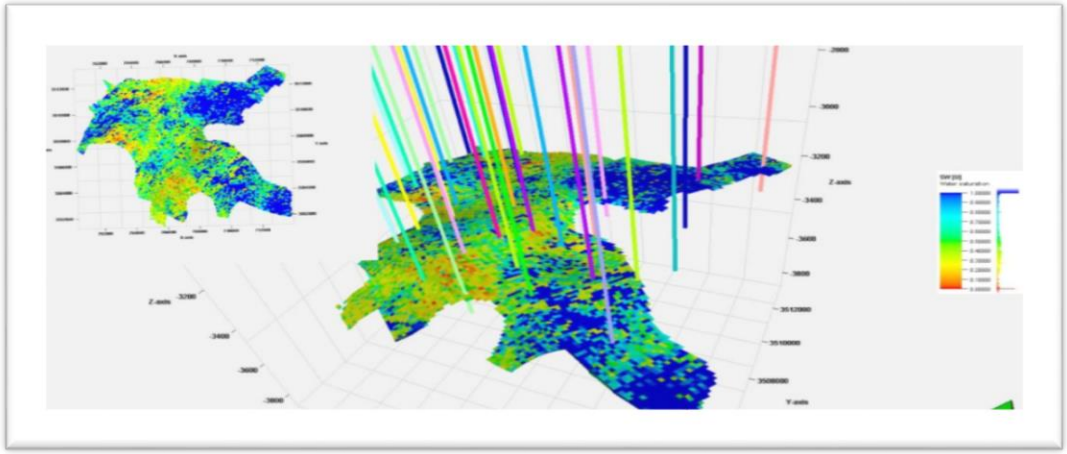

Figure 44: 3D,2D water saturation distributions in U1.

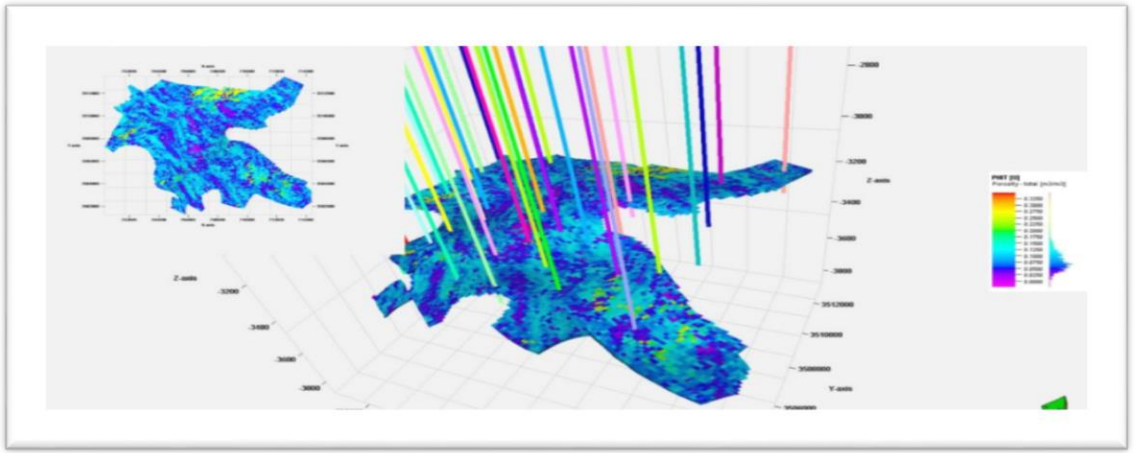

Figure 45: 3D,2D Porosity distributions in U2.

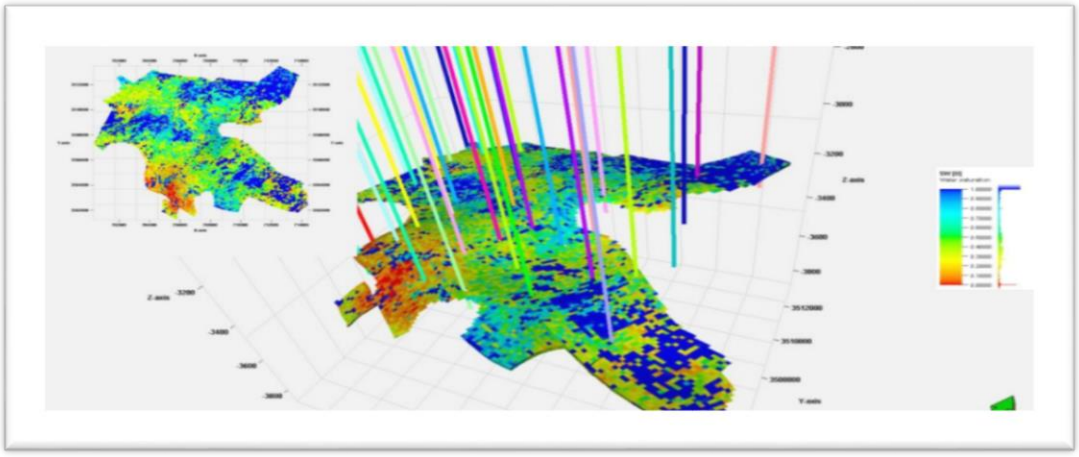

Figure 46: 3D,2D water saturation distributions in U2.

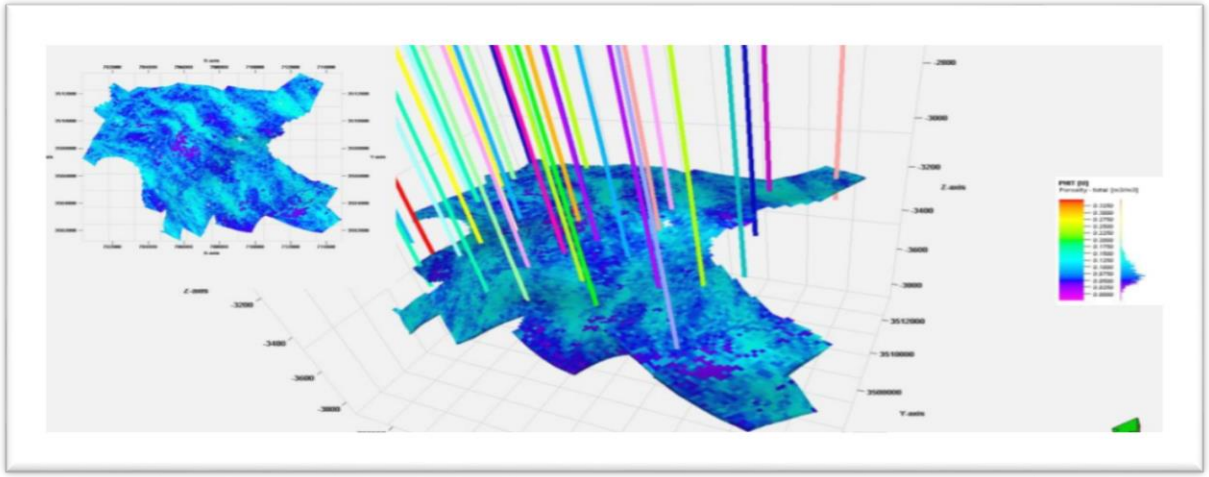

Figure 47: 3D,2D Porosity distributions in U3.

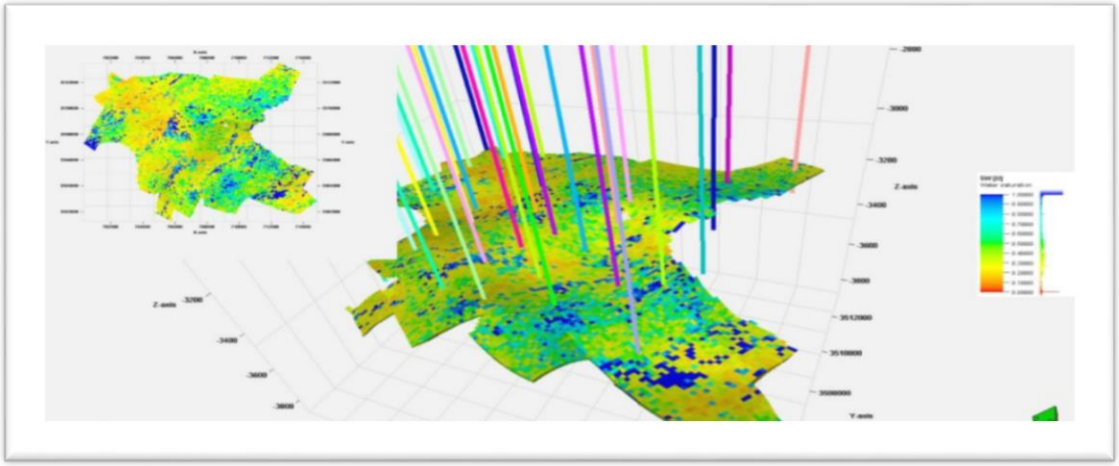

Figure 48: 3D,2D water saturation distributions in U3.

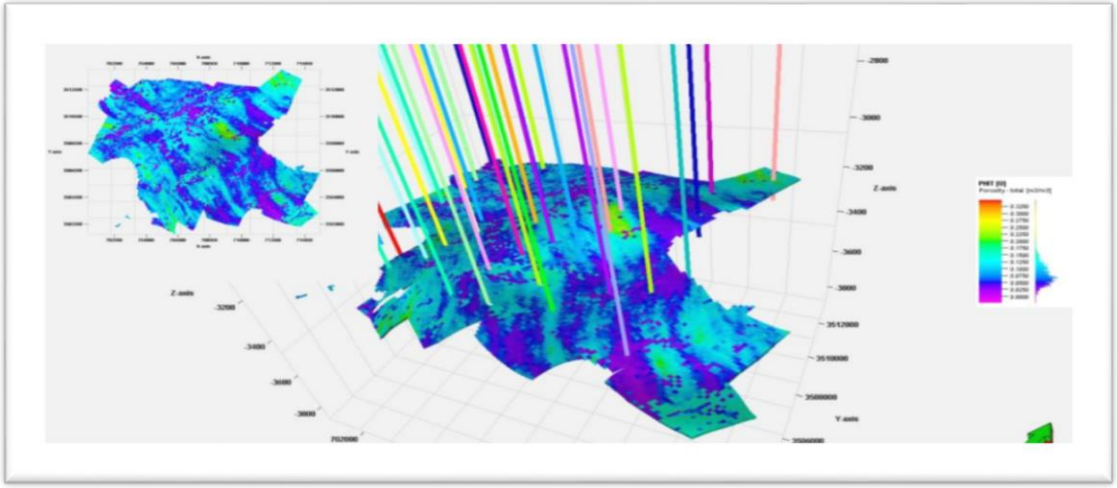

Figure 49: 3D,2D Porosity distributions in U4.

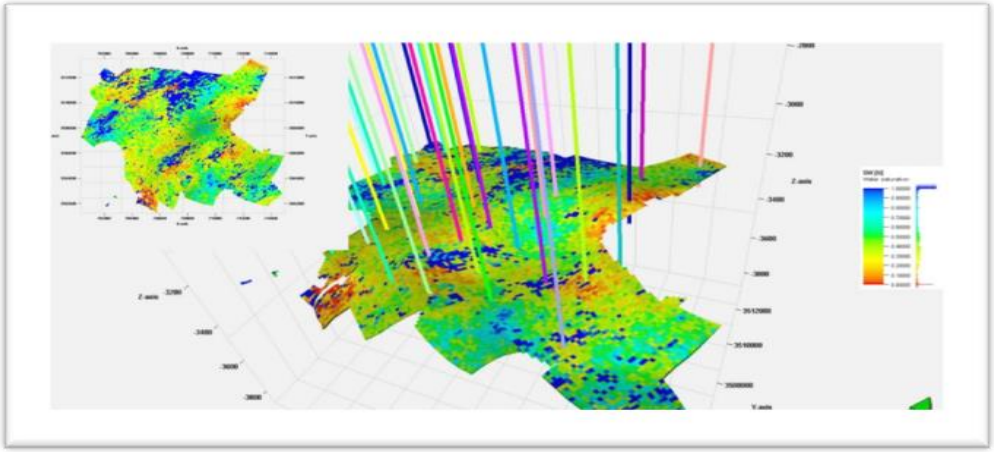

Figure 50: 3D,2D water saturation distributions in U4.

5. Model Validation

To validate the 3D geological model constructed in Petrel, three wells (OKS-28, OKS-49 , and OKS-34) were excluded from the initial modeling and simulation phases. Simulated porosity and water saturation values at these wells were later compared with available core data. The results are presented in the table below:

Tableau 4: Porosity and water saturation estimated values compared to core values.

Well	Property	Simulated Value	Core Value	Difference (%)
OKS-34	Porosity (%)	12.6	13.5	6.67
OKS-34	Water Saturation (%)	35.7	37.5	4.80
OKS-49	Porosity (%)	10.0	11.3	11.50
OKS-49	Water Saturation (%)	32.8	34.0	3.53
OKS-28	Porosity (%)	13.4	14.0	4.29
OKS-28	Water Saturation (%)	30.2	32.0	5.63

In five out of six cases, the percentage difference remained below 10%. One exception was observed in the porosity value at Well OKS-49 which showed a difference of 11.5%.

5.1. Discussion Model Performance and Reliability

The validation results show that the model reasonably replicates measured petrophysical properties. Most of the differences between simulated and core values were under the 10% threshold, which is commonly used as an acceptance criterion in reservoir modeling.

A single exception was noted in porosity at WellOKS-49, where the difference reached 11.5%. This may be due to localized heterogeneity, data resolution limits, or minor inaccuracies in core measurements. Given that this is an isolated case, it does not significantly affect the overall evaluation of the model.

The general consistency between simulated and measured values indicates that the interpolation and property distribution methods applied in the model are appropriate. The model can therefore be used for further static reservoir analysis, volumetric estimation, or as input to dynamic simulation.

Conclusion

The geological and structural study conducted on the southern zone of the BenKahla field has enabled the construction of a robust 3D geological model of the Triassic argillaceous-sandstone reservoir. This model integrates a wide range of data, including well log interpretations, petrophysical and facies analysis, stratigraphic correlations, and 3D structural modeling.

To ensure representative spatial coverage of the study area, three correlation profiles were carefully established: two parallel north–south profiles (OKS21–OKS23–OKS26 and OKS64–OKS54–OKS52) focused on vertical stratigraphic stacking, and one east–west profile (OKS26–OKT06–OKT17) aimed at analyzing the lateral evolution of facies and structures.

Stratigraphic correlation results revealed a progressive deepening trend of the tops of units T2, T1, and the underlying andesitic level, reflecting tectonic subsidence controlled by a dominant NE–SW fault system. These faults clearly compartmentalize the reservoir, significantly influencing its thickness, geometry, and lateral continuity.

Facies interpretation, based on electric and nuclear logs interpreted using the IP software and validated by Sonatrach, revealed an alternation of well-sorted fine to medium sandstones with high porosity—interpreted as channel deposits—and clayey to silty levels representing floodplain or low-energy depositional phases. This facies succession reflects a braided fluvial system , characterized by hydrodynamic fluctuations and active tectonic controls.

A detailed subdivision of the reservoir into five electrofacies units (Unit01 to Unit05) allowed for precise stratigraphic interpretation. These units display contrasting lithological and petrophysical characteristics: for example, Unit03 and Unit05 are rich in porous sandstones and show better connectivity, while Unit02 is more heterogeneous with a dominance of clay-rich facies.

The fundamental petrophysical properties porosity and water saturation provided by Sonatrach were integrated into the 3D geological model using appropriate variogram-based geostatistical methods, ensuring realistic spatial distribution and continuity of reservoir properties.

In summary, the Triassic reservoir of the southern BenKahla field is defined by a complex structural architecture influenced predominantly by a NE–SW oriented fault system. This structural framework has led to significant compartmentalization of the reservoir, directly impacting its geometry, thickness, and continuity. The reservoir also exhibits notable facies heterogeneity, reflective of a dynamic braided fluvial depositional environment characterized by alternating high-energy channel sandstones and low-energy floodplain deposits. Through detailed log interpretation, the reservoir was subdivided into five electrofacies units (Unit01 to Unit05), each representing distinct lithological and petrophysical characteristics that enhance both vertical and lateral understanding of the system. Petrophysical parameters such as porosity and water saturation, provided by Sonatrach, were rigorously integrated into the 3D geological model using geostatistical methods based on variograms to ensure a realistic spatial representation. This comprehensive, multidisciplinary approach has resulted in a robust and coherent static model, forming a solid basis for future dynamic simulation and effective field development strategies.

Generel conclusion

General conclusion

This thesis has addressed the geological and petrophysical characterization of the TAG reservoir in the Ben Kahla field, situated in the Oued Mya Basin of the Algerian Sahara. The approach integrated well log analysis, structural interpretation, and 3D geological modeling, offering a coherent understanding of the reservoir's internal architecture and its heterogeneities—essential elements for informed field development.

Through detailed diagraphic and petrophysical analysis, three Triassic reservoirs were identified in the OKS area. Of these, only the SI reservoir proved to have significant hydrocarbon potential. It lies entirely above the oil-water contact, with a reservoir pressure averaging 440 kg/cm². The T1 and T2 reservoirs were found to be clay-rich and of no economic interest.

Despite the absence of seismic data, the use of variography enabled the construction of a meaningful 3D geological model. This model provided insights into the spatial distribution of facies and petrophysical parameters such as porosity and saturation, which, although not strongly correlated, are generally of good quality. Five productive units were identified within the SI reservoir, deposited in a braided fluvial setting, emphasizing the complexity and heterogeneity of the system.

The cross-sectional interpretations and correlations demonstrated that the maximum reservoir thickness is concentrated in the central part of the structure, thinning towards the south—a pattern interpreted as bisection and likely defining the southern limit of reservoir extension. These findings help delineate the most favorable drainage zones for future drilling.

This study confirms that robust reservoir modeling is possible even in the absence of seismic data, provided that well log data is thoroughly analyzed and statistically integrated. However, certain limitations remain, particularly regarding structural precision and dynamic behavior forecasting.

And for recommendations for future work include we recommendate a:

Acquiring 3D seismic data to enhance structural resolution and fault interpretation.

Developing a dynamic reservoir model to simulate fluid flow and support production optimization.

Performing advanced core and laboratory analyses to refine petrophysical parameters.

Evaluating connectivity and communication between reservoir units, especially across faults and thin argillaceous barriers.

In conclusion, this work lays a solid foundation for improved understanding and management of the TAG reservoir. The integrated modeling approach applied here not only reduced geological uncertainties but also identified new opportunities for reservoir development in the Ben Kahla field.

Refrences

- **Aït Bali, A. & Sadoun, B. (2023).** *Étude sédimentologique et pétrophysique du Trias série inférieure du gisement de Benkahla-Bassin Oued Mya-province Triasique (Algérie)* [Rapport inédit].

- **Boudjemaa,A. 1987**.Evolution structural du bassin pétrolier "triasique" du Sahara Nord Oriental. Thèse Doctorat, Uni. Paris-Sud, Orsay.

- **BENMANSOUR Abdel Kamal & LAZREG Nesrine**, mémoire de fin d'études Master, Lithostratigraphie, organisation sédimentaire du Champ de Ben Kahla Est Aspect pétrolier du puits BKHE 2 Haoud Berkaoui - Bassin de Oued M'ya – Algérie. Université Abou Bakr Belkaid Tlemcen.

- **MEBROUKI Nacira**, mémoire du diplôme de MAGISTER, ETUDE GEOLOGIQUE DE L'EXTENSION DE LA ZONE DE BENKAHLA. Université Kasdi Merbah Ouargla

- **SAHRAOUI Ahmed & KABOUR Saad**, Mémoire de fin d'études master, InterprÈtation structurale 3D aux toits de l9Aptien et du SalifËre 8S49 du pÈrimËtre de Zelfana Bassin d'Oued Mya. Université M'HAMED BOUGARA DE BOUMERDES.
- **Serra, O. 1979** : Diagraphie différées, Base de l'Interprétation des données diagraphiques, Tome 2, SNEAP. P PAU-France.

- **SLB. (n.d.).** Practical Guide for Petrel at HMD. Schlumberger internal training document.
  Geostatistics Lessons. (n.d.). Sequential Indicator Simulation. https://geostatisticslessons.com/pdfs/sequentialindicatorsim.pdf .

- **Sonatrach, 2002** - **Rapport d'analyse pétrographique des réservoirs triasiques, Champ de Benkahla.*

- **Thiago A. Mizuno and Clayton V. Deutsh :** Sequential Indicator Simulation.
  Journel, A. G., & Alabert, F. (1989). Non-Gaussian data expansion in the Earth sciences. Terra Nova, 1(2), 123–134.

- **Truc, G., Fabre, J., Conrad, J. & Magnier, P. (1989).** Contrôles climatiques des séquences triasiques. *Bulletin de la Société Géologique de France*, *V*(3), 487-498.